

Comparing the photochemical potential of quinoa to maize under water stress conditions

C. Malan

 orcid.org/0000-0003-0680-503X

Thesis accepted for the degree [Doctor of Philosophy in Science](#)
[with Botany](#) at the North-West University

Promoter: Prof JM Berner

Graduation May 2020

22775366

PREFACE

The work presented here is a result of an original study conducted at the North-West University, Potchefstroom. The research was done under the supervision of Prof. J. M. Berner.

The sustainable production of crops is being threatened each year by severe abiotic stress. Recently South Africa has experienced extreme drought events resulting in a worrying yield reduction of important crops, such as maize. The introduction of climate resilient crops, for example, quinoa, could assist South Africa in adapting to climate change. In this study the acclimation strategy of both quinoa and maize was investigated by means of their photochemical potential and ability to produce osmoprotectants under water- stressed conditions.

I declare that the work presented in this PhD thesis is my own work, that it has not been submitted for any degree or examination at any other university and that all the sources I have used or quoted have been acknowledged by complete reference. I therefore, cede its copyright in favour of the North-West University, Potchefstroom.

ACKNOWLEDGEMENTS

Firstly, I am grateful to Almighty God for the good health and wellbeing that were necessary to complete this thesis.

I would like to express my sincere gratitude to my supervisors Prof. J. M. Berner for his support of my PhD study.

I would also like to thank William Weeks for providing the quinoa photos.

Additionally, I would also like to acknowledge Mmbulaheni Netshimbupfe, Linda van der Spuy and Marcell Slabbert for their help with the glasshouse trials.

I would also like to thank the NRF-DAAD and the North West University, for their financial support, which made it possible to complete this study.

Last but not the least; I would like to express my very profound gratitude to my family for supporting me throughout my years of study and through the process of researching and writing this thesis.

ABSTRACT

In the current context of climate change, drought events are one of the major causes of yield reduction in crops. Seeing that South Africa is a water scarce country and along with the future climate change predictions, the introduction of climate resilient crops is needed. Quinoa has been identified as a climate resilient crop that could provide farmers with an alternative option to mitigate the impact of climate change on crop production. Nevertheless, the question stands, whether the cultivation of quinoa would be successful in South Africa. The aim of this study is to investigate the physiological acclimation of quinoa, while subjected to water stress and compare it to the main staple crop, maize. In this trial, both quinoa and maize were planted in glasshouses at two different temperature regimes (20°C and 30°C) while subjected to water stress. The photochemical potential of PSII was measured by means of chlorophyll *a* fluorescence and the photochemical potential of PSI was measured by means of 820 nm reflection. The antioxidative capacity of the crops was assessed by measuring the superoxide dismutase (SOD) and glutathione reductase (GR) activities and proline content. In addition, the stomatal conductance, chlorophyll content, leaf water potential and membrane leakage was determined for both the crops. The higher proline levels of the water- stressed quinoa contributed to the ability of PSII to tolerate water deficit stress. PSI activity of the water- stressed quinoa was more stable under the water- stressed conditions compared to the water-stressed maize plants. The SOD and GR activities were higher in the water stressed quinoa, thereby playing an active role in minimizing oxidative damage. The physiological acclimation strategy of quinoa also included a decrease in the stomatal conductance, total leaf area, membrane leakage and higher leaf water content. Compared to the water stressed maize, quinoa was able to acclimate more successfully to water deficit stress. The ability of quinoa to protect its photosystems is a crucial acclimation strategy to ensure optimal photochemistry under water deficit conditions.

Keywords: Chlorophyll *a* fluorescence, Glutathione reductase, Hydrogen peroxide, Maize, Modulated reflection, Proline, Quinoa, Superoxide dismutase, Water stress

TABLE OF CONTENTS

CHAPTER 1 INTRODUCTION	1
1.1 The aim of this study.....	4
1.2 The objectives of the study	4
1.3 Hypothesis.....	4
1.4 Thesis layout	5
CHAPTER 2 LITERATURE STUDY	6
2.1 Quinoa	6
2.2 The acclimation strategy of plants to abiotic stress.....	11
2.2.1 Acclimation strategy of crops to drought.....	12
2.2.2 Acclimation strategy of crops to temperature.....	13
2.3 Comparing C ₃ species to C ₄ species subjected to stress	15
2.4 The role of osmoprotectants	18
2.4.1 Proline	19
2.4.2 Superoxide dismutase	21
2.4.3 Glutathione reductase	23
2.4.4 Hydrogen peroxide	25
2.5 Chlorophyll a fluorescence.....	27
CHAPTER 3 MATERIALS AND METHODS	36
3.1 Growth conditions.....	36
3.2 Plant cultivation.....	36
3.3 Water regimes.....	36
3.4 Experimental timeline	37

3.5 Prompt fluorescence	38
3.6 MR820 nm Modulated reflection.....	38
3.7 Membrane leakage	38
3.8 Relative leaf water potential	39
3.9 Stomatal conductance	39
3.10 Chlorophyll content.....	40
3.11 Proline content	40
3.12 Superoxide dismutase	41
3.13 Glutathione reductase.....	42
3.14 Hydrogen peroxide.....	43
3.15 Fresh and dry biomass	44
3.16 Statistical analysis	45
CHAPTER 4 RESULTS	46
4.1 Chlorophyll a fluorescence.....	46
4.1.1 JIP test	46
4.1.2 Difference in relative variable fluorescence (ΔV).....	48
4.1.3 Fluorescence parameters.....	55
4.1.4 Vitality index scale	64
4.1.5 Modulated reflection	65
4.2 Membrane leakage	70
4.3 Relative leaf water content	71
4.4 Stomatal conductance	72
4.5 Chlorophyll content.....	73

4.6 Proline content	75
4.7 Superoxide dismutase content.....	76
4.8 Glutathione reductase activity.....	77
4.9 Hydrogen peroxide content	79
4.10 Dry Biomass	81
CHAPTER 5 DISCUSSION.....	83
CHAPTER 6 CONCLUSIONS.....	97
CHAPTER 7 RECOMMENDATIONS AND FUTURE STUDIES.....	99
References	100
LAST UPDATED: 19 February 2020.....	135

LIST OF TABLES

Table 2-1: Formulae and definitions of terms used by the JIP-test for the analysis of chlorophyll *a* fluorescence transient OJIP in this study (from Strasser *et al.*, 2007; Tsimilli-Michael and Strasser, 2013; Kalaji *et al.*, 2017). 31

Table 3-1: Timeline of the experimental work during 2017 to 2019.....37

Table 4-1: Correlations of the JIP test parameters.....59

Table 4-2: The percentage difference between the water- stressed maize and quinoa at both the 20°C and 30°C regimes. 63

Table 4-3: A vitality index for quinoa and maize based on the PI_{TOTAL} values. 65

Table 4-4: Parameters derived from 820 nm modulated reflection (MR_t/MR₀) in leaves of both quinoa and maize under water stress conditions (severe drought stress, soil moisture content ≤ 0.01 m⁻³.m⁻³) at 20°C and 30°C. (MWS, maize water stress; MWW, maize well-watered; QWS, quinoa water stress; QWW, quinoa well-watered)..... 68

LIST OF FIGURES

Figure 2-1:	The five quinoa ecotypes and their geographic distribution (Hinojosa <i>et al.</i> 2018).	7
Figure 2-2:	(a) The panicle of quinoa; (b) Opened flowers with anthers and pollen (c) White quinoa seeds contained within the flower; (d) An unopened flower bud (Photos provided by William Weeks, 2018).....	8
Figure 2-3:	Phenological growth stages of quinoa (<i>Chenopodium quinoa</i>) (Sosa-Zuniga <i>et al.</i> , 2017).	10
Figure 2-4:	A representation of the carbon fixation pathways of C3 and C4 plants (Lara and Andreo, 2011).	16
Figure 2-5:	The metabolic pathways of proline in plants (Zhang and Becker, 2015).	20
Figure 2-6:	Localization of superoxide dismutase in a plant cell (Saibi and Brini, 2018).....	22
Figure 2-7:	Antioxidant pathway mediated by Glutathione reductase in response to external and inner cellular stresses (Trivedi <i>et al.</i> , 2013).....	24
Figure 2-8:	The production of hydrogen peroxide (H ₂ O ₂) in the different photosynthesising cells (Saxena <i>et al.</i> , 2016).....	27
Figure 2-9:	A typical chlorophyll a polyphasic fluorescence rise OJIP, exhibited by plants plotted on a logarithmic time scale (0.2 ms – 1 s). The different steps are labelled as O (20 μs), K (0.3 ms) J (2 ms), I (30ms), and P (≈300 ms).....	30
Figure 2-10:	A schematic presentation of the JIP-test (Tsimilli-Michael and Strasser, 2013).....	32
Figure 2-11:	Kinetics of modulated light reflection at 820 nm in dark-adapted leaves. oa ecotypes and their geographic distribution (Hinojosa <i>et al.</i> 2018).....	34
Figure 4-1:	The average chlorophyll a fluorescence transient (OJIP) taken over time as the volumetric moisture reached 0.01 m ⁻³ .m ⁻³ (A) quinoa at 20°C, (B) maize at 20°C, (C) quinoa at 30°C and (D) maize at 30°C. Comparative	

chlorophyll a fluorescence transients for (E) both quinoa and maize at 20°C and (F) both quinoa and maize at 30°C. The O-J-I-P transients (E and F) were normalized at 0.03 ms and plotted on a logarithmic time scale. (MWS, maize water stress; MWW, maize well watered; QWS, quinoa water stress; QWW, quinoa well watered). 47

Figure 4-2: (A) Difference in relative variable fluorescence ($\Delta V_{OP} = V_{OP} \text{ treatment} - V_{OP} \text{ control}$) of intact leaves of the quinoa and maize control and water stress treatments at 20°C, normalized between 0.03 μ s and 300 ms respectively to obtain the ΔV_{OJ} and ΔV_{JP} curves normalized between 0.03 and 300 ms. (B) Difference in relative variable fluorescence ($\Delta V_{OJ} = V_{OJ} \text{ treatment} - V_{OJ} \text{ control}$) normalized between 0.03 μ s and 2 ms. (C) Difference in relative variable fluorescence ($\Delta V_{JP} = V_{JP} \text{ treatment} - V_{JP} \text{ control}$) normalized between 2 ms and 300 ms. (D) Difference in relative variable fluorescence ($\Delta V_{KI} = V_{KI} \text{ treatment} - V_{KI} \text{ control}$) normalized between 0.3 ms and 30 ms. (MWS, maize water stress; MWW, maize well watered; QWS, quinoa water stress; QWW, quinoa well watered). 50

Figure 4-3: (A) Difference in relative variable fluorescence ($\Delta V_{OP} = V_{OP} \text{ treatment} - V_{OP} \text{ control}$) of intact leaves of the quinoa and maize control and water stress treatments at 30°C, normalized between 0.03 μ s and 300 ms respectively to obtain the ΔV_{OJ} and ΔV_{JP} curves normalized between 0.03 and 300 ms. (B) Difference in relative variable fluorescence ($\Delta V_{OJ} = V_{OJ} \text{ treatment} - V_{OJ} \text{ control}$) normalized between 0.03 μ s and 2 ms. (C) Difference in relative variable fluorescence ($\Delta V_{JP} = V_{JP} \text{ treatment} - V_{JP} \text{ control}$) normalized between 2 ms and 300 ms. (D) Difference in relative variable fluorescence ($\Delta V_{KI} = V_{KI} \text{ treatment} - V_{KI} \text{ control}$) normalized between 0.3 ms and 30 ms. (MWS, maize water stress; MWW, maize well watered; QWS, quinoa water stress; QWW, quinoa well watered). 52

Figure 4-4: The fluorescence transients were normalized between O-J ($\Delta V_{OJ} = V_{OJ} \text{ treatment} - V_{OJ} \text{ control}$) to visualize the ΔV_{K-} band. (MWS, maize water stress; MWW, maize well watered; QWS, quinoa water stress; QWW, quinoa well watered). 54

Figure 4-5: Variable fluorescence ($\Delta V_{OI} = V \text{ treatment} - V \text{ control}$) of intact leaves of the quinoa and maize control and water stress treatments normalized between 30 μ s and 300 ms respectively to obtain the curves (A) at 20°C

and (B) at 30°C. (MWS, maize water stress; MWW, maize well watered; QWS, quinoa water stress; QWW, quinoa well watered). 55

Figure 4-6: Changes in the (A) F_o , (B) F_m and (C) F_v/F_m parameters of PSII relative to the control treatments of both the water- stressed quinoa and water- stressed maize grown at 20°C and 30°C. Chlorophyll *a* fluorescence measurements were taken when the volumetric moisture content reached $0.01 \text{ m}^{-3}.\text{m}^{-3}$. (MWS, maize water stress; MWW, maize wellwatered; QWS, quinoa water stress; QWW, quinoa well watered). 56

Figure 4-7: Fractional changes in selected functional and structural parameters of PSII relative to the control treatments of both the water- stressed quinoa and water- stressed maize grown at 20°C and 30°C. Chlorophyll *a* fluorescence measurements were taken when the volumetric moisture content reached $0.01 \text{ m}^{-3}.\text{m}^{-3}$. The treatments were normalized according to their relevant controls and plotted on a multi parametric radar plot. (MWS, maize water stress; MWW, maize well watered; QWS, quinoa water stress; QWW, quinoa well watered). 58

Figure 4-8: Changes in selected functional and structural parameters of PSII relative to the control treatments of both the water- stressed quinoa and water- stressed maize grown at 20°C and 30°C. (A) Changes over time in Dlo/RC ; the energy flux for dissipation in the form of heat of both water- stressed quinoa and maize. (B) Changes over time in $y_{RC}/(1- y_{RC})$; the amount of electrons absorbed per RC. (C) Changes over time in $\phi_{Po}/(1- \phi_{Po})$; the maximum quantum yield of primary photochemistry. (D) Changes over time in $\psi_{Eo}/(1- \psi_{Eo})$; the efficiency of a trapped exciton to move an electron into the electron transport chain further than Q_A^- . (E) Changes over time in $\delta_{Ro}/(1- \delta_{Ro})$; the efficiency with which an electron from the intersystem electron carriers moves to reduce end electron acceptors at the PS1 acceptor side. Chlorophyll *a* fluorescence measurements were taken when the volumetric moisture content reached $0.01 \text{ m}^{-3}.\text{m}^{-3}$. (MWS, maize water stress; MWW, maize well watered; QWS, quinoa water stress; QWW, quinoa well watered). 62

Figure 4-9: The (A) PI_{ABS} and (B) PI_{TOTAL} values of both quinoa and maize at 20°C and 30°C compared to the declining soil moisture status (severe drought stress, soil moisture content $\leq 0.01 \text{ m}^{-3}.\text{m}^{-3}$). (MWS, maize water stress;

	MWW, maize well watered; QWS, quinoa water stress; QWW, quinoa well watered).....	64
Figure 4-10:	Kinetics of the modulated light reflection at 820 nm in dark adapted leaves under water stress (severe drought stress, soil moisture content $\leq 0.01 \text{ m}^{-3} \cdot \text{m}^{-3}$) for (A) quinoa at 20°C, (B) maize at 20°C, (C) quinoa at 30°C and (D) maize at 30°C. Comparative MR 820 nm reflection transients for (E) both quinoa and maize at 20°C and (F) both quinoa and maize at 30°C. (MWS, maize water stress; MWW, maize well watered; QWS, quinoa water stress; QWW, quinoa well watered).	66
Figure 4-11:	Parameters derived from 820 nm modulated reflection (MR_t/MR_0) in leaves of both quinoa and maize under water stress conditions over time (severe drought stress, soil moisture content $\leq 0.01 \text{ m}^{-3} \cdot \text{m}^{-3}$). (A) P700 oxidation rate of quinoa and maize at 20°C. (B) P700 oxidation rate of quinoa and maize at 30°C. (C) P700 ⁺ reduction rate of quinoa and maize at 20°C. (D) P700 ⁺ reduction rate of quinoa and maize at 30°C. (MWS, maize water stress; MWW, maize well watered; QWS, quinoa water stress; QWW, quinoa well watered).	69
Figure 4-12:	The difference between MR_0 and MR_{Min} representing the difference in the amplitudes and rise of increase of the MR820 nm signal of both quinoa and maize under water stress (severe drought stress, soil moisture content $\leq 0.01 \text{ m}^{-3} \cdot \text{m}^{-3}$) at (A) 20°C and (B) 30°C. (MWS, maize water stress; MWW, maize well watered; QWS, quinoa water stress; QWW, quinoa well watered).....	70
Figure 4-13:	The membrane leakage (%) of both quinoa and maize under water-stressed conditions (severe drought stress, soil moisture content $\leq 0.01 \text{ m}^{-3} \cdot \text{m}^{-3}$) at 20°C and 30°C. Treatment values not connected by the same letters are significantly different ($P < 0.05$). (MWS, maize water stress; MWW, maize well watered; QWS, quinoa water stress; QWW, quinoa well watered).....	71
Figure 4-14:	The relative leaf water content (%) of both quinoa and maize under water- stressed conditions (severe drought stress, soil moisture content $\leq 0.01 \text{ m}^{-3} \cdot \text{m}^{-3}$) at 20°C and 30°C. Treatment values not connected by the same letters are significantly different ($P < 0.05$). (MWS, maize water	

	stress; MWW, maize well watered; QWS, quinoa water stress; QWW, quinoa well watered).	72
Figure 4-15:	The stomatal conductance ($\text{mmol m}^{-2} \text{s}^{-1}$) of both quinoa and maize under water- stressed conditions (severe drought stress, soil moisture content $\leq 0.01 \text{ m}^{-3}.\text{m}^{-3}$) at (A) 20°C and (B) 30°C. (MWS, maize water stress; MWW, maize well watered; QWS, quinoa water stress; QWW, quinoa well watered).	73
Figure 4-16:	The chlorophyll content ($\mu\text{mol m}^2$) of both quinoa and maize under water- stressed conditions (severe drought stress, soil moisture content $\leq 0.01 \text{ m}^{-3}.\text{m}^{-3}$) at (A) 20°C and (B) 30°C. (MWS, maize water stress; MWW, maize well watered; QWS, quinoa water stress; QWW, quinoa well watered).	74
Figure 4-17:	The proline content ($\mu\text{mol.g}^{-1} \text{ FW}$) of both quinoa and maize under water- stressed conditions (severe drought stress, soil moisture content $\leq 0.01 \text{ m}^{-3}.\text{m}^{-3}$) at 20°C and 30°C. Treatment values not connected by the same letters are significantly different ($P<0.05$). (MWS, maize water stress; MWW, maize well watered; QWS, quinoa water stress; QWW, quinoa well watered).	76
Figure 4-18:	The superoxide dismutase activity ($A_{560} \text{ nm /mg protein/hour}$) of both quinoa and maize under water- stressed conditions (severe drought stress, soil moisture content $\leq 0.01 \text{ m}^{-3}.\text{m}^{-3}$) at 20°C and 30°C. Treatment values not connected by the same letters are significantly different ($P<0.05$). (MWS, maize water stress; MWW, maize well watered; QWS, quinoa water stress; QWW, quinoa well watered).	77
Figure 4-19:	The glutathione reductase activity ($\text{nmol of NADPH/ hour/ mg protein}$) of both quinoa and maize under water- stressed conditions (severe drought stress, soil moisture content $\leq 0.01 \text{ m}^{-3}.\text{m}^{-3}$) at 20°C and 30°C. Treatment values not connected by the same letters are significantly different ($P<0.05$). (MWS, maize water stress; MWW, maize well watered; QWS, quinoa water stress; QWW, quinoa well watered).	79
Figure 4-20:	The hydrogen peroxide content ($\text{mmol L}^{-1} \text{ g}^{-1} \text{ FW}$) of both quinoa and maize under water- stressed conditions (severe drought stress, soil moisture content $\leq 0.01 \text{ m}^{-3}.\text{m}^{-3}$) at 20°C and 30°C. Treatment values not	

connected by the same letters are significantly different ($P < 0.05$). (MWS, maize water stress; MWW, maize well watered; QWS, quinoa water stress; QWW, quinoa well watered). 80

Figure 4-21: (A) The above ground dry biomass (g/pot) and (B) Total leaf area (m^2/m^2) of both quinoa and maize under water- stressed conditions (severe drought stress, soil moisture content $\leq 0.01 m^{-3}.m^{-3}$) at $20^\circ C$ and $30^\circ C$. Treatment values not connected by the same letters are significantly different ($P < 0.05$). (MWS, maize water stress; MWW, maize well watered; QWS, quinoa water stress; QWW, quinoa well watered). 82

LIST OF ABBREVIATIONS

3-PGA	Phosphoglycerate
ABA	Abscisic acid
ABS	Absorption of light energy
APX	Ascorbate peroxidase
CAT	Catalase
CO ₂	Carbon dioxide
ET ₀	The conversion of excitation energy
F _M	Maximum fluorescence
F ₀	Initial fluorescence
GR	Glutathione reductase
GSSG	Oxidized glutathione
GSH	Reduced glutathione
H ₂ O ₂	Hydrogen peroxide
LEA	Late embryogenesis abundant
LHC II	Light-harvesting complex II
MAPKs	Mitogen-activated protein kinases
MR	Modulated reflection
MR _{Min}	Minimum of modulated 820-nm reflection intensity
MR ₀	Modulated 820-nm reflection intensity at Time "0"
MWS	Maize water stress

MWW	Maize well-watered
NADPH	Nicotinamide adenine dinucleotide phosphate
NAD-ME	NAD-malic enzyme
NADP-ME	NADP-malic enzyme
P5C	Pyrroline 5-carboxylate
P700 ⁺	Photosystem I primary donor
P680 ⁺	Photosystem II primary donor
PC ⁺	Plastocyanin
PAR	Photosynthetic active radiation
PEP	Phosphoenolpyruvate
PEPC	Phosphoenolpyruvate carboxylase
PEPCK	Phosphoenolpyruvate carboxykinase
Pheo	Pheophytin
PSI	Photosystem I
PSII	Photosystem II
PI _{TOTAL}	Performance index for energy conservation from exciton to the reduction of PSI end acceptors
PI _{ABS}	Performance index for energy conservation from exciton to the reduction of intersystem electron acceptors
PQ	Plastoquinone
RC	Reaction complex
RE ₀	Reduction of end electron acceptors

ROS	Reactive oxygen species
Rubisco	Ribulose-1, 5-bisphosphate carboxylase oxygenase
SOD	Superoxide dismutase
TLA	Total leaf area
TR ₀	Trapping
Q _A	Quinone A
Q _B	Quinone B
QWS	Quinoa water stress
QWW	Quinoa well-watered
RWC	Relative water content
OEC	Oxygen evolving complex
V _{ox}	P700 and PC oxidation velocity (maximum slope decrease of MR _i /MR ₀)
V _{red}	P700 and PC re-reduction velocity (maximum slope increase of MR _i /MR ₀)

CHAPTER 1 INTRODUCTION

It is no secret that abiotic stress is one of the main causes of crop loss, resulting in a worldwide yield loss of more than 50% (Hinojosa *et al.*, 2018). In recent years, the process of photosynthesis has been under an enormous amount of pressure due to an ever- changing climate. Consequently, these changes can cause a reduction in the photosynthetic pigments and components thereby diminishing the activities of the Calvin cycle and eventually, causing yield reductions (Farooq *et al.*, 2009). Today, drought is one of the most critical threats to the world food security and South Africa is of no exception. As a water scarce country, South Africa frequently experiences high temperatures and droughts (Vogel and van Zyl, 2016; Baudoin *et al.*, 2017). In South Africa, maize is considered as a crucial crop, as it is used as the main staple food and feed grain by the majority of South Africans (DAFF 2016, Mangani *et al.*, 2019). Globally South Africa is ranked ninth in terms of maize production (Estes *et al.*, 2013), with nearly 60% of the agricultural land comprised of maize cultivation (Mangani *et al.*, 2019).

On average, nearly 10.2 million tons of maize is produced annually of which 8 million tons of the production is used either for food or as feed for livestock (FAO, 2012). Mpumalanga, the Free State and the North West provinces are considered as the main maize production areas in South Africa, contributing between 21% and 39% of the total maize production in the 2011/2012 season (South African Grain Quality, 2011). These areas also experience mid-summer droughts, which vary from season to season and are hard to predict (Mangani *et al.*, 2019). Maize is also highly susceptible to changes in precipitation and temperature and as a result, climate change may have detrimental effects on its yield (Benhin, 2006; Durand, 2006; BFAP, 2007).

Throughout the 2015/2016 growing season, however, South Africa experienced one of the worst droughts yet recorded which coincided with heat waves. The production of maize decreased by 24.3% compared to the 2013/2014 growing season (DAFF, 2016). According to climate predictions these extreme weather conditions are expected to increase in the near future. Additionally, the human population is predicted to reach 9 billion within the next decades (Ziervogel *et al.*, 2014). Therefore, leaving an urgent

need for food production to increase despite the limited availability of cultivable land and water (Ruiz *et al.*, 2014).

As plants are immobile and cannot migrate to escape extreme climatic conditions, they have to develop mechanisms to either avoid or tolerate these adverse climatic conditions (Iqbal *et al.*, 2018). To survive adverse environmental conditions, plants adapted morphological, anatomical, physiological, biochemical and molecular strategies to survive (Solanki and Sarangi, 2014). Biochemically plants produce osmoprotectants such as, proline, which accumulates naturally in many plant species. Proline can also be produced as one of the major organic osmolytes during abiotic stress, such as drought, thereby behaving as a protective mechanism (Oukarroum *et al.*, 2012a). Other antioxidants include superoxide dismutase (SOD) and glutathione reductase (GR) and are key in protecting plant cells from the adverse effects of reactive oxygen species (ROS). For plants to perform vital cell functions the generation and metabolism of ROS must be well maintained and this is usually compromised during drought or high temperatures (Iqbal *et al.*, 2018).

To mitigate the negative impacts of climate change on agriculture, crops are needed that are able to acclimatize in an ever- changing climate (Jacobsen *et al.*, 2012; Ruiz *et al.*, 2014). This can be achieved through crop diversification, away from the overreliance on staple crops; therefore, species that are underutilized can also play an important role in agro-biodiversity (Kahane *et al.*, 2013; Yang *et al.*, 2016). The introduction of quinoa in Africa and more specifically South Africa could further advance the agricultural sector, and at the same time improve food security (Jacobsen *et al.*, 2003). Quinoa has the ability to tolerate various environmental stressors, for example, drought, frost and heat with temperatures ranging between -4 to 38°C and soils with a pH ranging from 4.8 to 9.5 (Jacobsen *et al.*, 2003; Gonzáles *et al.*, 2015). Additionally, quinoa can also grow in semi-desert conditions whilst producing seed in areas such as Chile, the arid mountain regions of Argentina and in the Altiplano area of Peru and Bolivia (Gonzáles *et al.*, 2015). These areas are extremely arid and have an annual rainfall of less than 200 mm. Acceptable yields were also produced in areas, for example, the Mediterranean, Asia, North Africa and the Near East (Gonzáles *et al.*, 2015). The ability of quinoa to be cultivated in arid environments makes it an excellent alternative crop in the face of climate change (Jacobsen *et al.*, 2012; Miranda-Apodaca *et al.*, 2018).

Understanding the physiological acclimation mechanisms that establish tolerance in quinoa is required to know how to utilize it as a crop (Jacobsen, 2011; Ruiz *et al.*, 2014). An effective way to evaluate the vitality of crop growth and performance is by using rapid and non-invasive techniques, for example chlorophyll *a* fluorescence, which demonstrates the operating quantum efficiency of electron transport through photosystem II (PSII) in the leaves (Strasser *et al.*, 2004). The effect of drought stress on PSII has been investigated widely (Oukarroum *et al.*, 2012a). Chlorophyll *a* fluorescence can provide vital information regarding the ability of a plant to acclimate to environmental stresses and to which degree those stresses can damage the photosynthetic apparatus (Maxwell *et al.*, 2000; Percival *et al.*, 2006; Chen *et al.*, 2016).

Since maize is a C₄ plant, it is expected that it would be less susceptible to photo-inhibition and photo-damage under water stress conditions when compared to quinoa, a C₃ species. However, various authors concluded that limitations caused by stomatal closure are more pronounced in C₄ species than in C₃ species (Wand *et al.*, 2001; Killi *et al.*, 2017), therefore leaving cause to believe that when exposed to water stress, C₃ species have the ability to perform equally or even more efficiently than C₄ species. Currently there is a shortage of comparative information available regarding the effect of abiotic stressors on the physiological acclimation of both C₄ and C₃ species. Furthermore, there is also a shortage of data available regarding the relation of the photosynthetic efficiency of quinoa and its ability to synthesis osmolytes or antioxidants under water- stressed conditions. Quinoa is one of the few crops with the innate ability to tolerate drought conditions based on its low water requirements, high photosynthetic efficiency and increased osmoprotectant content (Zurita *et al.*, 2015). On the other hand, severe water stress conditions tend to decrease the photochemical activity of maize drastically (Liu *et al.*, 2018).

As a result, this study is focused on comparing the different physiological acclimation strategies used by both quinoa and maize when subjected to water deficit stress. This was done by investigating the photosynthetic efficiency, proline production as well as the production of antioxidants of both quinoa and maize while subjected to water stress. In addition, both crops were grown at two different temperature regimes, 20°C and 30°C. Generally, quinoa is described as a summer crop with ideal growth temperatures of between 16°C and 20°C (Bertero *et al.*, 1999; Jacobsen *et al.*, 2003), whereas maize

grows optimally in temperatures between 25°C and 30°C (Farooq *et al.*, 2008). By evaluating the growth and response of both crops at 20°C and 30°C it could be determined whether differences in temperature will influence the acclimation strategy under water deficit stress.

1.1 The aim of this study

As quinoa is one of the few crops with the ability to grow in arid environments, the aim of this study is to investigate the acclimation strategy of both quinoa and maize subjected to water stress, by means of comparing the photochemical potential of quinoa and maize as well as the successful production of selected osmoprotectants.

1.2 The objectives of the study

- To investigate the acclimation potential of both quinoa and maize subjected to water stress.
- The use of prompt fluorescence and modulated 820 nm reflection to quantify the effects of water stress on the photochemical potential of both quinoa and maize.
- Investigating the relationship between the production of osmolytes (such as proline, superoxide dismutase and glutathione reductase) and the photosynthetic efficiency of both quinoa and maize subjected to water stress.
- Probing the biomass and leaf area reduction of both quinoa and maize under water- stressed conditions.

1.3 Hypothesis

Quinoa has a better acclimatization potential to water stress when compared to maize. This is due to the fact that quinoa possesses a higher osmoprotectant activity and photochemical potential when compared to maize, especially under water deficit conditions.

1.4 Thesis layout

This thesis conforms to the guidelines set for a standard thesis at the North-West University. This thesis includes seven chapters. A selection of the results has been submitted in article format to the Journal of Integrative Agriculture for possible publication. References cited in the text are included in the list of references at the end of the thesis. Abbreviations are defined in each chapter.

- Chapter 2
 - A detailed literature review related to the title of this study. Topics discussed include the acclimation of plants to water and high temperature stress, the production and activity of selected osmoprotectants and the morphology and growth of quinoa.
- Chapter 3
 - A detailed description of the materials and methods used in this study. This includes prompt fluorescence, modulated 820 nm reflection and the extraction and determination of selected osmoprotectant. In addition, the stomatal conductance, chlorophyll content, relative water content, membrane leakage and biomass methods has been described in detail.
- Chapter 4
 - All results generated during this study. This includes prompt fluorescence, modulated 820 nm reflection and the extraction and determination of selected osmoprotectant.
- Chapter 5
 - A detailed discussion regarding the results chapter. In short, how quinoa and maize were able to acclimatize to water deficit stress.
- Chapter 6
 - Concluding remarks.
- Chapter 7
 - Recommendations and future studies.

CHAPTER 2 LITERATURE STUDY

2.1 Quinoa

Quinoa pronounced as “kiuna” or “kinwa” in the Quechua language, belongs to the genus *Chenopodium* and is identified as an annual dicotyledonous crop. Scientifically quinoa is known as *Chenopodium quinoa* Willd (Wilson, 1990; Hinojosa *et al.*, 2018).

Geographically, quinoa can be found naturally from the south-central coast of Chile (43°S) to the southern parts of Colombia (2°N), stretching to the north-western region of Argentina and to the subtropical region in Bolivia (Ruize *et al.*, 2014). However, this crop was originally domesticated and cultivated close to Lake Titicaca in the southern parts of Peru and Bolivia almost 5000 years B.C. (Tapia, 1997). Archaeological evidence revealed that quinoa was cultivated alongside maize during the ancient Inca times (Zurita *et al.*, 2014). The quinoa seed served as a staple food in the Incan diet and was considered as a sacred plant (González *et al.*, 2015). This however, changed during the Spanish colonization in 1532 where the consumption and cultivation of other cereal crops (mainly maize) were enforced, thereby repressing the cultivation of quinoa (Tapia, 2009). In spite of this, the Andean people preserved this crop for centuries, therefore ensuring the conservation of the quinoa germplasm *in situ* (González *et al.*, 2015). However, during the green revolution massive setbacks in crop production were caused by severe droughts, but due to quinoa’s resilience to the harsh climatic conditions in the Andean region, the production of quinoa was restored (Cusack, 1984; Bhargava *et al.*, 2007). As a result of the cultural practices of the Andean people for preserving quinoa in its natural state, the United Nations General Assembly declared 2013 as the “International Year of Quinoa” (FAO, 2013). As of recently, quinoa has been introduced in Asia, Europe, North America and Africa (Jacobsen *et al.*, 2003; Ruiz *et al.*, 2014).

This crop has been widely cultivated and introduced to a variety of environments with altitudes ranging from sea levels to altitudes between 2000 and 4000 m (Pulvento *et al.*, 2010). As a result, five different ecotypes have been classified based on the geographic distribution and adaptation of quinoa (Figure 2-1) (Ruiz *et al.*, 2014; Tapia, 2015; Hinojosa *et al.*, 2018). The first is the “Valley” quinoa which grows at altitudes ranging

between 2000 and 3000 meters above sea level (m.a.s.l.). Valley quinoa is late-ripening, with plant heights reaching 150 to 200 cm and can be found in Colombia, Ecuador, Peru, and Bolivia. Second is the “Altiplano” quinoa, which grows in areas with altitudes higher than 3500 m.a.s.l. and are generally found around the Titicaca Lake on the border of Bolivia and Peru. Altiplano quinoa has the ability to resist severe frost and a low rainfall. Thirdly, the “Salares” quinoa can tolerate soils with a high salinity and is found in the salt flats of Bolivia and Chile (Ruiz *et al.*, 2014). Fourth is the low-altitude, sea level quinoa. These plants are commonly small (near 100 cm) with a small number of stems and they produce bitter grains. The Salares quinoas are also found in the southern and central areas of Chile. Lastly the subtropical quinoa can be found in the low-altitude, humid valleys of Bolivia. These plants tend to have small white or yellow grains (Ruize *et al.*, 2014; González *et al.*, 2015).

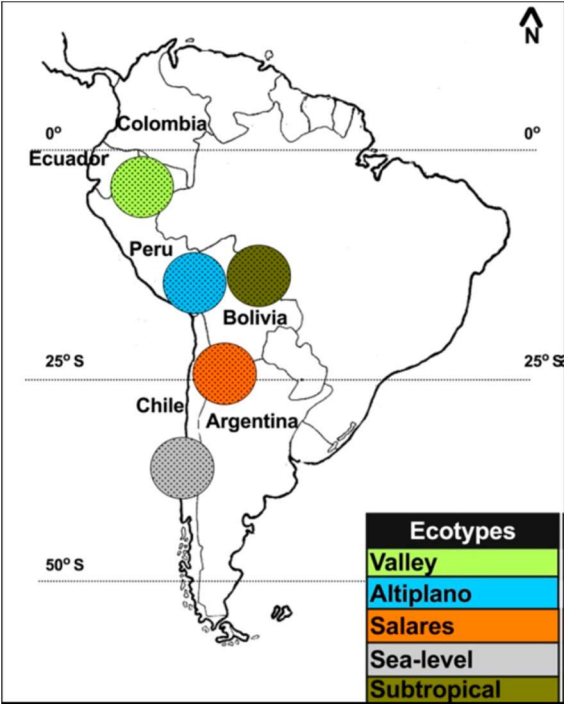


Figure 2-1: The five quinoa ecotypes and their geographic distribution (Hinojosa *et al.* 2018).

The quinoa species is naturally highly diverse with various different traits, for example, seed size, seed colour, inflorescence type, life-cycle duration, saponin content and salinity tolerance, therefore allowing quinoa to acclimate to various environments. All of

these different traits allow quinoa to adapt to several marginal agricultural soils and climatic conditions (Ruiz *et al.*, 2014; Hinojosa *et al.*, 2018).

Morphologically quinoa is a dicotyledonous annual herbaceous plant that ranges in height between 0.1 to 2 m tall depending on the environmental conditions and genotype (Geerts *et al.*, 2008). The taproot can range from 20 to 50 cm long and is lavishly branched, therefore forming a dense web of roots that can penetrate to approximately the same depth as the plant height (González *et al.*, 2015). Quinoa has alternating broad lobed leaves attached to a woody central stem (Mujica, 1994). The leaves are usually powdery, rarely smooth and depending on the species, can range in colours from green, purple and red, which occurs due to the varying betacyanin content. It has a straight stem which ends with a panicle containing small flowers (Figure 2-2). Panicles can also develop from the leaf junction on the stem (Mujica, 1994).

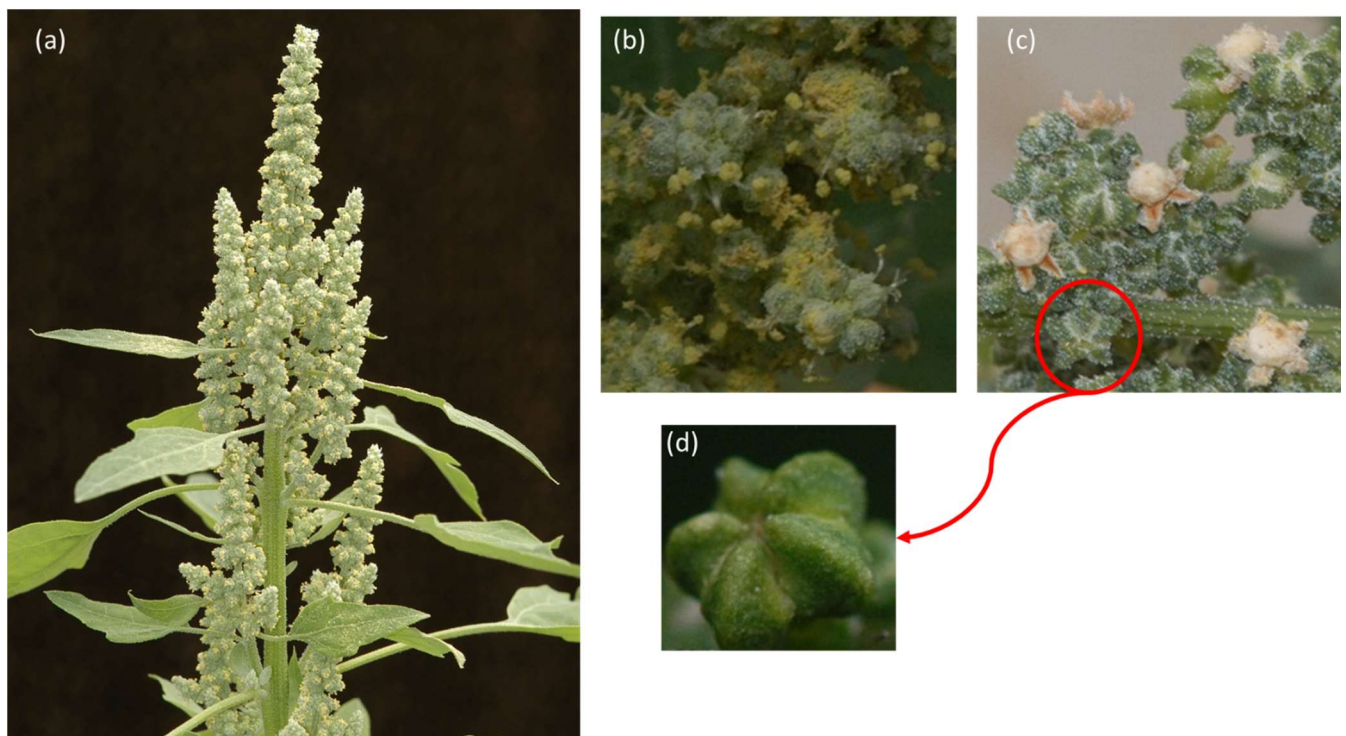


Figure 2-2: (a) The panicle of quinoa; (b) Opened flowers with anthers and pollen (c) White quinoa seeds contained within the flower; (d) An unopened flower bud (Photos provided by William Weeks, 2018).

Quinoa has hermaphrodite, pistillate, or male sterile flowers which are positioned at the distal end. These flowers can vary in sizes (± 1 mm in diameter) and weight (± 2 mg)

(Geerts *et al.*, 2008). The wide colour spectrum also extends to the vegetative organs and perigonium which in turn results in colourful inflorescences. These colours often range from orange, yellow, white, black and reddish-brown (Jacobsen and Stolen, 1993). The seeds are to some extent flat and measures to 1–2.6 mm. The pericarp of the seeds may often also contain saponins. As with the inflorescence, the seeds can also vary in size and colour between the different varieties. In general, black seeds are more dominant compared to the yellow, white and red seeds (Mujica, 1994).

Depending on the variety, the vegetative period of quinoa can vary between 120 and 240 days and is related to the photoperiod sensitivity. Some varieties from Chile can have a vegetative period ranging from 110 to 120 days (González *et al.*, 2015; Sosa-Zuniga *et al.*, 2017). Quinoa has nine principle growth stages (Sosa-Zuniga *et al.*, 2017). The first stage involves the emergence of the photosynthetic leaves attached to the main stem (Figure 2-3). Typically, the leaves emerge in pairs and are visible once the two leaves separate from each other. During the second stage, side shoots start to form (considered visible when 1 cm or more in length) and depending on the genotype, it will start to emerge before or after the formation of the inflorescence. The third stage involves the elongation of the stem and occurs simultaneously with leaf growth, side shoot development, inflorescence formation and flowering. The fourth stage includes the development of the harvestable vegetative parts (Sosa-Zuniga *et al.*, 2017).

During the fifth stage, the inflorescence develops fully in the main shoot. At emergence the inflorescence is covered by younger leaves and is not visible, but once elongation occurs, the inflorescence becomes visible. This stage concludes once the inflorescence is exposed and not covered with leaves. Next (stage six) the flowers start to develop within the main inflorescence and depending on the variety, the colour of the inflorescence could start to change (Sosa-Zuniga *et al.*, 2017). As flowering progresses, the perigone will change colour and once all visible anthers senesced, flowering is completed. Fruit development will occur next (stage seven) and starts when the ovary thickens and the first grains are visible. Stage eight refers to the ripening of the grains, during which the colour of the pericarp changes from green to either, yellow, white, red or black. Grains are considered ripe when it is difficult or impossible to crush it and it has a dry content. The last stage (nine) involves plant senescence. The first

senescence starts with the basal leaves and continues upwards. Once all leaves are dead the stem will finally start to senesce (Sosa-Zuniga *et al.*, 2017).

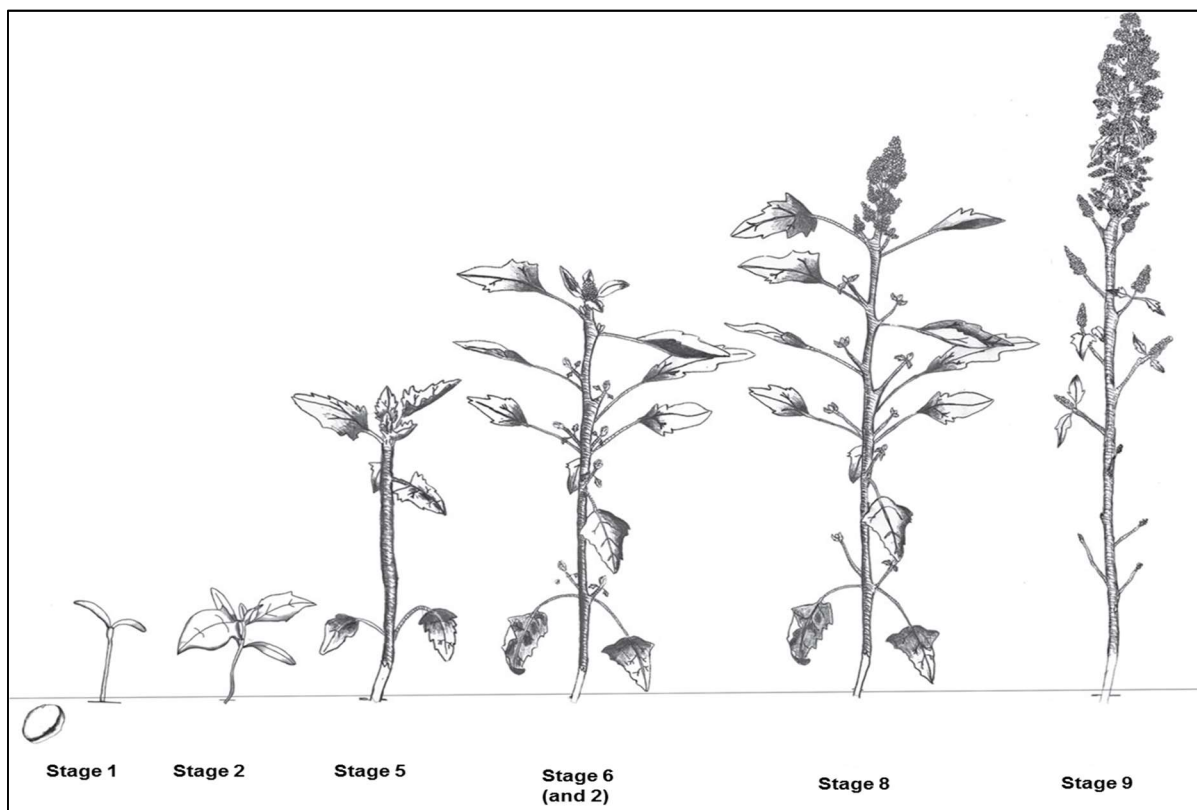


Figure 2-3: Phenological growth stages of quinoa (*Chenopodium quinoa*) (Sosa-Zuniga *et al.*, 2017).

Ideally, quinoa prefers well-drained semi- deep soils with a supply of nutrients. It thrives well in sandy–loamy soils containing organic material. Depending on the ecotype, quinoa is also capable of growing in acidic soils with a pH of 4.5, commonly found in Peru or alkaline soils with a pH of 9.5 as found in Bolivia (Mujica, 1994). Acceptable yields are also easily obtained in both sandy and clay soils. Ideal sowing conditions for quinoa seeds are at a depth of 1 to 2 cm with a minimum temperature of 8°C and 10°C and an approximate relative humidity of 60%. In the vegetative phase, quinoa can tolerate temperatures of -5°C depending on the ecotype. Some varieties have the ability to grow in temperatures of -8°C and still survive for 20 days (Mujica, 1994).

The required temperature for good growth is between 16°C and 22°C and a photoperiod of 10 to 12 hours (short day length) is needed as quinoa is sensitive to low photoperiods

(Bertero *et al.*, 1999; Jacobsen *et al.*, 2003). Depending on the ecotype the precipitation requirements for quinoa can vary from 250 mm (salt plains) to 1500 mm in the humid Andean valleys. According to Geerts *et al.* (2008), quinoa only requires 50 to 70 mm of precipitation during germination, flowering and seed formation. Though quinoa shows strong tolerance to drought, it needs adequate soil moisture during the start of cultivation (Lanino, 2006; Geerts *et al.*, 2008). During drought spells, the application of organic material with a low phosphorus and nitrogen fertilization can increase quinoa yields. Care should be taken during fertilization since the application of high levels of phosphorus and nitrogen could decrease the quinoa yields. The decrease in yields is usually caused by intense lodging and a delay in flowering and seed formation (Oelke *et al.*, 1992; Bhargava *et al.*, 2003).

Quinoa has also been recognized as a halophyte crop and when compared to crops, such as, barley, wheat and maize, it has a greater tolerance to salt stress (Gunes *et al.*, 2007; Peterson and Murphy, 2015). Generally, it has been speculated that the quinoa genotypes from the Bolivian Salares had a high salt tolerance; however, later various other quinoa genotypes have been described as salt tolerant. The wild relative of quinoa (*Chenopodium hircinum*) was reported as having a much higher tolerance to salt compared to the quinoa varieties (Orsini *et al.*, 2011; Schmöckel *et al.*, 2017). For this reason, it was found that the tolerance of quinoa towards salt stress does not relate to the geographical distribution of varieties. The reason being that varieties outside of the Salares ecosystem were found to have an equivalent or even higher tolerance to salt stress (Schmöckel *et al.*, 2017; Hinojosa *et al.*, 2018).

2.2 The acclimation strategy of plants to abiotic stress

Plants tend to respond to different abiotic stresses by using complex mechanisms which includes genetic molecular expressions and changes in the biochemical metabolism. For example, plants can escape stress by completing their life cycles earlier; developing more extensive root systems; enhancing their osmotic adjustment; altering metabolic pathways; leaf shedding and biochemical traits for plant evolution (Xu *et al.*, 2010). These changes can also occur simultaneously in response to abiotic stress.

2.2.1 Acclimation strategy of crops to drought

Plants tend to acquire different response mechanisms to counteract the effects associated with drought stress. These mechanisms can be grouped as, morphological strategies, physiological strategies and molecular strategies (Farooq *et al.*, 2009). Morphological strategies include the formation of deeper root systems, whereas physiological strategies involve antioxidant defences, plant growth regulation, cell membrane stability, regulated stomatal closure and osmotic adjustment (Farooq *et al.*, 2009; Hinojosa *et al.*, 2018).

To understand the effect of water stress on quinoa several studies have been conducted. One of the common responses of plants to water deficit stress is stomatal closure. Generally, an increase in the concentration of root abscisic acid (ABA) will reduce the turgor pressure in the stomata guard cells effectively closing the stomata (Jacobsen *et al.*, 2009; Coccozza *et al.*, 2013; Yang *et al.*, 2016). In addition, it was found that the ABA present in the xylem accumulated faster in the shoots compared to the roots during water stress.

Another drought response mechanism in plants is the synthesis of osmolytes, which actively scavenges for reactive oxygen species (ROS). This is an antioxidant defence mechanism and it involves the raffinose and ornithine pathways along with the accumulation of proline or soluble sugars which amongst other things are known to adjust the cellular osmotic potential (Bascunan-Godoy *et al.*, 2016; Muscolo *et al.*, 2016). Additionally, photosynthesis is also inhibited under drought stress conditions. This will usually result in an excess of excitation energy with the potential for photoinhibition to occur. Plants can alleviate or avoid damage to the photosystems via non-photochemical quenching, where radiant energy is dissipated as heat in the light harvesting antenna of photosystem II (PSII) (Yordanov *et al.*, 2000).

In addition, rapid stomatal closure reduces water loss, regulates cellular water deficit as well as the root to shoot ratios, thereby ensuring a higher water use efficiency (Bosque *et al.*, 2003; Jacobsen *et al.*, 2009; Killi and Haworth, 2017; Miranda-Apodaca *et al.*, 2018). Due to quinoa's low water requirement it has the innate ability to cope with water stress, and moreover to resume its former photosynthetic activity after a period of drought stress (Jacobsen *et al.*, 2009). Jensen *et al.* (2000) observed that the altiplano

quinoa variety was insensitive to water stress according to its stomatal response during the early growth stages. This could be justified by the fact that a specific leaf area and a high photosynthetic rate could support water uptake by larger root systems during the early growth stages, this will help to counteract drought at a later stage.

Delayed growth is another drought response mechanism of plants and this was apparent when a delayed growth was documented for quinoa between the fifth and sixth growth stages (Greets *et al.*, 2008). Prasad *et al.* (2011) demonstrated that water stress inhibited the grain weight, pistillate flower development and ovule functions of wheat. This was brought on by a decrease in the photosynthetic rate in response to stomatal closure (Reddy *et al.*, 2004). However, according to González *et al.* (2015) certain quinoa varieties which only receive 160 mm of rain in the growing season, displayed higher stomatal conductance levels while maintaining a high photosynthetic rate.

Lastly, the relationship between soil moisture and the root system has been studied in quinoa. Quinoa has a high water use efficiency which is evident by its ability to grow in soils lacking soil moisture while producing acceptable yields (Garcia *et al.*, 2003; Bertero *et al.*, 2004). Quinoa can tolerate up to three months of water deficit stress during the vegetative growth stage in which the stalk becomes fibrous and the roots strengthen (National Research Council, 1989). Compared to other crops, quinoa has the ability to produce roots faster along with rapid root elongation and branching which advances its foraging capacity (Alvarez-Flores *et al.*, 2013). A study recently conducted both in a dry habitat and a rainy habitat reported that the quinoa varieties grown in the dry habitat displayed accelerated root growth longer, coarser, and more roots compared to the rainy habitat variety (Hinojosa *et al.*, 2018). As a result, quinoa escapes the harmful effects caused by drought via the development of deep root systems, a reduced leaf area, stomatal closure, leaf dropping, small and thick-walled cells, which adapt to water loss while maintaining the turgor pressure (Jensen *et al.*, 2000; Adolf *et al.*, 2013).

2.2.2 Acclimation strategy of crops to temperature

Heat stress can be described as the increase in air temperature above the optimum growth temperature for an extended time causing reduced growth and development and finally cellular damage (Wahid *et al.*, 2007). Depending on the current growth stage of

the plants and the duration of the stress applied, plants tend to respond differently to heat stress (Prasad *et al.*, 2017). Heat stress can affect a plant in three ways. The first is morphological, for example a delay in the root and shoot growth with increased stem branching. Secondly, anatomical changes can occur, which include reduced cell size as well as an increase in the trichome and stomata densities. Thirdly, physiological changes can occur which can cause increased membrane leakage, protein denaturation, osmolyte accumulation, mitochondrial and chloroplast enzyme inactivation and changes in respiration and photosynthesis (Wahid *et al.*, 2007; Bitá and Gerats, 2013; Hinojosa *et al.*, 2018).

A change in the stomatal conductance of plants is one of the primary and rapidly occurring events during heat stress. These changes aim to regulate the flow of carbon dioxide (CO₂), water loss and leaf temperature (Zandalinas *et al.*, 2018). Generally, heat will cause an increase in the stomatal conductance so as to cool down the leaves via transpiration, whereas drought stress prevents any water loss (Mittler and Blumwald, 2010). Maintaining the leaf temperature during heat stress is imperative for tolerance to heat stress. In studies where tobacco plants were exposed to heat and drought stress, the leaf temperature was significantly higher compared to plants only subjected to heat stress. The increasing leaf temperature was therefore, caused by a lower stomatal conductance induced by the water stress (Rizhsky *et al.*, 2002).

Similar to drought stress, heat stress can also induce ROS and when present in high concentrations can be severely toxic. The production of osmolytes and antioxidants can reduce the increased accumulation of ROS. On the other hand, lower levels of ROS can act as signalling molecules, activating processes such as programmed cell death (Wahid *et al.*, 2007; Awasthi *et al.*, 2015). Depending on the variety and the growth stage, quinoa can tolerate a broad range of temperatures ranging between -8°C and 35°C and a relative humidity between 40% and 88% (Jacobsen *et al.*, 2005). Regardless of quinoas tolerance to heat stress, high temperatures during flowering and seed production can, however, reduce the yield production significantly (Geerts *et al.*, 2008; Bazil *et al.*, 2016; Eisa *et al.*, 2017). A high temperature during anthesis can also reduce the diameter of the seeds (Bertero *et al.*, 1999) and cause pollen sterility (Hunziker, 1943). Barnabas *et al.* (2008) concluded that the reproductive tissue of plants is more sensitive to heat stress compared to the vegetative tissue. Prasad *et al.*

(2011) also observed that heat stress affected the pollen fertility and grain number of wheat.

On the other hand, quinoa can also tolerate low temperatures of -8°C , however, temperatures lower than this can induce oxidative stress and when accompanied by ROS can result in cold-induced photo-inhibition. Additionally, frost causes visible damage on plants leading to foliar senescence (Cui *et al.*, 2003; Rapacz *et al.*, 2004; Bois *et al.*, 2006; Winkel *et al.*, 2009). Low temperatures during the night combined with high solar irradiance during the day can result in stunted growth and a long term reduction in photosynthesis. Colder temperatures will generally also delay seed germination, radicle elongation and seedling growth (Rosa *et al.*, 2004).

2.3 Comparing C₃ species to C₄ species subjected to stress

Since maize is a C₄ plant, it is expected that it would be less susceptible to photo-inhibition and photo-damage under water stress conditions when compared to quinoa, a C₃ species. In general, C₄ species, for example, sugarcane, maize and sorghum have remarkably higher photosynthetic levels compared to C₃ species, for example, rice, wheat (Kajala *et al.*, 2011) and quinoa (Gonzales *et al.*, 2015). This is as a result of the different morphological, anatomical and biochemical mechanisms existing in C₃ and C₄ species which are used during carbon fixation (Guidi *et al.*, 2019). In general, the Calvin-Benson cycle is practically used by all plants for the fixation of CO₂, including C₃ species (Sage *et al.*, 2014; Guidi *et al.*, 2019). During C₃ photosynthesis ribulose-1, 5-bisphosphate carboxylase oxygenase (Rubisco) catalyses the formation of phosphoglycerate (3-PGA), which is a three-carbon compound, therefore, referred to as the C₃ cycle (Figure 1-4) (Reddy *et al.*, 2010). This process occurs inside the chloroplasts of mesophyll cells. One of the common difficulties with the C₃ cycle is that rubisco is used to catalyse two opposing reactions namely carboxylation and oxygenation, (Portis and Parry, 2007). Therefore, if the oxygenation pathway is chosen, the carbon movement is directed towards the photorespiration pathway. As a result, 30% of the carbon fixed can be lost via this pathway (Long *et al.*, 2006). Abiotic stressors, such as drought and increased temperatures can result in an increase in the oxygenase reaction (Lara and Andreo, 2011).

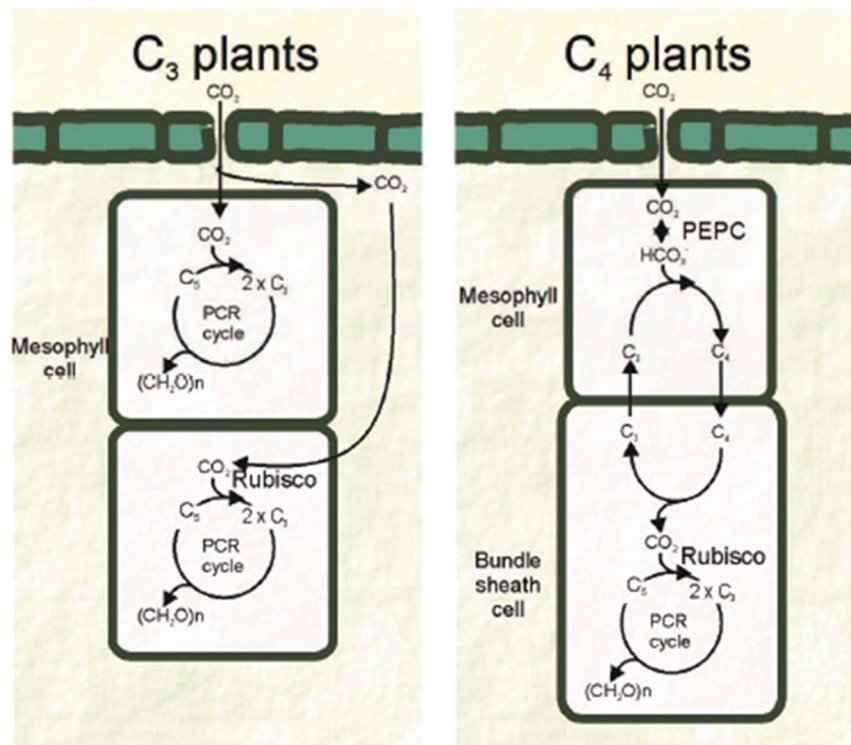


Figure 2-4: A representation of the carbon fixation pathways of C_3 and C_4 plants (Lara and Andreo, 2011).

On the other hand, the C_4 photosynthesis pathway overcomes the limitation of photorespiration by improving the photosynthetic efficiency and minimizing the water loss in warm environments (Figure 1-4) (Sage *et al.*, 2014). The C_4 photosynthetic activities are divided between the mesophyll and bundle sheath cells (both anatomically and biochemically distinct). C_4 plants utilize a biochemical CO_2 pump that relies on the spatial separation of the CO_2 fixation and assimilation. During the carboxylation of PEP (phosphoenolpyruvate) via PEPC (phosphoenolpyruvate carboxylase), four carbon-containing organic acids are produced in the cytosol of the mesophyll cells (Lara and Andreo, 2011; Sage *et al.*, 2014). The C_4 compounds are then relocated to the bundle sheath cells where they are decarboxylated to form CO_2 . Thereafter, the CO_2 is assimilated via Rubisco in the Calvin-Benson cycle (Lara and Andreo, 2011). Three carbon-containing organic acids (C_3) are released in addition during the decarboxylation reaction, which returned to the mesophyll cells to regenerate PEP via the enzyme pyruvate orthophosphate dikinase (PPDK) (Sage *et al.*, 2014). In this manner a CO_2 -concentrating mechanism is formed around Rubisco. Therefore, by elevating the CO_2

concentration at the site of Rubisco, photorespiration is suppressed in C₄ plants, because the activity of the oxygenase reaction is considerably reduced (Uzilday *et al.*, 2014).

By adopting this approach, C₄ species are able to increase the efficiency of energy consumption by means of energy conservation. Following this approach, C₄ species have the ability to maintain a higher photosynthetic performance and water use efficiency compared to C₃ species (Majeran *et al.*, 2010). Various authors speculated that over time the atmospheric CO₂ declined, which in turn induced changes in the CO₂ concentrating mechanism of C₄ species (Ehleringer *et al.*, 1991; Guidi *et al.*, 2019). Therefore, allowing C₄ species to preserve a larger diffusion gradient for CO₂. As a result, C₄ species can function at a lower conductance than C₃ species. In this way, C₄ species reduce water loss via transpiration and as a result ensuring a higher water use efficiency (Long, 1999).

In addition, C₄ species are also classified into different subtypes based on the different C₄ metabolic adaptations used by the species (Guidi *et al.*, 2019). The three subtypes are NADP-malic enzyme, NAD-malic enzyme and PEP carboxykinase (Hatch, 1987; Guidi *et al.*, 2019). These features assist C₄ plants to tolerate high temperatures and light intensities. As a result, C₄ plants will typically be found in warmer subtropical regions (Moore *et al.*, 2014). Additionally, these traits assist C₄ plants to maintain a higher growth and photosynthetic rate under high light and temperature conditions. This is achieved by a greater availability of water and an efficient use of nitrogen and carbon (Edwards *et al.*, 2010; Sage *et al.*, 2014). As C₄ plants are normally found in warm areas, they seldom occur in cooler environments as their distribution is associated to the amount of rainfall in certain areas (Ghannoum *et al.*, 2011; Lara and Andreo, 2005). C₄ photosynthesis tends to function poorly in colder environments. This could be due to the limited competency of Rubisco at colder temperatures (Kubien *et al.*, 2003). On the other hand, C₃ plants have increased photosynthetic activities compared to C₄ plants in cooler environments (Sage and McKown, 2006).

Compared to C₃ species it can be expected that C₄ species would be less susceptible to photo-inhibition and photo-damage when exposed to drought, high or low temperatures and high soil salinity levels. In most cases, these stressors would lead to an excess of

energy, which is absorbed by the leaves relative to altered CO₂ assimilation in C₄ plants. Various authors, however, questioned the truth of this reasoning (Guidi *et al.*, 2019). In agreement with this, Ghannoum (2009) questioned the lack of C₄ plant species, as it currently only represents $\pm 4\%$ of the world's total flora, while Sage and Sultmanis (2016), contemplated the lack of "C₄ forests" as the majority of forests are C₃. While their reasoning sparks for interesting conversation, there is currently a shortage of information available comparing the effect of abiotic stressors on the photosynthetic efficiency of both C₄ and C₃ species.

2.4 The role of osmoprotectants

One of the primary causes of crop loss is abiotic stress and often crops are exposed to several stresses. The severity and frequency of the abiotic stressors are increasing mainly due to a diminishing rainfall pattern and the manner in which crops respond to environmental stress seems to be overlapping (Dutta *et al.*, 2019). Often the various stressors will result in the production of ROS, signifying that a plant is under oxidative stress. Generally, ROS are produced as by-products of several metabolic pathways, though the over-production of ROS and its by-products are extremely reactive and toxic to plants, which cause oxidative stress in plants (Yousuf *et al.*, 2012). Oxidative stress causes severe damage to proteins, lipids, nucleic acids and carbohydrates, causing cell death. Alternatively, low levels of ROS, can in contrast act as signalling molecules which regulate the vital processes in plants, this includes growth, development, cell cycle, programmed death, pathogen defence, abiotic defence and systemic signalling (Dar *et al.*, 2017; Zandalinas *et al.*, 2018).

For plants to perform these vital cell functions, the generation and metabolism of ROS must be well maintained. In order to do this, plants trigger a series of biochemical events in response to abiotic stress. Tolerance to stress is granted by transcriptionally regulating specific gene families (Joshi *et al.*, 2018). Based on their function, the gene families are classified into three groups. The first group includes the genes that are involved in osmoprotection, for example, antioxidant enzymes, osmoprotectants, late embryogenesis abundant proteins and heat shock proteins (Dutta *et al.*, 2019). The second group contains the genes that are responsible for ion transport and facilitates the uptake of water. The third group involves genes responsible for signal perception

and transcriptional regulation, for example, mitogen-activated protein kinases and salt overly sensitive kinases (Ji *et al.*, 2013). Water stress is responsible for cellular dehydration which alters the cellular homeostasis. To reduce water loss, protect proteins and to maintain the integrity of cells, plants have developed different strategies to produce osmolytes (Dutta *et al.*, 2019). Some of the important osmoprotectants that accumulate in plants are proline, glycine betaine, polyols, sugar alcohols, superoxide dismutase (SOD), glutathione reductase (GR) and soluble sugars. These osmoprotectants are involved in maintaining the cellular redox potential, stabilizing membranes and proteins structures, osmotic adjustments and scavenging of ROS (Dutta *et al.*, 2019).

2.4.1 Proline

Proline is an amino acid that plays an important role both in stress defence and regulating the development and growth of a plant subjected to stress (Ahanger *et al.*, 2014). The synthesis of proline is common in most plant species under both stressed and non-stressed conditions. Typically, proline is actively involved in the formation of seeds and the development of embryos (Mattioli *et al.*, 2009). Proline also acts as a precursor for the synthesis of various enzymes and proteins (Vives- Peris *et al.*, 2017). In addition, proline has a superior conformational rigidity, which allows it to play an important role as a molecular chaperone for stabilizing protein structures (Funck *et al.*, 2012). During recovery, proline acts as a reservoir for cellular nitrogen and carbon (Kavi Kishor *et al.*, 2005).

When under stress, plants tend to accumulate a high level of proline (Per *et al.*, 2017; Mansour and Ali, 2017) where a high concentration of proline is a valuable indicator of drought injury in plants (Zlatev and Stotanov, 2005). Signorelli *et al.* (2013) found that the concentration of proline can increase up to tenfold in the leaves of *Lotus japonicas* when under drought stress. As an osmoprotectant, proline can assist plants during stress, by repairing or preventing the unfavourable effects caused by oxidative and/or osmotic stress. During extended periods of water stress, increased proline concentrations accumulate in the cytoplasm of plants. As a result, proline is actively involved in preventing oxidative stress by scavenging free radicals. In addition, it controls the redox potential and cellular homeostasis of cells (Heuer, 2003). Recent

studies, however, revealed that various important crops, including, maize, wheat and rice are not capable of synthesising the necessary levels of proline needed to counteract the damaging effects of drought stress (Slama *et al.*, 2015).

Proline is synthesised in the cytosol of plants via two pathways which include the glutamate or ornithine pathway (Suprasanna *et al.*, 2016; Zarattini and Forlani, 2017). The glutamate pathway requires two Nicotinamide adenine dinucleotide phosphate (NADPH) molecules and is completed in two enzyme dependent steps (Figure 2-5). The first step in the glutamate pathway is ATP dependent and it involves the phosphorylation of glutamate, therefore resulting in its activation (Jawahar *et al.*, 2019).

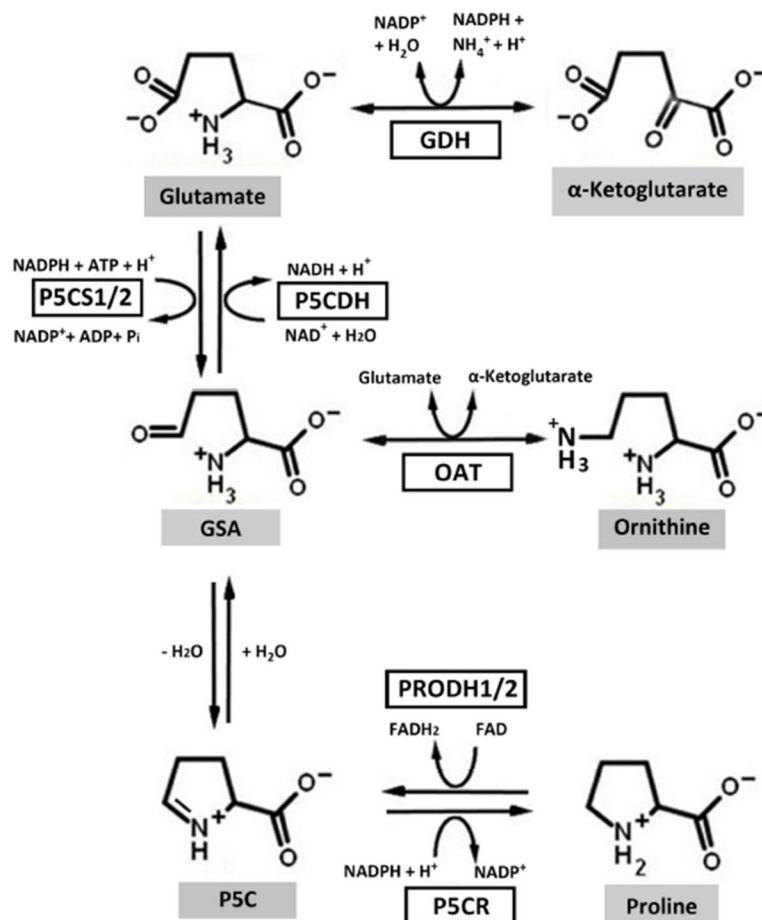


Figure 2-5: The metabolic pathways of proline in plants (Zhang and Becker, 2015).

Secondly, the activated glutamate is reduced to glutamatic-γ-glutamyl kinase following its cyclization to pyrroline 5-carboxylate (P5C). The cyclization of glutamatic-γ-glutamyl kinase to P5C is catalysed by the enzyme pyrroline 5-carboxylate synthetase. Finally,

P5C is reduced to proline via the pyrroline 5-carboxylate reductase enzyme (Dutta *et al.*, 2019).

Alternatively, ornithine is used in the ornithine pathway as the predecessor for the synthesis of proline instead of glutamate. During this pathway ornithine is transaminated to P5C and catalysed by Orn-D-aminotransferase. Thereafter, P5C is reduced to proline by the enzyme pyrroline 5-carboxylate reductase (Dutta *et al.*, 2019; Jawahar *et al.*, 2019).

The synthesis of proline has been studied in various model plants and from these findings the two enzymes pyrroline 5-carboxylate synthetase and pyrroline 5-carboxylate reductase were identified as capable of regulating the production of proline under abiotic stress (Dutta *et al.*, 2019). The genes responsible for the coding of these enzymes have been integrated into many economically important crops in order to contradict the effects of drought stress.

2.4.2 Superoxide dismutase

SOD is a metallo-enzyme working in conjunction with Cu, Zn, Mn or Fe, Ni and can be categorized into four groups based on the metal cofactor at its active side (Gill *et al.*, 2015). The four groups can be identified as, Cu/Zn-SOD, Mn-SOD, Fe-SOD and Ni-SOD and have different functions, structures and they occur in different locations (Figure 2-6) (Saibi and Brini, 2018). Cu/Zn-SOD can be located in the cytosol, chloroplasts, and peroxisomes, whereas Fe-SOD is mainly situated in the chloroplasts and to some extent in the peroxisomes and apoplast, while Mn-SOD can be found in the mitochondria (Corpas *et al.*, 2006). Ni-SOD, however, can be found in marine-eukaryote, cyanobacteria and marine gammaproteobacteria (Dupont *et al.*, 2008).

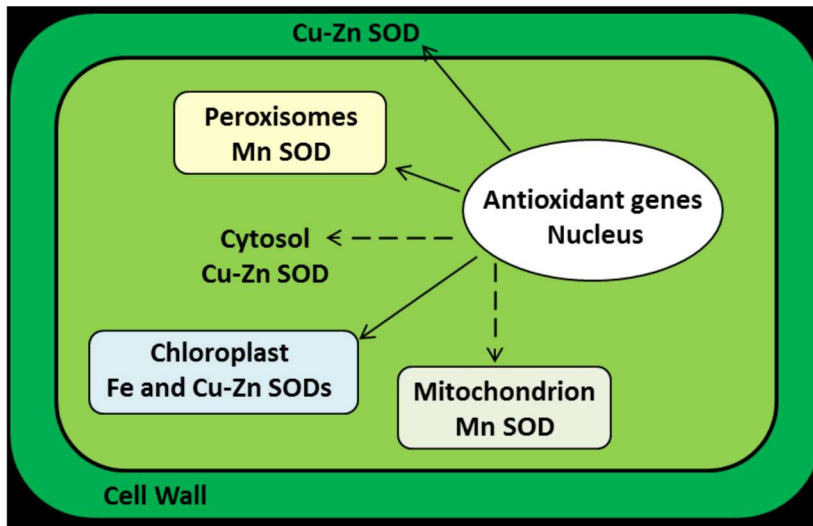


Figure 2-6: Localization of superoxide dismutase in a plant cell (Saibi and Brini, 2018).

SOD occurs in all oxygen metabolizing cells as well as in all sub-cellular compartments, such as, chloroplasts, mitochondria, nuclei, peroxisomes, cytoplasm, and apoplasts (Fink and Scandalios, 2002). SOD is described as one of the most effective components in combating ROS toxicity and often represents the first line of antioxidant defence by converting it into hydrogen peroxide (H_2O_2) and oxygen (O_2) (Alscher *et al.*, 2002; Gill and Tuteja, 2010; Saibi and Brini, 2018). SOD mainly catalyses the conversion of superoxide radicals into either O_2 or H_2O_2 (Gill *et al.*, 2015).



From this point H_2O_2 is detoxified, once the cellular antioxidant defence mechanisms become sufficient. Catalase (CAT), a tetrameric heme containing enzyme, has the ability to convert H_2O_2 into H_2O and O_2 (Garg and Manchanda, 2009). CAT can also be found in glyoxysomes and peroxisomes or in any related organ where an excess of H_2O_2 is present. CAT mainly scavenges ROS, for example H_2O_2 and has the ability to dismutate approximately six million H_2O_2 molecules per minute (Gill and Tuteja, 2010).

It could be stated that superoxide dismutase is central in the defence mechanism, because its activity regulates the amount of O_2 and H_2O_2 present in cells. Even so, it is important to note that superoxide is produced as a by-product of the oxygen metabolism

and if it is not regulated, it can also cause a series of cell damage (Gill *et al.*, 2015). Additionally, SOD also has the ability to overcome the electrostatic repulsion between two oxygen radicals (Saibi and Brini, 2018). This will usually occur in two ways, with the first being a reaction between the Fe-, Mn-, and Cu/Zn-SODs to the oxygen radical molecules, one at a time. Secondly, SOD will manipulate the negative charge of the oxygen radicals to rather encourage a specific binding with substrates and not with products (Miller, 2004). Furthermore, SOD also has the ability to protect PSII against oxygen radicals, which are produced due to water stress (Martinez *et al.*, 2001).

Various plants have been identified with increased SOD activities when exposed to water- stressed conditions, for example, *Oryza sativa* (Sharma and Dubey, 2005), *Vigna unguiculata* (Manivannan *et al.*, 2007) and *Catharanthus roseus* (Jaleel *et al.*, 2007). Zhang and Kirkham (1995) found that the SOD activity in *Triticum aestivum* increased or remained unaffected during the early phase of water stress, however, it decreased with prolonged water stress. Ahmed *et al.* (2013) observed that the SOD activity increased significantly under both drought and salinity stress during the anthesis period of the wild *Hordeum vulgare* genotypes. Bose *et al.* (2014) also found that halophytes generally have a higher level of SOD activity, thereby supporting its ability to rapidly convert superoxide radicals into H₂O₂. Hereafter, a series of adaptive responses are initiated where various other antioxidants could play a role in reducing the basal levels of H₂O₂ (Gill *et al.*, 2015).

2.4.3 Glutathione reductase

Glutathione reductase is a flavo-protein and is known to use NADPH as a reductant to catalyses the reduction of glutathione disulphide to the sulphhydryl form of glutathione (GSH) (Yousuf *et al.*, 2012). This process occurs in two phases. The first phase involves the reductive half reaction phase, where FAD (the prosthetic group of GR) is reduced by NADPH (Figure 2-7). Secondly the resulting dithiol will then react with the glutathione disulphide. Hereafter, the final electron acceptor, oxidized glutathione (GSSG), is reduced to two GSH molecules at the GR active site (Yousuf *et al.*, 2012).

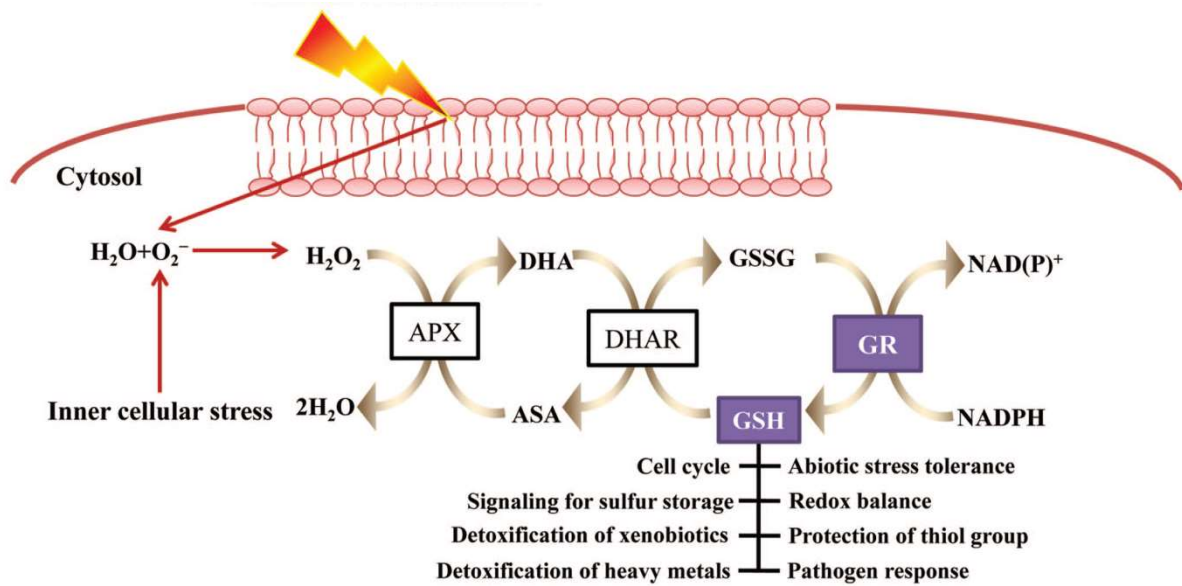


Figure 2-7: Antioxidant pathway mediated by Glutathione reductase in response to external and inner cellular stresses (Trivedi *et al.*, 2013).

Glutathione reductase can primarily be found in the chloroplasts, but some isoforms of the enzyme have been found in the mitochondria, peroxisomes and the cytosol in small amounts (Edwards *et al.*, 1990; Jiménez *et al.*, 1997; Trivedi *et al.*, 2013). There are three isoforms of GR, identified based on their location. Thus, there are cytosolic isoforms, chloroplastic isoforms and mitochondrial isoforms (Mullineaux *et al.*, 1996; Kaminaka *et al.*, 1998). The concentrations of the different isoforms can also change in the sub-cellular compartments in response to environmental stress. Different environmental stressors can also activate each isoform with their different functions during stress (Stevens *et al.*, 1997).

Together GR and GSH play important roles in establishing tolerance in plants in response to different stressors. GR ensures that proteins function normally by conserving the reduced state of the intracellular glutathione pool (Yousuf *et al.*, 2012). Small amounts of GSH also respond as important redox buffers by forming a barrier between protein cysteine groups and ROS (Korniyev *et al.*, 2003). In addition, GSH also limits metal-induced oxidative stress. GR activities in leaf tissue are responsible for scavenging ROS such as, H_2O_2 and O_2^- , and maintaining a high ratio of reduced oxidized glutathione (Alscher, 1989). Another important feature of GR is that it's also

thermo-stable. Yousuf *et al.* (2012) also found that an overexpression of GR can result in tolerance in various crop plants to abiotic stressors due to its efficient ROS scavenging capacity.

2.4.4 Hydrogen peroxide

Hydrogen peroxide occurs in the peroxisomes, chloroplasts, mitochondria, the endoplasmic reticulum, nucleus and plasma membranes of all photosynthesising cells (Figure 2-8) (Edwards *et al.*, 2009; Saxena *et al.*, 2016). The production of H₂O₂ in chloroplasts mainly occurs in the chlorophyll molecules related to the photosynthetic electron transport chain (the main source of O₂) (Hossain *et al.*, 2015). During this process, superoxide radicals are formed via the photo-reduction of molecular oxygen. Hereafter, singlet oxygen is produced via an energy transfer to the triplet oxygen in PSII. The excitation of PSII will then result in the oxidation of water to oxygen. In peroxisomes, H₂O₂ is produced during the oxidation of glycolate in the C₂ cycle (Saxena *et al.*, 2016). During this process, xanthine oxidase catalyses the oxidation of xanthine or hypoxanthine to uric acid, which produces oxygen and in turn is converted to H₂O₂ (Saxena *et al.*, 2016).

Hydrogen peroxide is also actively present in the development of plants (Hung *et al.*, 2005), despite being toxic at high concentrations and causing cell death (Dat *et al.*, 2000). Regardless of its reactive perception, H₂O₂ is involved in the last step of converting ROS (Filippou *et al.*, 2013). When present at low concentrations, H₂O₂ acts as a messenger molecule when a plant experiences biotic or abiotic stress (Mittler *et al.*, 2004). A series of acclimation mechanisms based on biochemical and physiological changes are involved when exposed to stress (Fukao and Bailey-Serres, 2004).

These mechanisms usually involve the coding of antioxidants, defence proteins, signal proteins, and transcription factors (Hung *et al.*, 2005). Drought, temperature and salinity stress induces oxidative stress in plants. Once plants are exposed to low temperatures, the early accumulation of H₂O₂ leads to the activation and production of antioxidant enzymes (Filippou *et al.*, 2013). Other studies also revealed that the exogenous application of H₂O₂ assisted sweet potato and sweet peppers to acclimate to low temperatures (Lin and Block, 2010). In addition, the exogenous application of H₂O₂ under a long photo-period had beneficial effects compared to its application under a

short photo-period. These observations lead to the belief that the H₂O₂-mediated priming phenomena could also be regulated by other factors, either intra- or extracellular. Furthermore, Kumar *et al.* (2010) also proposed that brassinosteroids, for example, 24-epibrassinolide are involved in the H₂O₂-induced acclimation against chilling stress. These authors found that 24-epibrassinolide assisted in preventing the harmful effect of H₂O₂ via the production of antioxidants.

Similar results were found in tomato plants, during which the exogenous application of H₂O₂ relieved the effects of oxidative stress caused by water stress through the activation of antioxidant enzymes (Behnamnia *et al.*, 2009; Filippou *et al.*, 2013). Comparable results were also found by Larkindale and Huang (2004), when plants were exposed to heat stress. In cucumber leaves, the exogenous application of H₂O₂ decreased lipid peroxidation, thereby protecting the ultrastructure of the chloroplasts. In addition, H₂O₂ is also responsible for the up-regulation of Hsp20 and Hsps chaperones, which are involved in cellular protection during stress conditions (Rhee *et al.*, 2011). Therefore, H₂O₂ is believed to be a vital prerequisite factor in the heat stress signalling pathway to effectively express heat shock genes (Volkov *et al.*, 2006).

The acclimation of plants to salt stress can also be linked to an increase in the antioxidant enzyme activity, along with certain stress-related genes (Wahid *et al.*, 2007; Filippou *et al.*, 2013). This includes the expression of transcripts for genes encoding D - pyrroline-5-carboxylate synthase, sucrose-phosphate synthase, and small Hsp 26 (Uchida *et al.*, 2002).

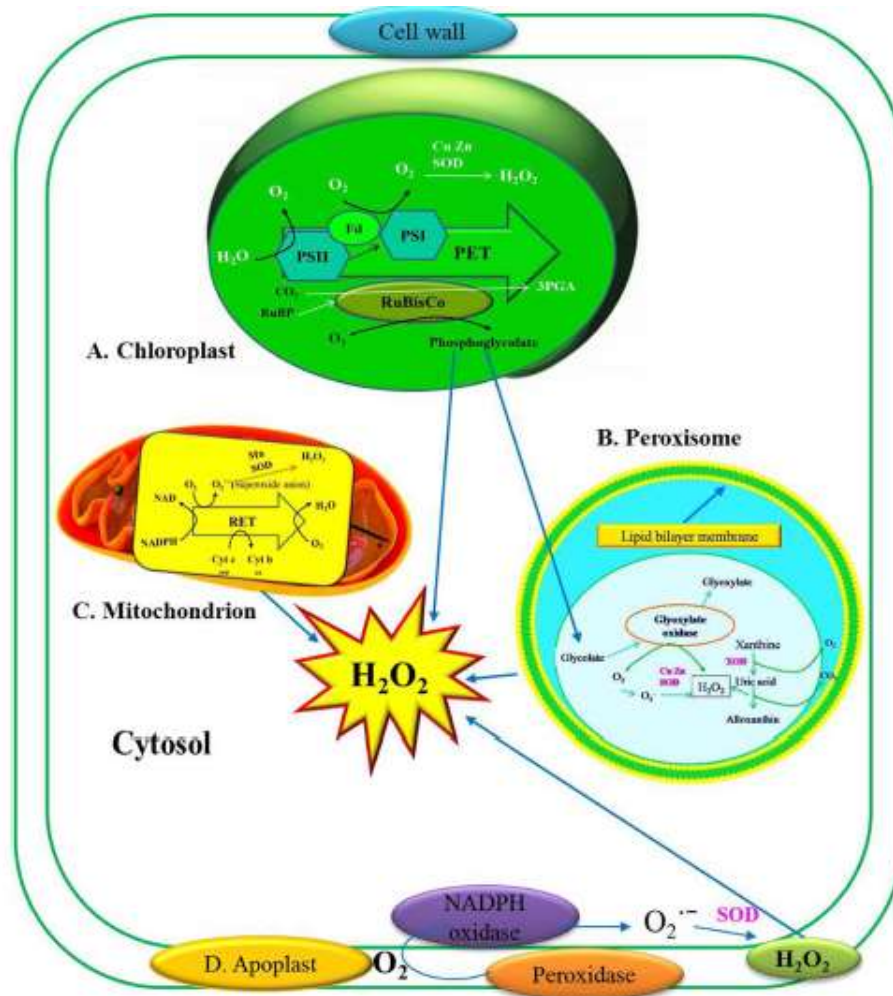


Figure 2-8: The production of hydrogen peroxide (H_2O_2) in the different photosynthesising cells (Saxena *et al.*, 2016).

2.5 Chlorophyll a fluorescence

When photosynthetic organisms are illuminated by an approximate wavelength of 400-700 nm, a red to far red light is produced, which is known as chlorophyll fluorescence (McCree, 1972; Kalaji *et al.*, 2017). Within this spectrum, the chlorophyll molecules are excited more efficiently by red and blue light compared to green light. Chlorophyll a fluorescence only represents 0.5- 10% of the absorbed energy and its intensity is oppositely proportional to the energy used during photosynthesis (Porcar-Castell *et al.*, 2014). In addition, it is also inversely correlated to the changes in the dissipative heat emissions; therefore, a decrease in the fluorescence emission yield is caused by an increase in the yield of heat emission (Kalaji *et al.*, 2017). As a result, chlorophyll a

fluorescence can easily be used to investigate the photosynthetic efficiency of plants, as well as the regulatory processes which affect the photosystem II (PSII) antenna.

The primary donor of photosystem II (P680⁺) is a strong quencher of chlorophyll *a* fluorescence and can easily allow the study of the different redox states as the lifetime of P680⁺ is S state dependent, therefore turning chlorophyll *a* fluorescence into a great tool to study photosynthesis *in vivo* (Kalaji *et al.*, 2017). This includes quenching analysis (Schreiber *et al.*, 1986), JIP test (Strasser *et al.*, 2004), non-photochemical quenching (Horton and Hague, 1988), electron transport rate (Krall and Edwards, 1990), rapid light curves (Ralph and Gademann, 2005), OJIP transients and dark adaptation (Schansker *et al.*, 2005), photo-acoustic spectroscopy (Bukhov *et al.*, 1997), 820-nm absorbance (Schansker *et al.*, 2003), the wavelength dependence of photosynthesis (Schreiber *et al.*, 2012), delayed fluorescence (Gorbe and Calatayud, 2012), and the measurements of parameters (Bussotti *et al.*, 2011).

Chlorophyll *a* fluorescence can also be used to study a wide variety of topics, for example, plant breeding, seed vigour and seed quality assessment, the quality of fruit and vegetables and postharvest regulation, senescence and climate change effects (Kalaji *et al.*, 2017). In addition, chlorophyll *a* fluorescence has also been used to investigate the effects of abiotic stress on plants (Digrado *et al.*, 2017; Banks, 2018; Pšidová *et al.*, 2018). This includes, heat stress, drought, photo-inhibition, UV stress and salinity stress.

In this study, a M-PEA fluorometer was used to measure the prompt fluorescence (JIP-test). The theory of energy flow in thylakoid membranes describes the inflow and outflow of energy in photosynthetic pigments, therefore forming the basis of the JIP-test (Kalaji and Loboda, 2007). The physiological state of the plant, due to different biotic and abiotic stressors, will determine the shape of the OJIP-transient (Strasser *et al.*, 2001, Strasser *et al.*, 2004). As plants cannot move to avoid different stressors, they have to acclimatize in order to survive. The ability of plants to adapt to different stressors is therefore, studied through the vitality of PSII and PSI (Guo *et al.*, 2008, Longenberger *et al.*, 2009). The JIP- test allows for a separate assessment of the maximum yield of primary photochemistry. As a result, the JIP- test explores the possibility with which an electron would move into the electron transport chain beyond

Q_A^- (Quinone A) (Kalaji, *et al.*, 2017). The reduction of the electron transport chain is represented by the shape of the OJIP transient which is used to investigate the photochemical potential of plants under stress.

When plotted on a logarithmic time scale the fluorescence rise kinetics can be described as polyphasic with steps J (2 ms), I (30 ms) and P (300 ms) found between F_0 (initial) and F_M (maximum) (Kalaji *et al.*, 2017) (Figure 2-9). From the JIP test, two events can be distinguished, the single turn over event (0 – 2 ms) and the multiple turnover event (2 – 300 ms) (Vredenberg *et al.*, 2006). The single turnover event represents the photosynthetic light events during which a single reduction of Q_A^- occurs (Tsimilli-Michael and Strasser, 2008). The multiple turnover event further describes the reaction from Q_A^- to the reduction of the end electron accepters (Vredenberg *et al.*, 2006).

To fully visualize and understand the changes in the redox potential of the O-J-I-P transient, the difference in variable fluorescence from stressed and non-stressed plants are normalized and plotted on a logarithmic time scale. By doing this, different ΔV -bands (O, L, K, J, I, G, H, P) will be revealed, which describe the efficiency of electron flow through the electron transport chain (Tsimilli-Michael and Strasser, 2008). A ΔV_O -band ($\approx 0.02 - 0.05$ ms) reveals information regarding the oxidised primary quinone acceptor. The ΔV_L -band (0.15 ms) refers to the energetic connectivity or grouping between the PSII units (Oukarroum *et al.*, 2007). The ΔV_K -band (0.3 ms) is associated with the activation of the oxygen evolving complex (OEC) and the flow of electrons moving from the reaction centre towards the acceptor side, as well as the flow of electrons moving towards the reaction centre from the donor side of PSII (Strasser *et al.*, 2007; Yusuf *et al.*, 2010; Bussotti *et al.*, 2011; Chen *et al.*, 2016; Kalaji *et al.*, 2017; Kalaji *et al.*, 2018). A ΔV_J -band (2 ms), represents an oxidized primary quinone acceptor Q_A^- (Strasser *et al.*, 2007) and whether electrons will move beyond Q_A^- . A ΔV_I -band (30 ms) represents the transport of electrons between the PSII and photosystem I (PSI) reaction centres. The ΔV_H -band (20 ms) refers to the reduction of the secondary quinone acceptor, but two electrons are used to reduce it (Strasser *et al.*, 2007). The ΔV_G -band (100 ms) refers to the reduction of $NADP^+$ to Nicotinamide adenine dinucleotide phosphate (NADPH). The ΔV_P -band (≈ 300 ms) reveals information regarding the fully reduced electron carriers.

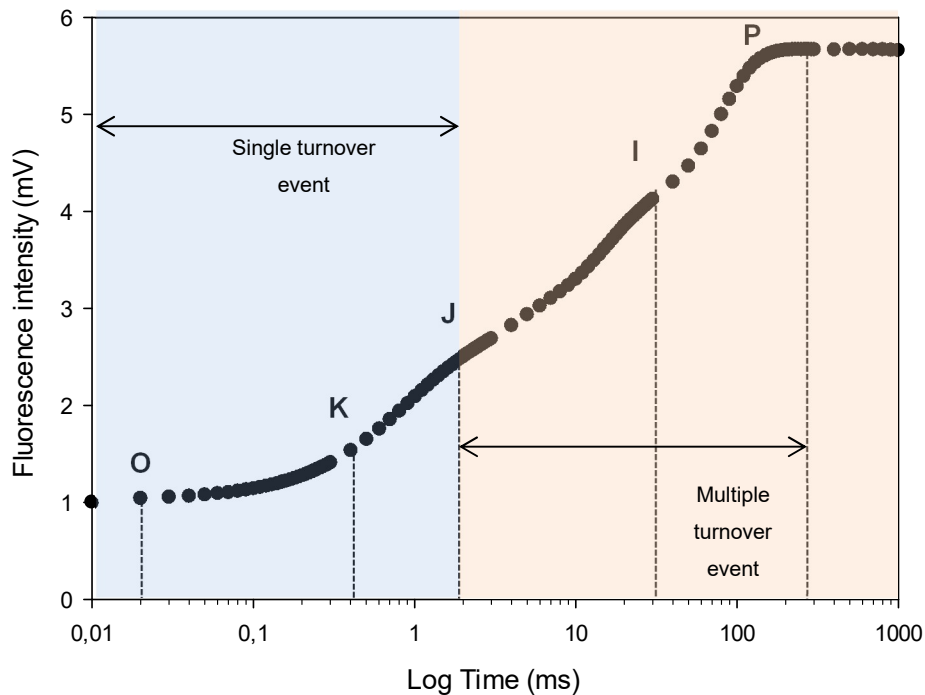


Figure 2-9: A typical chlorophyll a polyphasic fluorescence rise (OJIP), exhibited by plants plotted on a logarithmic time scale (0.2 ms – 1 s). The different steps are labelled as O (20 μ s), K (0.3 ms), J (2 ms), I (30ms), and P (\approx 300 ms).

In addition, a set of parameters are also calculated by the JIP-test which have been proven to be sensitive to stress initiated by adverse environmental conditions. These parameters are based on the theory of energy flow in membranes and can be presented using a Z-scheme of photosynthesis, expressed by sequential energy fluxes (Figure 2-10).

The specific energy fluxes are: Absorption of light energy (ABS), trapping of light energy (TR_0), the conversion of excitation energy (ET_0) and the reduction of end electron acceptors (RE_0) which regulate the initial stage of the photosynthetic activity of a reaction complex (RC) (Table 2-1).

These four independent steps contributing to photosynthesis leads to the introduction of the multi-parametric expression (Strasser *et al.*, 2004). The PI_{TOTAL} incorporates these four steps, thereby capturing the kinetics of electron flow through the photosynthetic

apparatus and making it one of the most sensitive parameters (van Heerden *et al.*, 2007).

Table 2-1: Formulae and definitions used by the JIP-test for the analysis of chlorophyll a fluorescence transient OJIP in this study (from Strasser *et al.*, 2007; Tsimilli-Michael and Strasser, 2013; Kalaji *et al.*, 2017).

Fluorescence parameters derived from the extracted data	
$F_0 = F_{20\mu s}$	Minimal fluorescence, when all PS II RCs are open
$F_P (F_M)$	Maximal fluorescence, when all PS II RCs are closed
$F_V = F_M - F_0$	Maximal variable fluorescence
$V_t = (F_t - F_0)/(F_M - F_0)$	Relative variable fluorescence at time t
$V_J = (F_J - F_0)/(F_M - F_0)$	Relative variable fluorescence at the J-step
$V_I = (F_I - F_0)/(F_M - F_0)$	Relative variable fluorescence at the I-step
Specific energy fluxes (per QA-reduced PSII reaction centre)	
$ABS/RC = M_0 (1/V_J) (1/\phi_{P_0})$	Flux for absorption per RC
$TR_0/RC = M_0 (1/V_J)$	Flux for trapping energy per RC
$ET_0/RC = M_0 (1/V_J)\psi_0$	Flux for electron transport per RC
$DI_0/RC = (ABS/RC) - (TR_0/RC)$	Energy flux for dissipation in the form of heat, not intercepted by an RC
Yields or energy flux ratios	
$\phi_{Pt} = TR_t/ABS = F_t/F_m$	The quantum yield for primary photochemistry at time t .
$\phi_{P_0} = TR_0/ABS$	The maximum quantum yield for primary photochemistry.
$\phi_{E_0} = ET_0/ABS$	The quantum yield for electron transport.
$\phi_{R_0} = RE_0/ABS$	The quantum yield, at the PSI acceptor side, for the reduction of end electron acceptors.
$\psi_{E_0} = ET_0/TR_0$	The probability of the transportation of an electron beyond Q_A^- .
$\phi_{R_0} = RE_0/ABS = [1 - (F_0/F_m)](1 - V_I)$	Quantum yield for reduction of end electron acceptors at the PSI acceptor side (RE)
Performance indexes	
$PI_{ABS} = \left[\frac{\gamma_{RC}}{1 - \gamma_{RC}} \right] \times \left[\frac{\phi_{P_0}}{1 - \phi_{P_0}} \right] \times \left[\frac{\psi_{E_0}}{1 - \psi_{E_0}} \right]$	Performance index (potential) for energy conservation from exciton to the reduction of intersystem electron acceptors
$PI_{total} = PI_{ABS} \times [\delta_{R_0}/(1 - \delta_{R_0})]$	Performance index (potential) for energy conservation from exciton to the reduction of PSI end acceptors

The yield or energy fluxes include: (1) $TR_0/ABS = \phi_{P_0} = 1 - (F_0/F_M)$, which is described as the maximum quantum yield of primary photochemistry; (2) $ET_0/TR_0 = \psi_{E_0} = (1 - V_J)$, refers to the efficiency with which an electron can move into the electron transport chain

further than Q_A^- ; (3) $ET_0/ABS = \varphi_{P_0} \cdot \psi_{E_0}$, the quantum yield of electron transport further than Q_A^- ; (4) $RE_0/ET_0 = \delta_{R_0} = (1 - V_1)/(1 - V_2)$, the efficiency with which an electron can move from the reduced intersystem electron carriers to the PSI end electron acceptors; (5) $RE_0/ABS = \varphi_{R_0} = \varphi_{P_0} \cdot \psi_{E_0} \cdot \delta_{R_0}$, the quantum yield for reduction of PSI end electron acceptors; (6) $RE_0/TR_0 = \psi_{R_0} = \psi_{E_0} \cdot \delta_{R_0}$, the efficiency with which an electron can move into the electron transport chain from Q_A^- to the PSI end electron acceptors (Table 2-1).

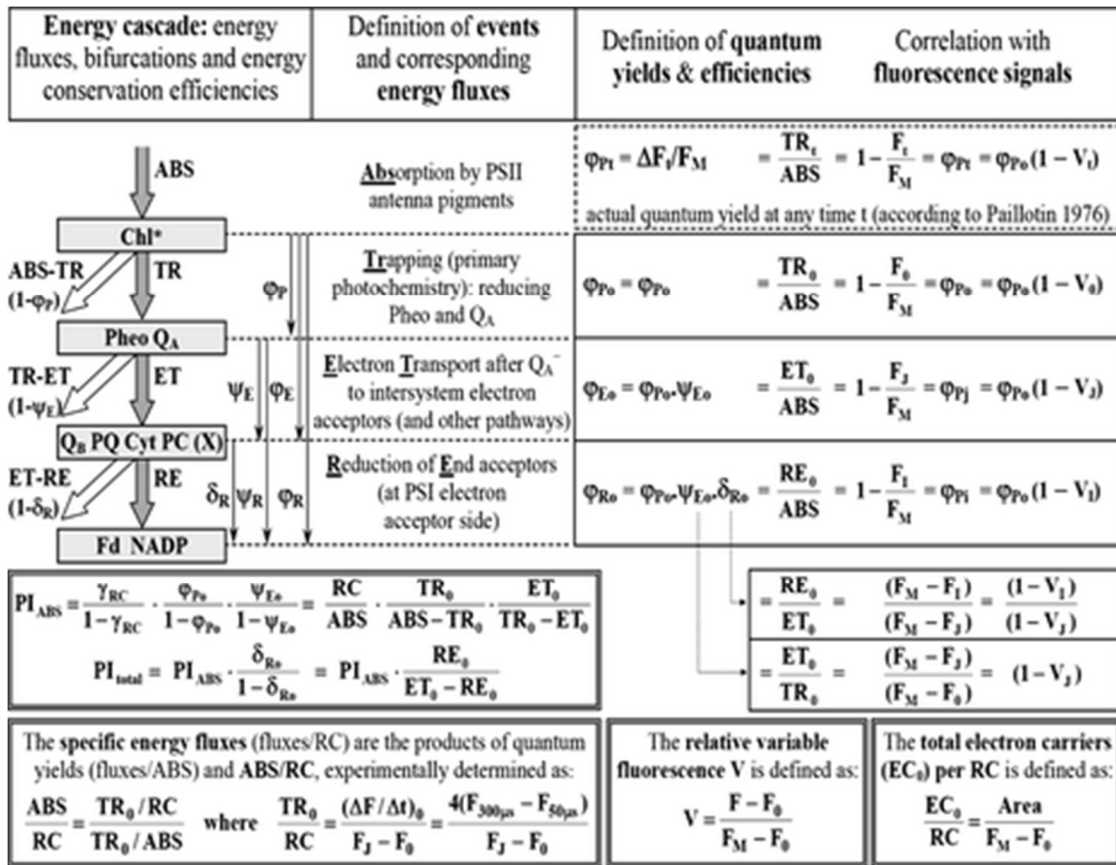


Figure 2-10: A schematic presentation of the JIP-test (Tsimilli-Michael and Strasser, 2013).

In addition, the M-PEA also measures the photo-induced changes in the light reflection at 820 nm. In this case, the light beam (820 nm wavelength) is modulated in order to increase the signal sensitivity (Kalaji *et al.*, 2017). The oxidation of the electron donors of PSI is reflected within the first 15-20 ms. When exposed to the actinic red light, both photosystems are excited and the photochemical reaction in the reaction centres are induced. This will occur during the initial period of illumination. As PSII is activated, the

electron carriers, Q_A , Quinone B (Q_B), plastoquinone and pheophytin (Pheo) in the electron transport chain are reduced and as a result of the oxidation of the water molecules, the oxidized chlorophyll ($P680^+$) decreases rapidly (Kalaji *et al.*, 2017). It is important that the electron donation to the oxidized chlorophyll is limited; this is to avoid the stationary concentration of $P680^+$ being too low during the light period.

In contrast, the situation in PSI is slightly different, because the pool of intersystem carriers is mainly oxidized, due to being dark adapted for a longer period, therefore, there are no electron donors available for the reduction of plastocyanin (PC^+), the primary donor of photosystem I ($P700^+$) (Schreiber *et al.*, 1989; Schansker *et al.*, 2003; Kalaji *et al.*, 2016). Due to this, the concentration of the PSI carriers (in the oxidized state) increases, which would lead to a proportional decrease in the scattered light signal MR820. Between 15 and 20 ms of illumination, the induction curve will reach a minimum. At the same time, the electron donated from the primary photochemical reactions in PSII, would reach PC^+ and $P700^+$ (Kalaji *et al.*, 2018).

This occurrence will cause a reduction in the rate of MR820 decrease and increase the reflection in order to reach the initial dark level. This will occur for approximately 200 ms and during this time, the MR820 signal will undergo two phases (Kalaji *et al.*, 2016). The first phase (0-20 ms) refers to the initial decrease, which is related to the photo-induced oxidation of $P700^+$ (Figure 2-11). The second phase (20-200 ms) involves the increase in reflecting a photo-induced reduction of oxidized $P700^+$. The first phase ends when the plastoquinone (PQ) pool is semi-reduced and occurs simultaneously with the prompt fluorescence transition between ΔV_J and ΔV_I (Van Heerden *et al.*, 2007; Oukarroum *et al.*, 2012b; Gao *et al.*, 2014). The second phase reflects the secondary reduction of PC^+ and $P700^+$ (movement of electrons from PSII to the PQ pool) and occurs at the same time with the prompt fluorescence transition between ΔV_I and ΔV_P (Schansker *et al.*, 2003; Strasser *et al.*, 2010). The kinetics of the MR820 signal can, therefore, be described as the rate of $P700$ oxidation which is often referred to as the fast phase and secondly the reduction of $P700^+$ also known as the slow phase (Kalaji *et al.*, 2016).

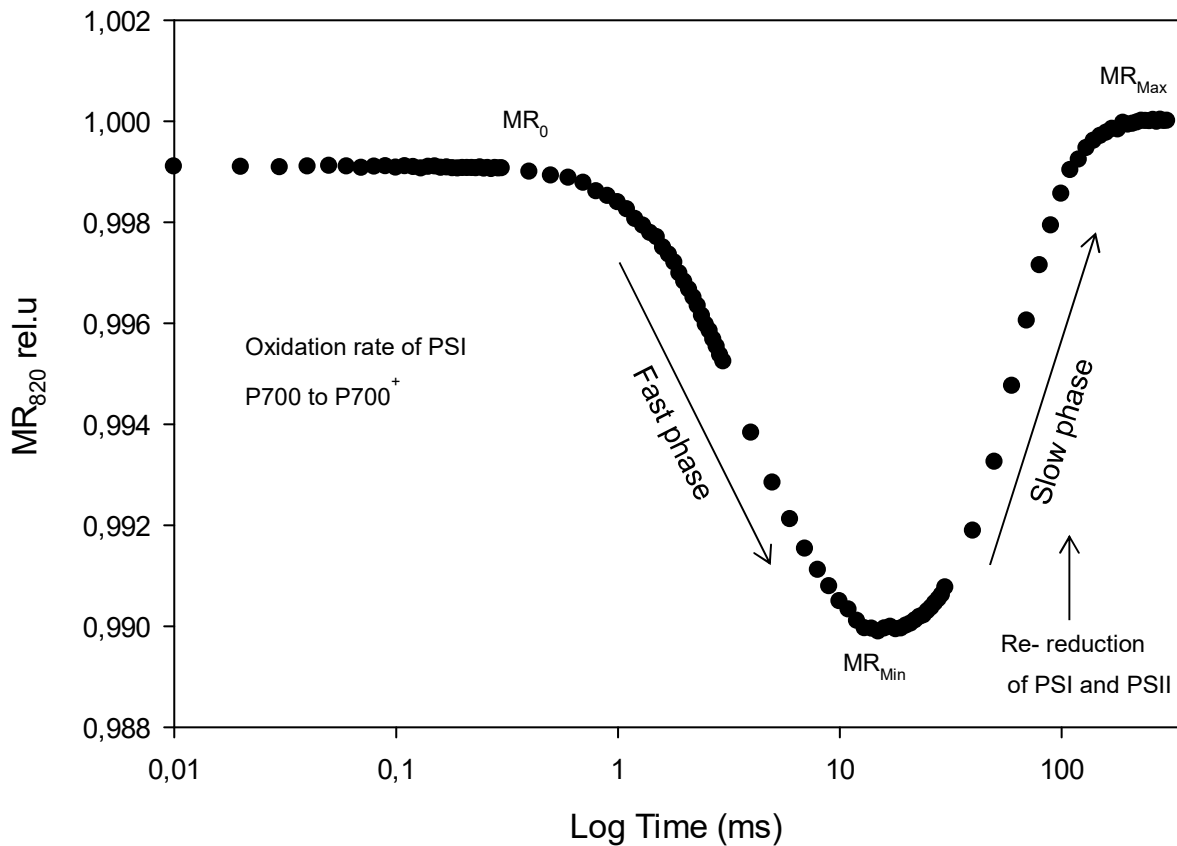


Figure 2-11: Kinetics of modulated light reflection at 820 nm in dark-adapted leaves.

However, during stress conditions, the changes that occur with the photo-induced transitions of the MR₈₂₀ modulated reflection signal can transpire in several successive stages. The first change to occur influences the amplitude and the rate of increase in the slow phase; this will usually refer to the inhibition of electron donors from PSII (Dabrowski *et al.*, 2019). When the effect of stress is significantly higher, the initial decline in the signal in the fast phase is delayed and can be ascribed to an inhibition of the photochemical reaction in PSI (Goltsev *et al.*, 2012).

With a decrease in the water content, the MR signal will also be modified. In terms of the fast phase, Goltsev *et al.* (2012) found that if the relative water content drops below 10% changes are induced in the P700 redox state. Whereas, the slow phase, which refers to P700⁺ re-reduction, was more sensitive as it dropped quickly when the relative water content dropped to 30% and disappearing with a relative water content of 3%.

Therefore, with a very low water content, the primary photochemical reactions of both PSI and PSII are deactivated (Goltsev *et al.*, 2012; Kalaji *et al.*, 2016).

In response to a decrease in the water content, four drought specific effects were identified; (1) a decrease in the flow of electrons in PSII will be observed, (2) a delay of electron transport from the reduced PQ pool to P700⁺ will occur, (3) the re-oxidation of Q_A will be inhibited and (4) a delay in the photo-induced electron transport from P680⁺ to Q_A will occur simultaneously with a reduction in the photo-induced kinetics of the MR signal (Schansker *et al.*, 2003; Goltsev *et al.*, 2012).

CHAPTER 3 MATERIALS AND METHODS

3.1 Growth conditions

The maximum day temperatures in the glasshouses were set to 30°C and 20°C and the night temperatures were set to 16°C. The day length was set to 13 hours by means of fluorescent light tubes. The photosynthetic active radiation (PAR) during the day ranged between 600 and 800 $\mu\text{mol m}^{-2} \text{s}^{-1}$.

3.2 Plant cultivation

Quinoa (*Chenopodium quinoa* Willd) seeds, as well as maize (*Zea mays*) seeds were hand sown in 2 L pots containing a moistened Hygromix[®] (Hygrotech, RSA) and potting soil substrate (3:2). Hygromix[®] is a soilless sterile growth medium, consisting of inert and stable components. The plants were fertilized with Osmocote Pro 3-4 months (25 kg); a controlled release fertilizer, with a NPK ratio of 17:11:10. The fertilizer was mixed with the growth medium (20 mL per pot) prior to planting.

3.3 Water regimes

Two water regimes were used during this trial, namely a well-watered and a water-stressed treatment. During germination, the plants were watered twice a day through an automated irrigation system. The water stress treatment was initiated 4 weeks after emergence (vegetative stage). Decagon[®] soil moisture sensors GS3 (CS Africa (Pty) Ltd, Stellenboch RSA) were used to measure the hourly soil moisture status. The water stress conditions were maintained until the soil water content reached a level of 0.01 $\text{m}^3 \cdot \text{m}^{-3}$. At this point the water stress treatment was stopped to avoid permanent wilting.

3.4 Experimental timeline

Table 3-1 below provides details and dates regarding the activities and experiments conducted during this study and include the activity, area of activity and time of completion.

Table 3-1: Timeline of the experimental work during 2017 to 2019.

Date	Activity	Time to completion	Area of activity
2017/01/08	Literature study	4 months	Office
2017/02/05	Plant seed of quinoa and maize	Germination to vegetative stage \pm 4 weeks	Greenhouse a and b
2017/03/12	Conduct first trial, commence water stress, start chlorophyll <i>a</i> fluorescence measurements.	2 weeks	Greenhouse a and b
2017/06 - 2017/12	Adjust trial according to problems found during first trial. Ventilation system upgrade	7 month	Greenhouse a and b
2018/04/02	Start second trial, commence water stress, include stomatal conductance, chlorophyll content, biomass and leaf area measurements	2 weeks	Greenhouse a and b
2018/06/11	Start third trial, repeat second trial	2 weeks	Greenhouse a and b
2018/08/20	Start fourth trial, commence water stress, focus on chlorophyll <i>a</i> fluorescence and proline measurements	3 weeks	Greenhouse a and b Lab work
2019/02/05	Start fifth trial, commence water stress, focus on chlorophyll <i>a</i> fluorescence and SOD measurements	3 weeks	Greenhouse a and b Lab work
2019/05/14	Start sixth trial, commence water stress, focus on chlorophyll <i>a</i> fluorescence and GR measurements	3 weeks	Greenhouse a and b Lab work
2019/07/08	Start seventh trial, commence water stress, focus on chlorophyll <i>a</i> fluorescence and H ₂ O ₂ measurements	3 weeks	Greenhouse a and b Lab work
2017- 2019	Write-up of results (After each trial)		Office
22/12/2019	Conclusion of thesis		Office

3.5 Prompt fluorescence

The kinetics of the polyphasic prompt fluorescence rise was measured *in vivo* using the M-PEA fluorometer (Hansatech Instrument Ltd, King's Lynn, Norfolk, UK). Prior to the start of the measurements, the plants were dark adapted for at least one hour. The measurements were taken on five different spots on the adaxial surface of the fully developed canopy leaves. Chlorophyll *a* fluorescence measurements were recorded after illumination by a red actinic light of 3000 $\mu\text{mol photons m}^{-2}\text{s}^{-1}$ provided by 3 light-emitting diodes with 5 mm diameter focus spot and 12-bit resolution in one second (Strasser *et al.*, 2004; Strasser *et al.*, 2007; Kalaji and Loboda, 2007; Guo *et al.*, 2008; Tsimilli-Michael and Strasser, 2008; Longenberger *et al.* 2009). PEA Plus (v 1.10) software was used to calculate the photosynthetic (O-J-I-P) curves, as well as the photosynthetic parameters. The PI_{TOTAL} parameter was also used to construct an estimated vitality index based on the photosynthetic performance of quinoa and maize under water- stressed conditions.

3.6 MR820 nm Modulated reflection

In addition, the MPEA fluorometer was also used to measure the photo-induced changes in the light reflection at 820 nm. In this case, the light beam with a wavelength of 820 nm was modulated in order to increase the signal sensitivity. As with the prompt fluorescence, five measurements were taken on the adaxial surface of the fully developed canopy leaves. PEA Plus (v 1.10) software was used to calculate the kinetics of the modulated light reflection at 820 nm as well as the parameters of the relative MR signal.

3.7 Membrane leakage

The method of Sullivan (1971) was used to measure the membrane leakage of both quinoa and maize. The membrane leakage was determined by sampling three 10 mm discs per plant with a cork borer (0.6 mm in diameter). The leaf discs were rinsed three times to remove excess electrolytes and placed in separate tubes (15 mL) containing 10 mL de-ionized water. Hereafter, the samples were placed in the dark for 24 hours, after which the initial ionic leakage was measured with an EC meter (Primo 5, HANNA Instruments, USA). The samples were autoclaved for 20 minutes to dissociate all

cellular cytosols into solution. The final ionic leakage was measured after the samples were cooled to room temperature and calculations were performed as an injury index percentage at 100 °C.

$$\text{Membrane leakage (\%)} = 1 - \frac{\text{Final} - \text{Initial}}{\text{Initial}} \times 100$$

Where “final” and “initial” represents the membrane leakage measurements.

3.8 Relative leaf water potential

Leaf discs were cut from the leaves, approximately 1.5 cm in diameter and large veins were avoided (Barr and Weatherley, 1962). The samples were weighed to obtain the initial weight, after which the samples were immediately hydrated to full turgidity for 4 h. Leaf discs were hydrated by floating on de-ionized water in closed petri dishes at normal room temperature. After this, the samples were taken out of the water and dried quickly and lightly with tissue paper and weighed immediately to obtain the turgid weight. The leaf samples were dried at 80°C for 24 h to determine the dry weight. The relative water content (RWC) was determined as:

$$\text{RWC (\%)} = \left(\frac{\text{FW} - \text{DW}}{\text{TW} - \text{DW}} \right) \times 100$$

Where FW represents the fresh weight, DW the dry weight and TW the turgid weight.

3.9 Stomatal conductance

Stomatal conductance measurements were taken on the abaxial surface of the fully expanded upper canopy leaves of the quinoa and the top visible dewlap of the maize. A steady state photometer (Model AP4, Delta-T Devices, Cambridge, UK) was used to record the measurements. Measurements were taken each day during the water stress trial. Five readings were taken per plant. Measurements were taken daily between 11:00 am and 13:00 pm.

3.10 Chlorophyll content

The chlorophyll content of both quinoa and maize was measured using a CCM 300 chlorophyll content meter (Opti-science, USA). Soil Plant Analysis Development (SPAD) values were obtained which determined the leaf chlorophyll content. The chlorophyll content was measured at five different spots on both the quinoa and maize leaves, avoiding large veins. The chlorophyll content was measured daily.

3.11 Proline content

Plant material and extraction:

A simple and fast ninhydrine-based method as described by Carillo and Gibon (2011) was used to determine the free proline content in both quinoa and maize leaves. The proline was extracted using a cold extraction method. Following this method, 50 mg fresh plant material was weighed and mixed with 1 mL of an ethanol: water (40:60 v/v) mixture. This mixture was left over night at 4°C. Thereafter, it was centrifuged at 14 000 g for five minutes and stored at -20°C.

Proline determination:

A reaction mixture containing 1% ninhydrine (w/v), 60% acetic acid (v/v) and 20% ethanol (v/v) was prepared. This mixture is sensitive to light. In 1.5 mL Eppendorf tubes, the following was added; 1000 µL of the reaction mix and 500 µL of the ethanol extract. The Eppendorf tubes were closed and placed in a block heater at 95°C for 20 minutes. Hereafter, the samples were centrifuged at 10 000 rpm for one minute. The supernatant was transferred to a 1.5 mL cuvette and the absorbance was read at 520 nm. A respective calibration curve was also generated with known concentrations ranging from 0.04 to 1 mM.

The following equation was used to calculate the amount of proline ($\mu\text{mol.g}^{-1}$) in the extracts:

$$\text{Proline} = \left(\frac{\text{Abs extract} - \text{Abs blank}}{\text{Slope}} \right) \times \frac{\text{Vol extract}}{\text{Vol aliquot}} \times \frac{1}{\text{FW}}$$

Where Abs_{extract} was the absorbance determined with the extract, and Abs_{blank} was the absorbance determined without the extract. The slope (expressed as absorbance·nmol⁻¹) was determined via linear regression. Vol_{extract} was the total volume of the extract and Vol_{aliquot} is the volume used in the assay. FW (mg) refers to the amount of plant material used for the extraction.

3.12 Superoxide dismutase

The principle:

For the superoxide dismutase (SOD) activity measurements, the method described by Beauchamp and Fridovich, (1971) was followed. SOD catalyses the dismutation of superoxide radicals to H₂O₂. The SOD activity assay is based on the ability of superoxide dismutase to inhibit the reduction of nitro-blue tetrazolium (NBT) via superoxide. In this method, riboflavin is illuminated in the presence of O₂ and methionine (an electron donor) which in turn will produce superoxide anions. In the absence of any SOD activity, superoxide radicals (O₂⁻) will interact with NBT, thereby reducing the yellow tetrazolium to a blue precipitate (Formazan). The control reaction, which is done without any enzyme, will show a maximum blue colour. In the presence of an enzyme, the intensity of the colour decreases with an increase in the enzyme activity.

Plant material and extraction:

To prepare the extract, 200 mg fresh plant material was pre-weighed and homogenized in 1.5 mL of a 50 mM ice cold sodium phosphate buffer (pH 7.0), containing 2 mM EDTA, 5 mM β-mercaptoethanol and 4% PVP-40. Hereafter the extract was centrifuged at 30 000 g for 30 minutes at 4°C.

The following stock solutions were prepared:

A sodium phosphate buffer (pH 7.8) was prepared with a 50 mM. A 0.12 mM riboflavin solution was prepared and stored in a dark bottle. A 1.72 mM Nitroblue tetrazolium (NBT) solution was prepared and stored at 4°C. Lastly a 201 mM Methionine solution as well as a 1% Triton X-100 solution was prepared.

Reaction mixture:

From the above stock solutions, a reaction mixture was prepared containing; 27 mL of the 50mM sodium phosphate buffer (pH 7.8), 1 mL of the NBT solution, 1.5 mL of the Methionine solution and 0.75 mL of the Triton X-100 solution.

Procedure:

In an Eppendorf tube, 1 mL of the reaction mixture was added with 0.1 mL of the enzyme extract and 0.03 mL riboflavin. The tubes were placed in a light box to provide uniform light intensity. A box lined with foil was used with an internally mounted 40 W fluorescent bulb. The tubes were incubated for 30 minutes under illumination. The reaction was stopped by switching off the illumination and the absorbance was recorded at 560 nm using a spectrophotometer. Hereafter, the samples were stored at -20°C and used for the protein determination.

Protein determination:

The protein content was determined using a simple BioRAD method (Bradford, 1976). The microplate method was followed and the absorbance was read at 595 nm. A blank was prepared containing 160 µL H₂O and 40 µL BioRAD. In addition, a STD was prepared with 150 µL H₂O, 40 µL BioRAD and 10 STD (0.5 µL Globulin & Albumin). The sample consisted of 150 µL H₂O, 40 µL BioRAD and 10 µL of the extract solution.

Furthermore, the maximum attainable absorbance at 560 nm was determined by irradiating a sample without the crude enzyme. The SOD activity (A₅₆₀ mg protein⁻¹ hour⁻¹) was expressed (Keppler and Novacky, 1987) as:

$$SOD\ activity = \log \frac{A_{560} (with\ crude\ extract) mg / protein}{A_{560} (without\ crude\ extract)}$$

3.13 Glutathione reductase

The principle:

The method described by Schaedle and Bassham, (1977) was used to measure the glutathione reductase (GR) activity. In this process GR catalysed the reduction of

oxidized glutathione (GSSG) to reduced glutathione (GSH) using Nicotinamide adenine dinucleotide phosphate (NADPH) as a reductant.

Plant material and extraction:

The plant material was extracted according to the same method used during the SOD extraction. To prepare the extract, 200 mg fresh plant material was homogenized in 1.5 mL of a ice cold 50 mM sodium phosphate buffer (pH 7.0) containing 2 mM EDTA, 5 mM β -mercaptoethanol and 4% PVP-40. Lastly the extract was centrifuged at 30 000 g for 30 minutes at 4°C.

The following solutions were prepared:

Three solutions were prepared and numbered as A, B and C. Solution A contained a 100 mM phosphate buffer (pH 7.5) and 7.2 mM $MgCl_2$. Solution B contained a 3.6 mM NADPH mixture and lastly solution C contained 15 mM oxidized glutathione.

Procedure:

In an Eppendorf tube (3 mL volume) the following was mixed, 1.5 mL of solution A, 0.1 mL of solution B, 0.1 mL of solution C, 0.3 mL of the enzyme extract and 1 mL distilled water. The total volume was 3 mL. The reaction was started once solution B is added and the reaction mixture without solution B (NADPH) serves as the blank. The decrease in absorbance was recorded at 340 nm at intervals of 60 seconds up to five minutes. The enzyme activity was calculated based on the extinction coefficient of NADPH $6.22 \text{ mM}^{-1}\text{cm}^{-1}$ and expressed as $\text{nmol NADPH} \cdot \text{min}^{-1} \cdot \text{mg protein}^{-1}$.

3.14 Hydrogen peroxide

Plant material and extraction:

To determine the hydrogen peroxide (H_2O_2) content present in quinoa and maize leaf tissue, a simple $TiCl_4$ method was used as explained by Breenan and Frenkel (1977). Accordingly, 200 mg fresh plant material was weighed and mixed with 1 mL ice cold acetone. The extract mixture was placed in an Eppendorf and centrifuged at 10000 g for 20 minutes and stored at -20°C.

Hydrogen peroxide determination:

The supernatant was placed into new Eppendorf tubes. A 20 % (v/v) TiCl_4/HCl solution was prepared of which 0.1 mL was added to the supernatant. While gently shaking the tubes, 0.7 mL NH_4OH (1/5 strength) was added drop wise to the supernatant. While adding the NH_4OH a precipitate started to form. Hereafter, the tubes were centrifuged at 10000 g for five minutes. In order to ensure that the supernatant was colourless the precipitate was washed repetitively with 1 mL acetone after which it was centrifuged at 10000 g for five minutes. Once the supernatant was colourless, the precipitate was dissolved in 2 mL of 2N H_2SO_4 . After this the samples were centrifuged again at 10000 g for five minutes and the content was placed into glass cuvettes. The absorbance was read at 415 nm. A corresponding calibration curve was generated with known concentrations ranging from 0.2 to 2 mM.

The concentration H_2O_2 ($\text{mol L}^{-1}\text{g}^{-1}$) was determined using Beer's Law while incorporating the fresh mass of the sample used:

$$A = \epsilon bc \times \left(\frac{1}{FW}\right)$$

Where A is the absorbance, ϵ is the extinction coefficient (0.3278), b is the path length, c refers to the concentration and FW represents the fresh weight of the plant material used in the extraction.

3.15 Fresh and dry biomass

The aboveground biomass was sampled once the soil moisture reached $0.01 \text{ m}^{-3}.\text{m}^{-3}$. The pots were sampled destructively by cutting the stalks at the soil surface. The fresh weight of both quinoa and maize was determined. Hereafter, the samples were dried in an oven at 70°C for one week after which the dry mass was determined. The percentage weight difference was determined.

Additionally, the total leaf area (TLA) of both quinoa and maize was determined as the leaf area multiplied by the total number of the leaves present ($\text{m}^2 \text{ Plant}^{-1}$). The leaf area (A) was calculated using a biometric relation between the lengths of the leaves (L), the widths of the leaves (W) and the k- coefficient (Schurr, 1997). The k- coefficient of the

maize was 0.75 (Tanko and Hassan, 2106) and for the quinoa it was 0.59 (Schurr, 1997). The following formulas were used to determine the total leaf area:

$$A = L \times W \times (\text{either } 0.59 \text{ or } 0.75)$$

$$TLA = A \times \text{number of leaves}$$

3.16 Statistical analysis

Statistical analysis was implemented using SigmaPlot v12.0 software (Systat Software, Inc., San Jose California USA). Data sets with parametric distribution and differences between treatments were subjected to a one-way analysis of variance to compare treatments at the 5% significance level (Tukey test). Additionally, the correlations between variables with the same sample size were tested by Pearson's rank-order correlation for each treatment.

CHAPTER 4 RESULTS

4.1 Chlorophyll a fluorescence

4.1.1 JIP test

When analysing the OJIP curves, statistical analysis was run according to the different time intervals on the OJIP curve, for example, between 0 and 2 ms, 2 and 30 ms and 30 and 300 ms. At both the 20°C and 30°C temperature regimes, no significant differences were found between 0 and 2 ms (single turnover event) for both quinoa and maize at both temperature regimes (Figure 4-1). However, significant differences ($p < 0.05$) were found between 2 and 300 ms (multiple turnover events). In figures 4-1 A to D the changes in the chlorophyll a fluorescence transients were observed over time. At the 20°C regime (Figure 4-1 A and B) a significant decrease in the amplitudes was observed for both quinoa and maize. The same observation was found at the 30°C regime (Figure 4-1 C and D). As the water stress period progressed, the shape of the OJIP transients changed significantly, revealing the negative effect of the water stress on the photochemical potential of quinoa and maize. After 11 days of water stress, a significant difference ($p < 0.001$) was found between the control and water- stressed treatments in the multiple turnover event.

The water- stressed quinoa had a higher OJIP transient than the water- stressed maize at both temperature regimes (Figure 4-1 E and F). Once the soil water status reached $0.01 \text{ m}^{-3} \cdot \text{m}^{-3}$, the OJIP transient of the water- stressed maize decreased significantly ($p \leq 0.05$) when compared to the water- stressed quinoa. The OJIP transients of the water- stressed quinoa were significantly higher in comparison to the water- stressed maize. However, at the 20°C regime no significant differences were found between the water- stressed quinoa and the well- watered maize, signifying that the optimal fluorescence intensity of the water- stressed quinoa was equal to that of the well- watered maize. (Figure 4-1 E). When the plants were subjected to the 30°C temperature regime, quinoa had a significantly higher fluorescence intensity compared to the maize in both the well- watered and water- stressed treatments (Figure 4-1 F).

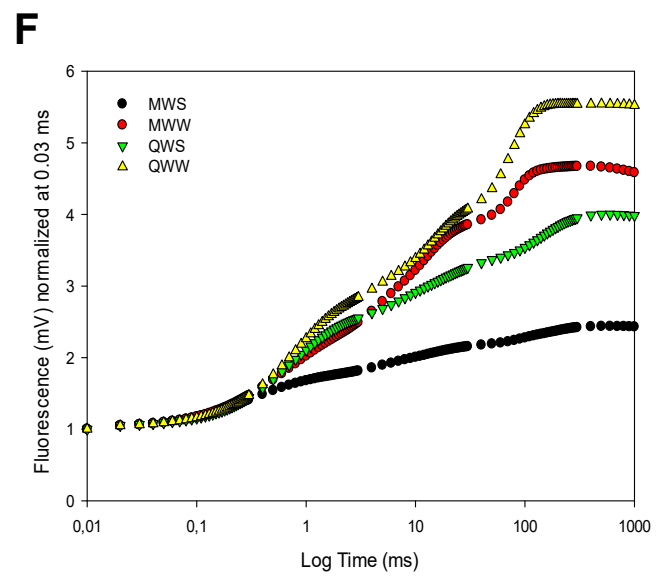
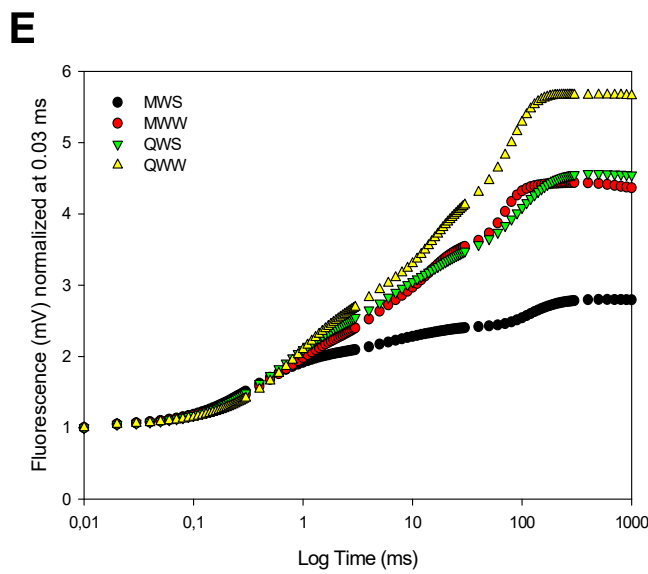
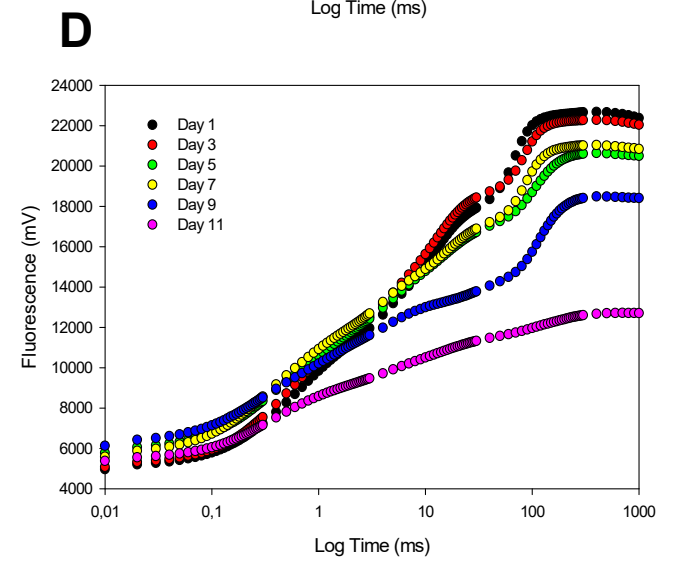
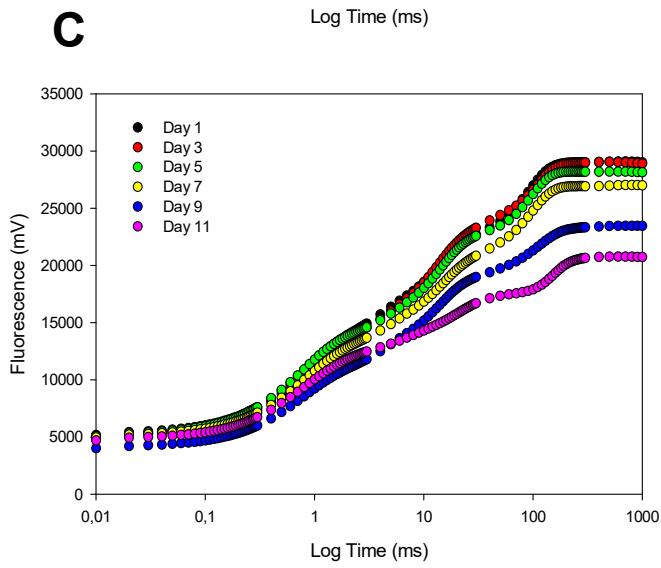
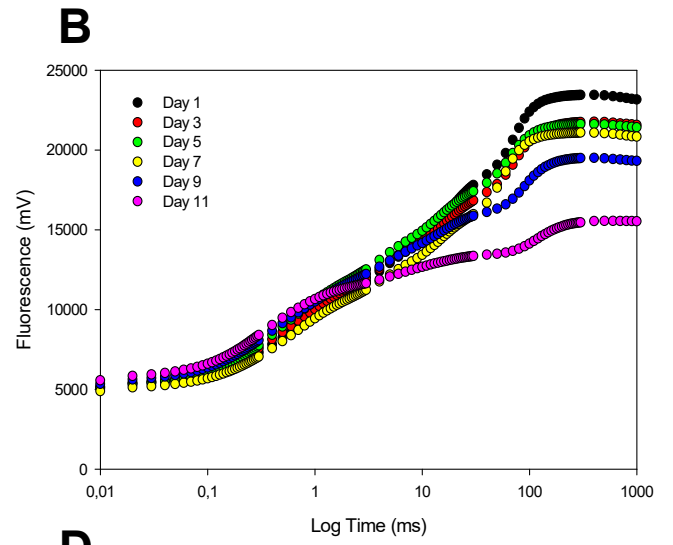
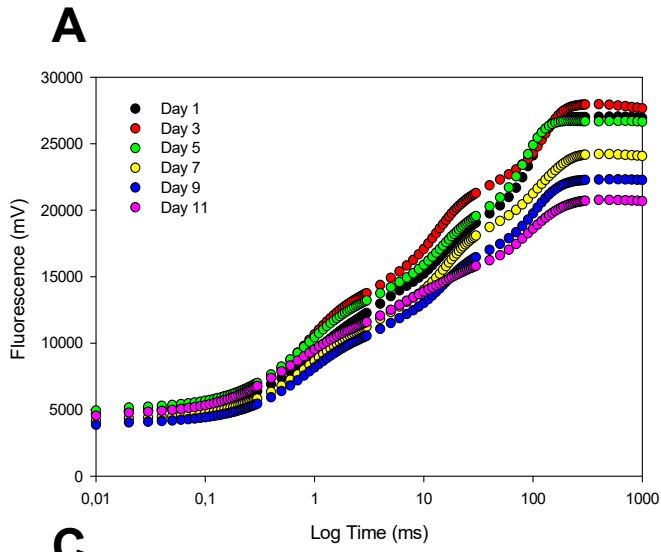


Figure 4-1: The average chlorophyll a fluorescence transient (OJIP) taken over time as the volumetric moisture content reached $0.01 \text{ m}^{-3}.\text{m}^{-3}$ (A) quinoa at 20°C , (B) maize at 20°C , (C) quinoa at 30°C and (D) maize at 30°C . Comparative chlorophyll a fluorescence transients for (E) both quinoa and maize at 20°C and (F) both quinoa and maize at 30°C . The O-J-I-P transients (E and F) were normalized at 0.03 ms and plotted on a logarithmic time scale. (MWS, maize water stress; MWW, maize well watered; QWS, quinoa water stress; QWW, quinoa well watered).

4.1.2 Difference in relative variable fluorescence (ΔV)

To fully visualize and understand the changes in the redox potential of the O-J-I-P transient, the difference in variable fluorescence (ΔV) was normalized and plotted on a logarithmic time scale. Different ΔV -bands were revealed, which describes the efficiency of electron flow through the electron transport chain. Under severe water stress, both quinoa and maize displayed $+\Delta V_K$, $+\Delta V_J$ and $-\Delta V_G$ bands (Figures 4-2 and 4-3 B, C and D). However, the water- stressed quinoa had an additional $+\Delta V_I$ band at the 30°C temperature regimes (Figures 4-3 C). The amplitudes of the Δ -bands were more apparent in the water- stressed maize. Positive ΔV -bands indicate that the flow of electrons was less efficient when compared with the control, while negative ΔV -bands values indicate that the flow of electrons was more efficient.

The ΔV_K – band

The ΔV_K - band (0.3 ms) is associated with the inactivation of the oxygen evolving complex (OEC), leading to an imbalance in the flow of electrons leaving the reaction centre and moving towards the acceptor side as well as the flow of electrons moving to the reaction centre from the donor side of photosystem II (PSII) (Yusuf *et al.*, 2010; Bussotti *et al.*, 2011; Chen *et al.*, 2016; Kalaji *et al.*, 2017; Kalaji *et al.*, 2018). In this trial a positive ΔV_K -band was found for both the water- stressed quinoa and water- stressed maize at the 20°C temperature regime. This indicated that the flow of electrons was delayed by the water stress between the acceptor side and the donor side of PSII (when the soil moisture reached $0.01 \text{ m}^{-3}.\text{m}^{-3}$) (Figure 4-2 B).

The ΔV_J – band

A positive ΔV_J - band (2 ms), indicates that the primary quinone acceptor, Quinone A (Q_A^-), is in an oxidized state (Strasser *et al.*, 2007). For this reason, the water stress influenced the flow of electrons from the reaction centre to the acceptor side for both crops at the 20°C temperature regime (Figure 4-2 D). Consequently, the flow of electrons was less efficient not being able to move beyond Q_A^- to the secondary quinone acceptor.

The ΔV_G – band

The negative ΔV_G - band (100 ms) was found in both crops at the 20°C temperature regime (Figure 4-2 C). The negative ΔV_G - band implies that there was no accumulation of plastoquinol in the thylakoid membrane (Strasser *et al.*, 2007). Consequently, there was no decrease in the reduction potential of $NADP^+$ to NADPH.

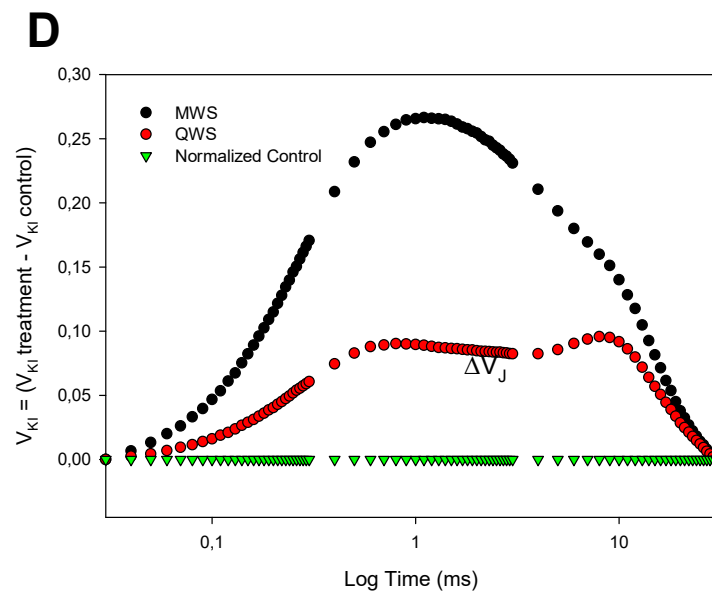
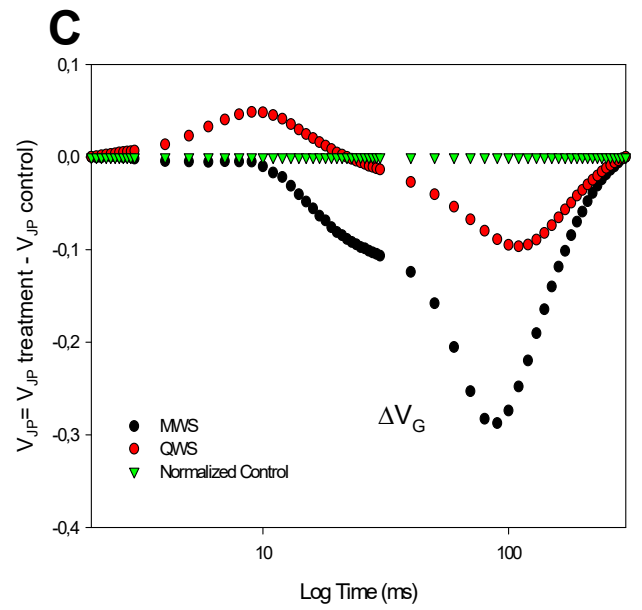
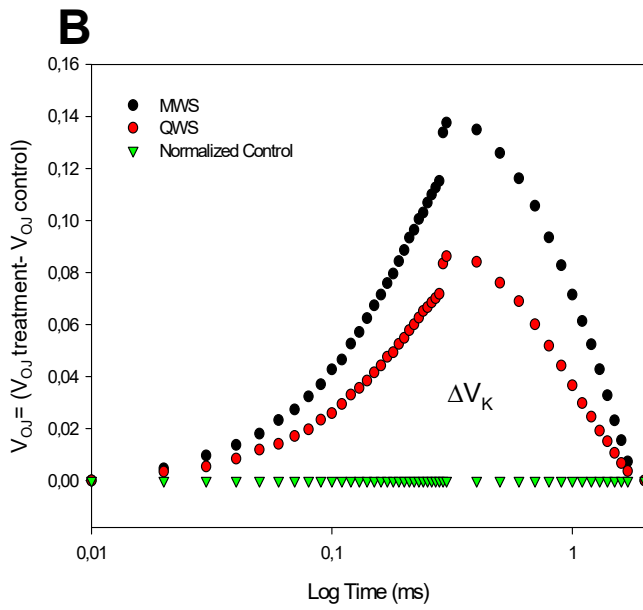
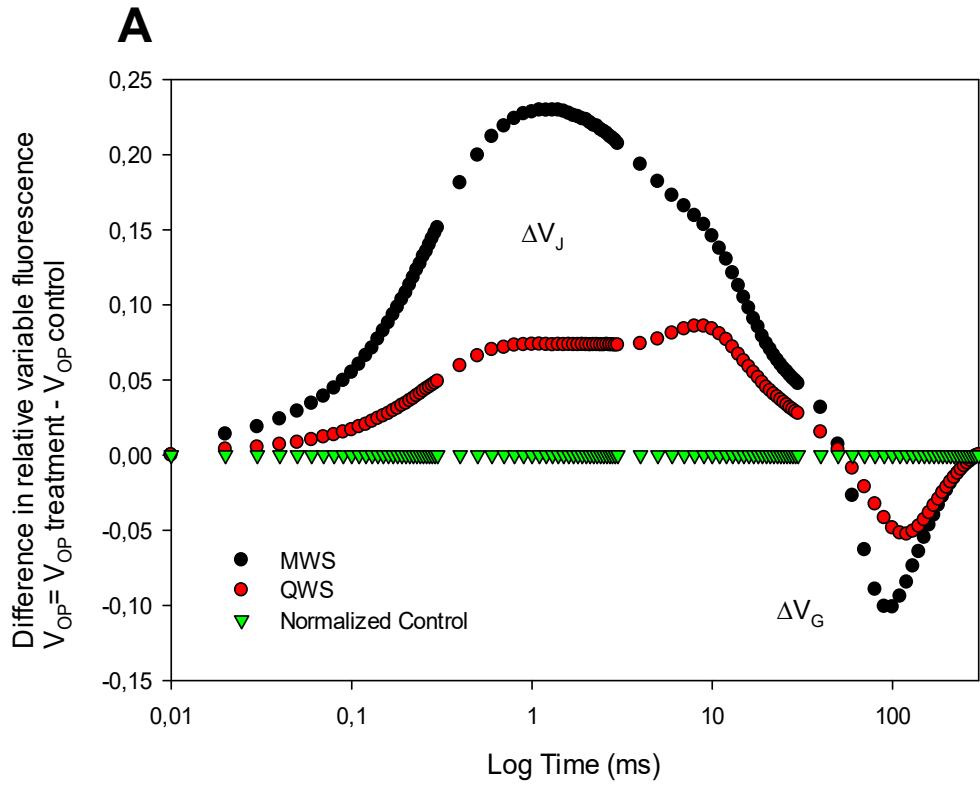


Figure 4-2: (A) Difference in relative variable fluorescence ($\Delta V_{OP} = V_{OP} \text{ treatment} - V_{OP} \text{ control}$) of intact leaves of the quinoa and maize control and water stress treatments at 20°C, normalized between 0.03 μs and 300 ms respectively to obtain the ΔV_{OJ} and ΔV_{JP} curves normalized between 0.03 and 300 ms. (B) Difference in relative variable fluorescence ($\Delta V_{OJ} = V_{OJ} \text{ treatment} - V_{OJ} \text{ control}$) normalized between 0.03 μs and 2 ms. (C) Difference in relative variable fluorescence ($\Delta V_{JP} = V_{JP} \text{ treatment} - V_{JP} \text{ control}$) normalized between 2 ms and 300 ms. (D) Difference in relative variable fluorescence ($\Delta V_{KI} = V_{KI} \text{ treatment} - V_{KI} \text{ control}$) normalized between 0.3 ms and 30 ms. (MWS, maize water stress; QWS, quinoa water stress).

Compared to the 20°C temperature regime, the same trend was observed at the 30°C temperature regime. A positive ΔV_K -band was found for the water- stressed quinoa and water- stressed maize at the 30°C temperature regime. This suggests that the water deficit stress delayed the flow of electrons between the acceptor side and the donor side of PSII (Figure 4-3 B). A positive ΔV_J - band (2 ms), was found for both the quinoa and maize. It should be noted that the amplitude of the ΔV_J - band was significantly higher compared to the water- stressed quinoa (Figure 4-3 D). This caused a reduction in the ability of electrons to move beyond Q_A^- to the secondary quinone acceptor. Additionally, both the water- stressed quinoa and maize had positive ΔV_I - bands (30 ms) (Figure 4-3 C). A positive ΔV_I – band (30 ms) implies that the transport of the electrons was affected due to the accumulation of plastoquinol. As a result, it affected the activation state of ferredoxin, NADP⁺ reductase and possibly the inhibition of the reduction of the end electron acceptors (Figure 4-3 C). This data agrees with the decrease that was observed for the amount of light energy trapped per RC ($\phi_{Po}/(1-\phi_{Po})$) (Figure 4-7). The same trend was observed for the efficiency with which an electron will move further than Q_A^- ($\psi_{Eo}/(1-\psi_{Eo})$). (Figure 4-7). The negative ΔV_G - band (100 ms) found for both crops at the 30°C temperature regime (Figure 4-3 C), implies that there was no accumulation of plastoquinol in the thylakoid membrane and no decrease occurred in the reduction of NADP⁺ to NADPH.

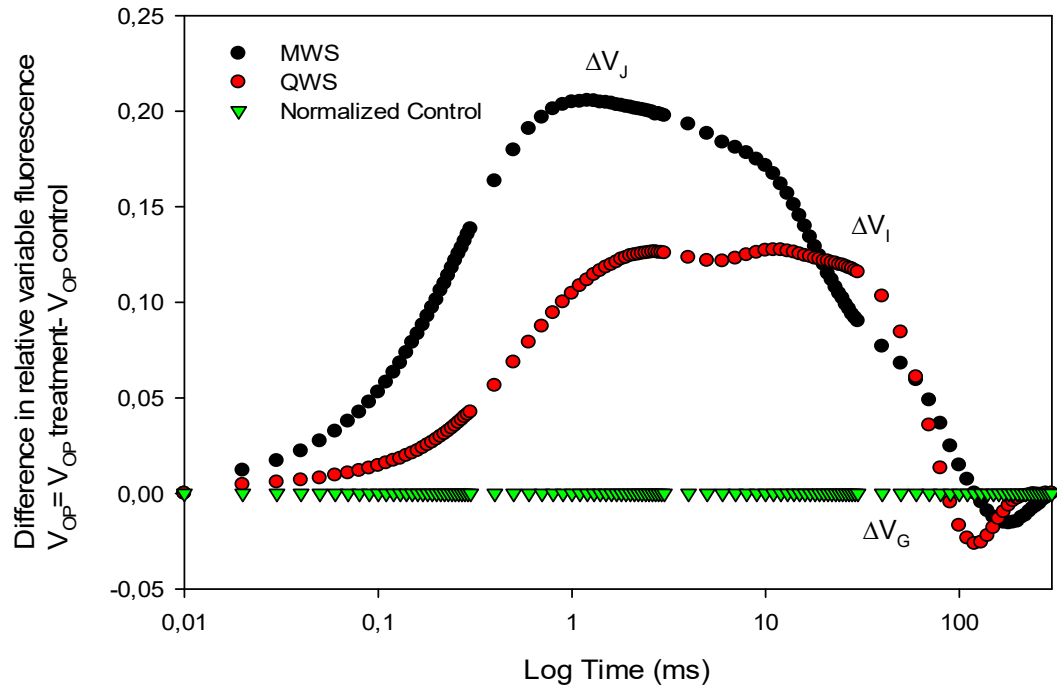
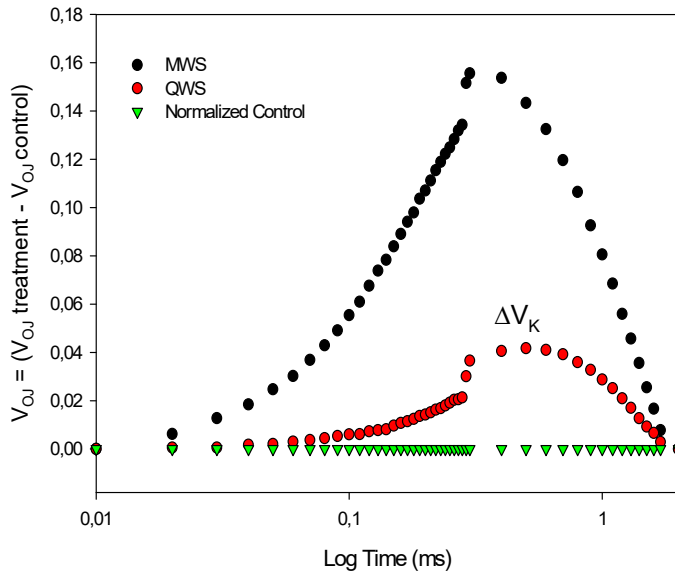
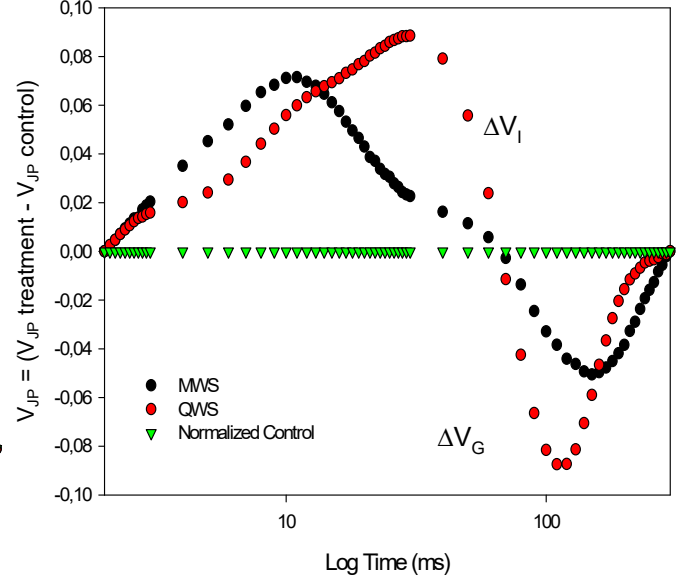
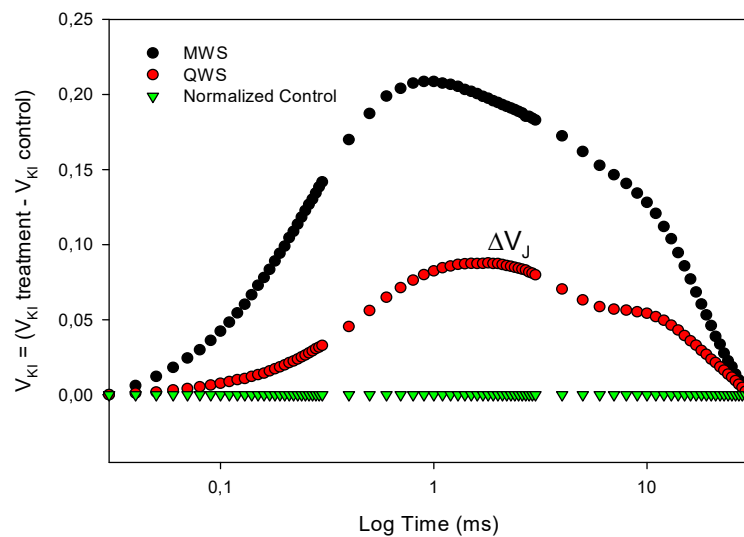
A**B****C****D**

Figure 4-3: (A) Difference in relative variable fluorescence ($\Delta V_{OP} = V_{OP} \text{ treatment} - V_{OP} \text{ control}$) of intact leaves of the quinoa and maize control and water stress treatments at 30°C, normalized between 0.03 μs and 300 ms respectively to obtain the ΔV_{OJ} and ΔV_{JP} curves normalized between 0.03 and 300 ms. (B) Difference in relative variable fluorescence ($\Delta V_{OJ} = V_{OJ} \text{ treatment} - V_{OJ} \text{ control}$) normalized between 0.03 μs and 2 ms. (C) Difference in relative variable fluorescence ($\Delta V_{JP} = V_{JP} \text{ treatment} - V_{JP} \text{ control}$) normalized between 2 ms and 300 ms. (D) Difference in relative variable fluorescence ($\Delta V_{KI} = V_{KI} \text{ treatment} - V_{KI} \text{ control}$) normalized between 0.3 ms and 30 ms. (MWS, maize water stress; QWS, quinoa water stress).

A comparative assessment was made of the ΔV_K - band for both crops at both temperature regimes (Figure 4-4). The water- stressed maize had a lower ΔV_K - band (amplitude) compared to the water- stressed quinoa. A distinct difference was observed between both temperature regimes. The water- stressed maize had a higher ΔV_K - band at the 30°C temperature regime compared to the 20°C temperature regime. This indicated that the effect of the water stress was more intense at the 30°C temperature regime having a greater effect on the OEC. However, the water- stressed quinoa had a higher ΔV_K - band at the 20°C temperature regime compared to the 30°C temperature regime. The effect of the water stress caused a delay in the flow of electrons between the acceptor side and the donor side of PSII of the water- stressed quinoa at the 20°C temperature regime.

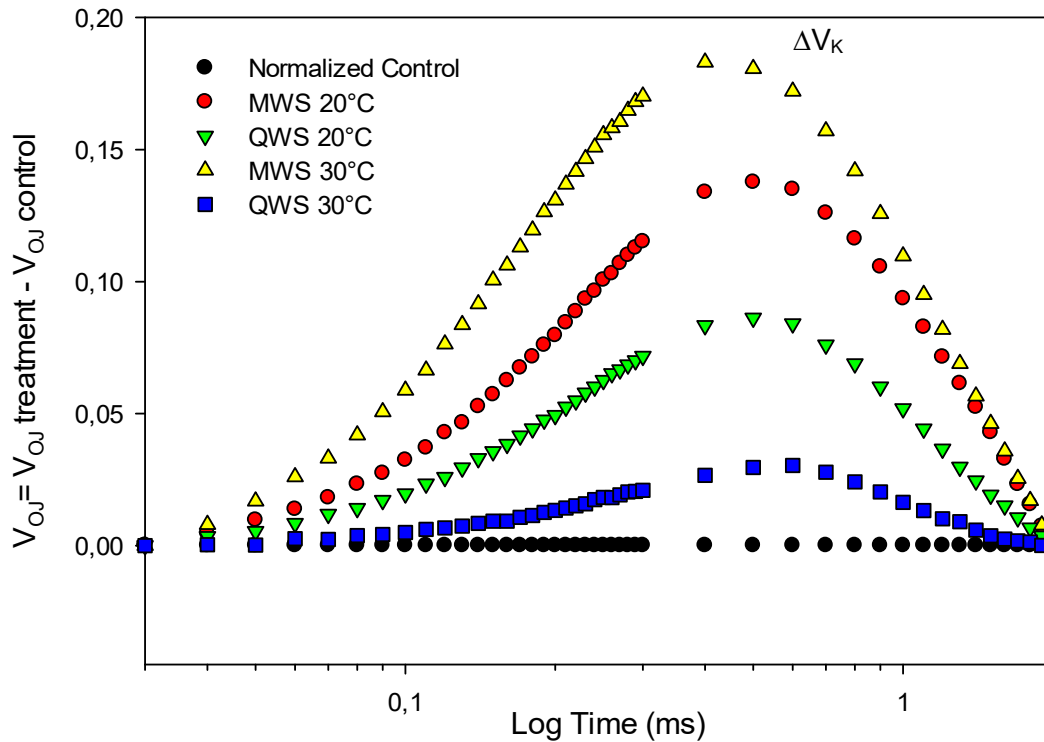


Figure 4-4: The fluorescence transients were normalized between O-J ($\Delta V_{OJ} = V_{OJ}$ treatment - V_{OJ} control) to visualize the ΔV_K - band. (MWS, maize water stress; MWW, maize well watered; QWS, quinoa water stress; QWW, quinoa well watered).

Additionally, the effect of the water stress on the I-P phase was further investigated (Figure 4-5 A and B). These transients were normalized between 30 ms and 300 ms and plotted on a logarithmic time scale. The I-P amplitude of the fluorescence rise represents the pool size of the end electron acceptors at the acceptor side of PSI (Yusuf *et al.*, 2010; Redillas *et al.*, 2011). A significant decrease ($p < 0.001$) in the pool size of the water- stressed maize was noted when compared to the respected well-watered control treatment, indicating that the regulation of the pool size had no effect on the regulation of the reduction of the end electron acceptor pool (Yusuf *et al.*, 2010). However, no significant differences ($p > 0.05$) were found between the water- stressed quinoa when compared to the well-watered quinoa at the 20°C temperature regime (Figure 4-5 A). The effect of the water deficit stress was again more pronounced at the 30°C temperature regime and significant differences were found for both the water- stressed quinoa and maize (Figure 4-5 B).

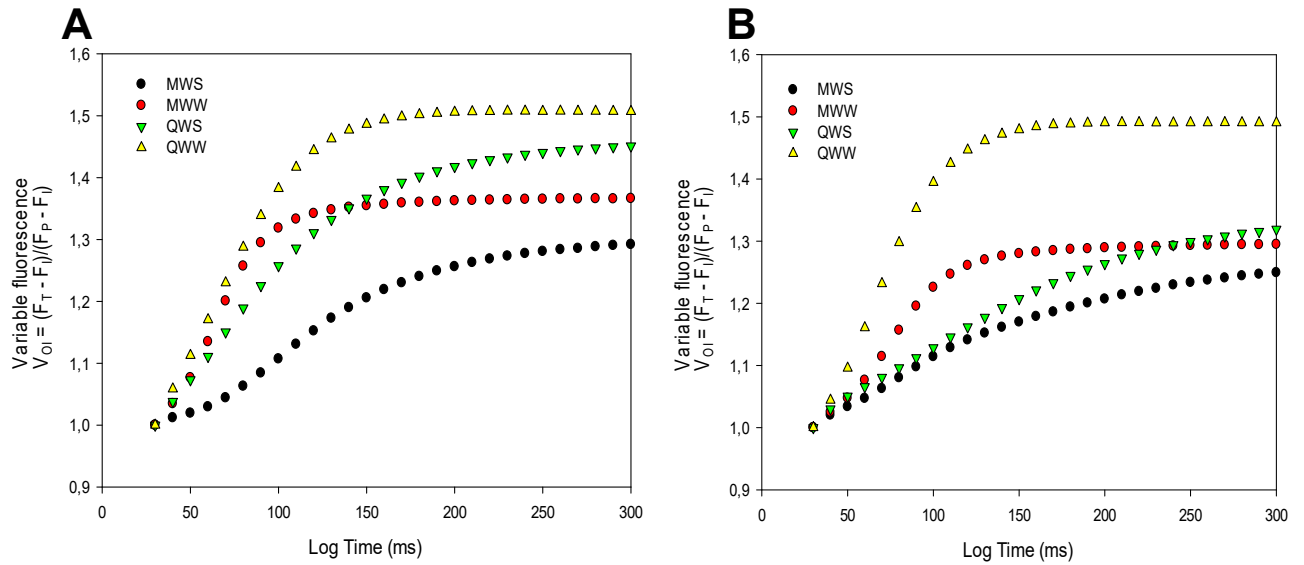


Figure 4-5: Variable fluorescence ($\Delta V_{OI} = V \text{ treatment} - V \text{ control}$) of intact leaves of the quinoa and maize control and water stress treatments normalized between 30 μs and 300 ms respectively to obtain the curves (A) at 20°C and (B) at 30°C. (MWS, maize water stress; MWW, maize well watered; QWS, quinoa water stress; QWW, quinoa well watered).

4.1.3 Fluorescence parameters

Based on the data collected (once the soil moisture status reached $0.01 \text{ m}^{-3} \cdot \text{m}^{-3}$) no significant changes were observed in the minimum fluorescence intensity (F_0) (Figure 4-6 A). This observation was found for both crops at both temperature regimes. However, the water- stressed conditions had a greater effect on the maximum fluorescence intensity (F_M) (Figure 4-6 B). No, significant differences were found in the F_M when comparing the well-watered quinoa and the water- stressed quinoa at both temperature regimes. The F_M of the water- stressed maize, decreased significantly ($p < 0.001$) compared to the well-watered maize. The same trend was observed for F_V/F_M (Figure 4-6 C). The water- stressed maize had a significantly lower ($p < 0.05$) F_V/F_M value (0.580) at 30°C when compared to the well-watered maize at 20°C ($F_V/F_M = 0.703$). No significant differences were found between the well-watered quinoa and the water- stressed quinoa when comparing the F_V/F_M . Both the well-watered quinoa and water- stressed quinoa had F_V/F_M values ranging between 0.818 and 0.816 at both temperature regimes.

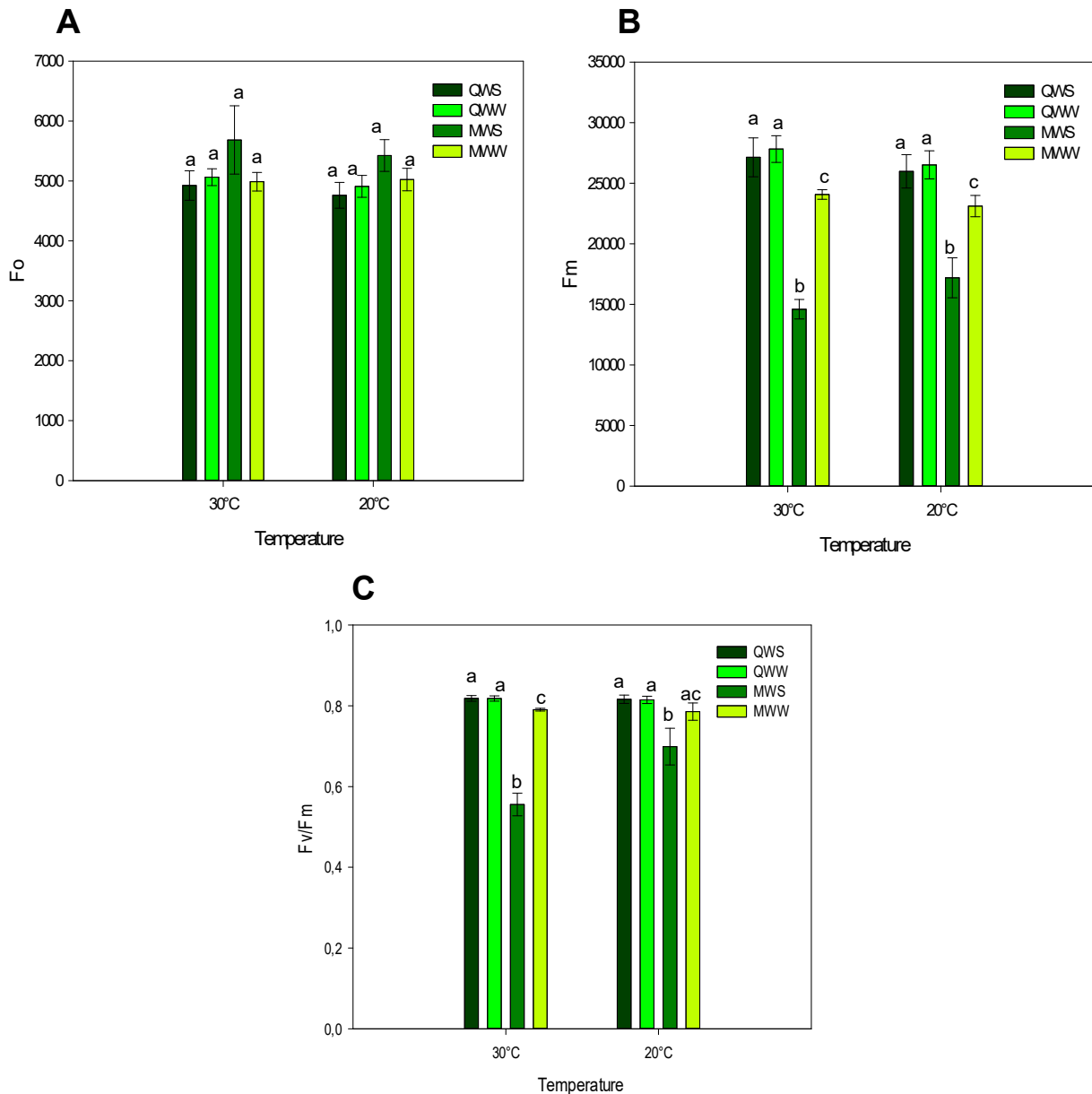


Figure 4-6: Changes in the (A) Fo, (B) Fm and (C) Fv/Fm parameters of PSII relative to the control treatments of both the water- stressed quinoa and water- stressed maize grown at 20°C and 30°C. Chlorophyll a fluorescence measurements were taken when the volumetric moisture content reached 0.01 m⁻³.m⁻³. (MWS, maize water stress; MWW, maize well watered; QWS, quinoa water stress; QWW, quinoa well watered).

A statistical ($p < 0.05$) decrease in the electron transport per reaction centre (ET_0/RC) was observed and an increase in the dissipation of heat energy per reaction centres (DI_0/RC) was found. This occurred due to an increase in the effective antenna size of

active RCs (ABS/RC) (Figure 4-7). The high amount of energy lost in the form of heat dissipation (DI_o/RC) (energy that is not utilized by photosynthesis) indicated that the maize plants were under water stress (Lauriano *et al.*, 2006; Kalaji *et al.*, 2017). The density of the active reaction centres (RCs) of the maize plants decreased significantly under water deficit stress compared to its corresponding well-watered treatment. However, no significant differences were observed for the water-stressed quinoa when compared to the well-watered plants.

Furthermore, the down regulation of PSII was influenced by the decrease in the ability to absorb light energy ($\gamma_{RC}/(1-\gamma_{RC})$), a decreased excitation of trapping energy (TR_o/RC) and a decrease in the movement of electrons between the reaction centres and Q_A^- ($\psi_{E_o}/(1-\psi_{E_o})$) (Figure 4-7). This observation was found for the water-stressed maize at both temperature regimes when compared to the respective controls. However, no significant ($p>0.05$) changes were found in the ability of the water-stressed quinoa to absorb light energy, to trap energy and to move electrons further than Q_A^- compared to the well-watered quinoa. The PSII activity of the water-stressed maize decreased significantly ($p<0.05$) compared to the water-stressed quinoa. Additionally, the water-stressed quinoa had a significantly higher ability to reduce the end electron acceptors at the PSI acceptor side ($\delta_{R_o}/(1-\delta_{R_o})$), therefore, the ability to reduce $NADP^+$ to NADPH increased compared to its respective control treatment. In contrast, the ability of the water-stressed maize to reduce $NADP^+$ to NADPH decreased significantly ($p<0.05$) when compared to the control treatments (Figure 4-7).

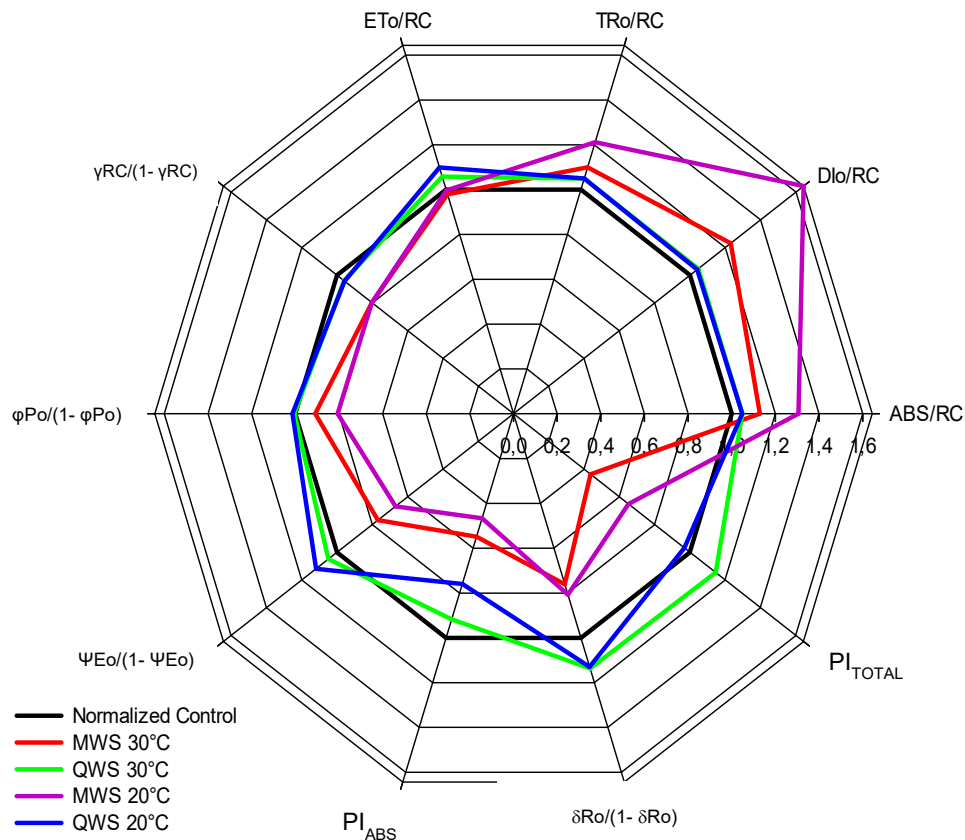


Figure 4-7: Fractional changes in selected functional and structural parameters of PSII relative to the control treatments of both the water- stressed quinoa and water- stressed maize grown at 20°C and 30°C. Chlorophyll *a* fluorescence measurements were taken when the volumetric moisture content reached 0.01 m³.m⁻³. The treatments were normalized according to their relevant controls and plotted on a multi parametric radar plot. (MWS, maize water stress; MWW, maize well watered; QWS, quinoa water stress; QWW, quinoa well watered).

In addition, the correlation between these parameters is also shown in Table 4-1 which coincides with Figure 4-7. The values marked in *italics* in Figure 4-7, are significant at $p < 0.05$. The pair of variables with positive correlation coefficients and P values below 0,050 tends to increase together. For the pairs with negative correlation coefficients and P values below 0,050, one variable tends to decrease while the other increases. For pairs with P values greater than 0,050, there is no significant relationship between the two variables.

Table 4-1: Correlation between the JIP parameters.

Crop treatment	Variables	ETo/RC	TRo/RC	Dlo/RC	ABS/RC	$\delta Ro/(1-\delta Ro)$	$\phi Po/(1-\phi Po)$	$\Psi Eo/(1-\Psi Eo)$	PI _{ABS}	$\delta Ro/(1-\delta Ro)$	PI _{TOTAL}
QWS 20°C	ETo/RC	1	0.214	0.00145	0.138	-0.0792	0.241	0.69	0.458	0.0903	0.502
	TRo/RC		1	0.913	0.988	-0.979	-0.749	-0.543	-0.678	-0.0646	-0.702
	Dlo/RC			1	0.965	-0.964	-0.944	-0.665	-0.773	0.218	-0.736
	ABS/RC				1	-0.994	-0.839	-0.601	-0.728	0.0418	-0.73
	$\delta Ro/(1-\delta Ro)$					1	0.859	0.647	0.781	-0.0352	0.778
	$\phi Po/(1-\phi Po)$						1	0.754	0.827	-0.311	0.764
	$\Psi Eo/(1-\Psi Eo)$							1	0.973	0.088	0.947
	PI _{ABS}								1	0.12	0.968
	$\delta Ro/(1-\delta Ro)$									1	0.248
	PI _{TOTAL}	0.502	-0.702	-0.736	-0.73	0.778	0.764	0.947	0.968	0.248	1
QWS 30°C	ETo/RC	1	0.901	0.794	0.922	-0.918	-0.285	0.318	-0.588	0.264	-0.053
	TRo/RC		1	0.73	0.984	-0.98	-0.0952	-0.122	-0.757	-0.0636	-0.404
	Dlo/RC			1	0.839	-0.843	-0.749	0.242	-0.659	0.171	-0.273
	ABS/RC				1	-0.998	-0.269	-0.0344	-0.774	-0.00659	-0.392
	$\delta Ro/(1-\delta Ro)$					1	0.281	0.0323	0.788	0.000972	0.392
	$\phi Po/(1-\phi Po)$						1	-0.476	0.178	-0.338	-0.014
	$\Psi Eo/(1-\Psi Eo)$							1	0.286	0.798	0.787
	PI _{ABS}								1	-0.199	0.677
	$\delta Ro/(1-\delta Ro)$									1	0.87

	PI_{TOTAL}										1
MWS 20°C	ETo/RC	1	0,509	0,234	0,353	-0,491	-0,426	0,00552	-0,234	0,456	0,038
	TRo/RC		1	0,869	0,95	-0,993	-0,971	-0,808	-0,918	0,693	-0,752
	DIo/RC			1	0,98	-0,866	-0,9	-0,722	-0,715	0,748	-0,598
	ABS/RC				1	-0,946	-0,958	-0,781	-0,811	0,724	-0,673
	$\delta Ro/(1-\delta Ro)$					1	0,988	0,816	0,949	-0,66	0,746
	$\phi Po/(1-\phi Po)$						1	0,817	0,909	-0,701	0,662
	$\Psi Eo/(1-\Psi Eo)$							1	0,837	-0,465	0,868
	PI_{ABS}								1	-0,47	0,829
	$\delta Ro/(1-\delta Ro)$									1	-0,107
		PI_{TOTAL}									
MWS 30°C	ETo/RC	1	0,261	0,901	-0,65	0,509	0,618	0,822	0,632	0,162	0,508
	TRo/RC		1	0,991	0,184	-0,515	-0,414	-0,292	-0,312	0,224	-0,466
	DIo/RC			1	0,997	-0,968	-0,98	-0,366	-0,922	0,733	-0,478
	ABS/RC				1	-0,918	-0,923	-0,79	-0,853	0,35	-0,717
	$\delta Ro/(1-\delta Ro)$					1	0,979	0,84	0,963	-0,391	0,851
	$\phi Po/(1-\phi Po)$						1	0,876	0,979	-0,373	0,829
	$\Psi Eo/(1-\Psi Eo)$							1	0,833	-0,0397	0,863
	PI_{ABS}								1	-0,407	0,849
	$\delta Ro/(1-\delta Ro)$									1	-0,113
		PI_{TOTAL}									

Changes over time in the energy flux for dissipation in the form of heat of both water-stressed quinoa and maize (DI_o/RC); the amount of electrons absorbed per RC ($y_{RC}/(1-y_{RC})$); the maximum quantum yield of primary photochemistry ($\phi_{P_o}/(1-\phi_{P_o})$); the efficiency of a trapped exciton to move an electron into the electron transport chain further than Q_A^- ($\Psi_{E_o}/(1-\Psi_{E_o})$); the efficiency with which an electron from the intersystem electron carriers moves to reduce end electron acceptors at the PS1 acceptor side ($\delta_{R_o}/(1-\delta_{R_o})$) are presented in Figure 4-8. The water-stressed maize had a significantly higher ($p < 0.05$) dissipation of heat energy compared to the water-stressed quinoa throughout the trial. This was observed at both temperature regimes (Figure 4-8 A). The water-stressed quinoa had a greater ability to absorb more electrons per RC compared to the water-stressed maize (Figure 4-8 B). The water-stressed maize also had a significantly ($p < 0.05$) higher $y_{RC}/(1-y_{RC})$ value at 20°C compared to the 30°C temperature regime. Additionally, the water-stressed quinoa had a greater maximum quantum yield of primary photochemistry compared to the water-stressed maize (Figure 4-8 C). The water-stressed maize also had a significantly ($p < 0.05$) higher $\phi_{P_o}/(1-\phi_{P_o})$ value at 20°C compared to the 30°C temperature regime. In addition, the efficiency of a trapped exciton to move an electron into the electron transport chain further than Q_A^- was observed in Figure 4-8 D. The water-stressed quinoa had a greater ability to move an electron further than Q_A^- compared to the water-stressed maize. Significant differences ($p < 0.05$) were observed between the water-stressed quinoa at both temperatures. The water-stressed quinoa also had a greater ability to move an electron further than Q_A^- at 30°C. The same trend was observed for the water-stressed maize which had a greater ability to move an electron further than Q_A^- at the 20°C temperature regime (Figure 4-8 D). Furthermore, the probability with which an electron is transferred to the reduced end electron acceptors at the PSI acceptor side was observed in Figure 4-8 E. Significant difference ($p < 0.005$) occurred between the water-stressed quinoa and water-stressed maize. Although, no significant differences were observed between the two temperature regimes for the water-stressed maize. However, the water-stressed quinoa had a greater ability to reduce the end electron acceptors at the PSI acceptor side at 20°C compared to the 30°C temperature regime (Figure 4-8 E).

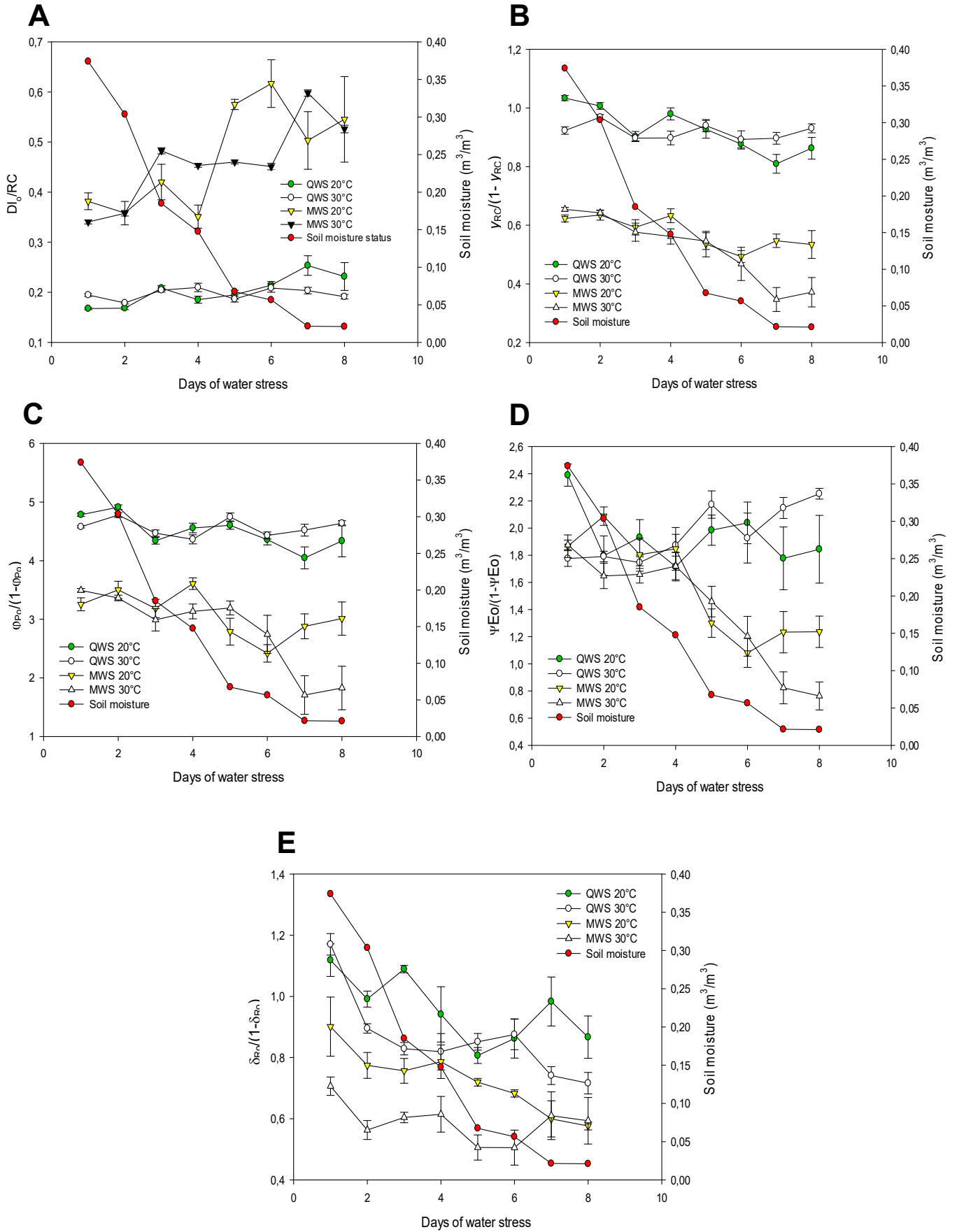


Figure 4-8: Changes in selected functional and structural parameters of PSII relative to the control treatments of both the water- stressed quinoa and water- stressed maize grown at 20°C and 30°C. (A) Changes over time in Dl_o/RC ; the energy flux for dissipation in the form of heat of both water- stressed quinoa and maize. (B) Changes over time in $y_{RC}/(1- y_{RC})$; the amount of electrons absorbed per RC. (C) Changes over time in $\phi_{Po}/(1- \phi_{Po})$; the maximum quantum yield of primary photochemistry. (D) Changes over time in $\Psi_{Eo}/(1- \Psi_{Eo})$; the efficiency of a trapped exciton to move an electron into the electron transport chain further than Q_A^- . (E) Changes over time in $\delta_{Ro}/(1- \delta_{Ro})$; the efficiency with which an electron from the intersystem electron carriers moves to reduce end electron acceptors at the PS1 acceptor side. Chlorophyll a fluorescence measurements were taken when the volumetric moisture content reached $0.01 \text{ m}^{-3} \cdot \text{m}^{-3}$. (MWS, maize water stress; MWW, maize well watered; QWS, quinoa water stress; QWW, quinoa well watered).

A decline in both the PI_{ABS} and PI_{TOTAL} values were observed, but in both cases the water- stressed quinoa had a significantly ($p < 0.05$) higher PI_{ABS} and PI_{TOTAL} compared to the water- stressed maize. In Figure 4-8, a steady decline in both the PI_{ABS} and PI_{TOTAL} was noted for both quinoa and maize compared to the declining soil moisture status. However the water- stressed quinoa had significantly higher PI_{ABS} and PI_{TOTAL} values. Table 4-1, indicates the percentage difference between the water- stressed maize and quinoa.

Table 4-2: The percentage difference between the water- stressed maize and quinoa at both the 20°C and 30°C regimes.

	20°C	30°C
PI_{TOTAL}	164.99 %	150.34 %
PI_{ABS}	139.56 %	130.37 %

Water stress conditions (severe drought stress, soil moisture content $\leq 0.01 \text{ m}^{-3} \cdot \text{m}^{-3}$). Note these percentages are based on the last day of the water- stressed trial.

The higher PI_{ABS} and PI_{TOTAL} values observed in the quinoa suggest that the water stressed quinoa had a more efficient photochemical efficiency compared to water- stressed maize. This trend was observed at both the 20°C and 30°C temperature

regimes. However, the effect of water deficit stress was significantly ($p < 0.05$) higher at the 30°C temperature regime compared to the 20°C temperature regime.

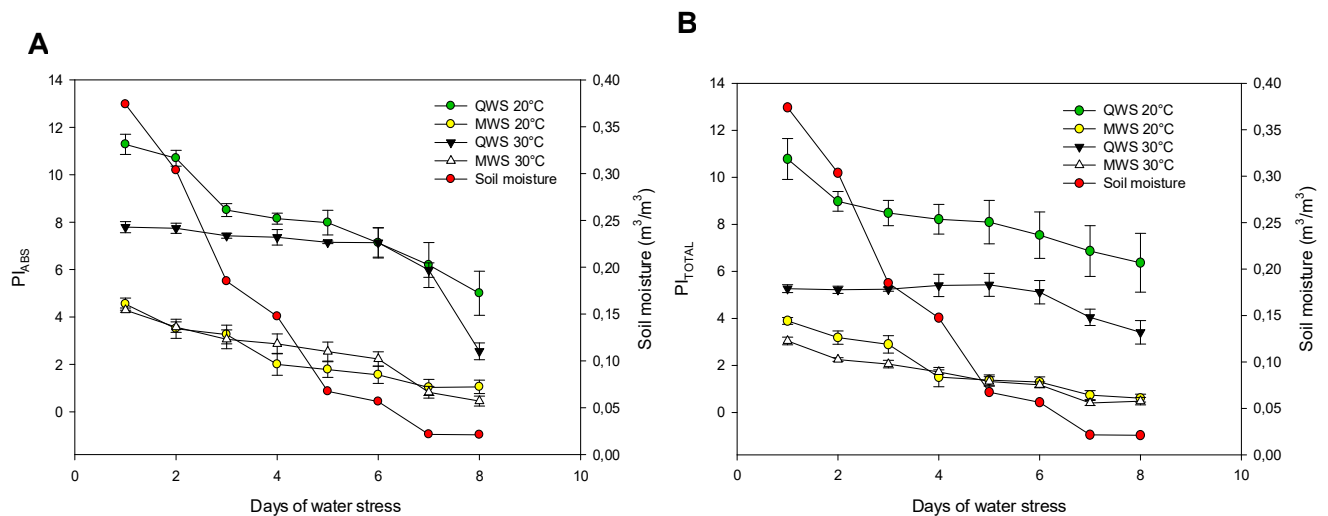


Figure 4-9: The (A) PI_{ABS} and (B) PI_{TOTAL} values of both quinoa and maize at 20°C and 30°C compared to the declining soil moisture status (severe drought stress, soil moisture content $\leq 0.01 \text{ m}^{-3} \cdot \text{m}^{-3}$). (MWS, maize water stress; MWW, maize well watered; QWS, quinoa water stress; QWW, quinoa well watered).

4.1.4 Vitality index scale

Additionally, a vitality index was created for both quinoa and maize using the data collected for the PI_{TOTAL} (Table 4-2). Yusuf *et al.* (2010) described the PI_{TOTAL} as the most sensitive parameter, since it incorporates several parameters that are evaluated from the OJIP transient. This index could be helpful to farmers in quantifying the physiological vitality of crop species during various stress conditions, in this case, water deficit stress. The steady decrease in the PI_{TOTAL} , which was in accordance with the decrease in the soil moisture status, provided information regarding the performance of the photosynthetic apparatus of both quinoa and maize over time during the water stress trial. Generally, the maize had significantly ($p < 0.05$) lower PI_{TOTAL} values compared to the quinoa. A PI_{TOTAL} value of above 4 (maize) and 6 (quinoa) could indicate that the crops were not under any stress and that it had an optimal photochemical potential. Whereas, any values below 1 (maize) and 2 (quinoa) indicated that the plants were under severe stress.

Table 4-3: A vitality index for quinoa and maize based on the PI_{TOTAL} values.

	Maize	Quinoa
Good- No stress	≥ 4	≥ 6
Fine	1 – 3	3 – 5
Poor conditions- severe stress	< 1	< 2

Note that these are estimated values.

4.1.5 Modulated reflection

During stress conditions, a series of changes can occur with the photo-induced transitions of the MR820 signal. Firstly, the amplitude and rate of increase in the slow phase will change which coincides with the inhibition of electron donors from PSII. Secondly, the initial decline in the signal in the fast phase is delayed due to an inhibition of the photochemical reaction in photosystem I (PSI) (Goltsev *et al.*, 2012). Changes in the modulated light reflection at 820 nm can be seen over time in Figures 4-9 A to D. At both temperature regimes little to no changes were observed in the MR_{min} parameters of the water- stressed quinoa (Figures 4-9 A and C). As the water stress period progressed, significant changes were observed in the MR_{min} parameters for the water-stressed maize. Based on the results obtained, it should be noted that the transition at 820 nm was significantly ($p < 0.05$) affected by the water stress in the maize at both temperature regimes (Figure 4-9 E and F). At both 20°C and 30°C the value of the MR_{min} parameters were the highest for the water- stressed maize. The value of the MR_{min} parameters of the water- stressed quinoa was lower than both the water-stressed and well-watered maize at the 20°C temperature regime (Figure 4-9 E).

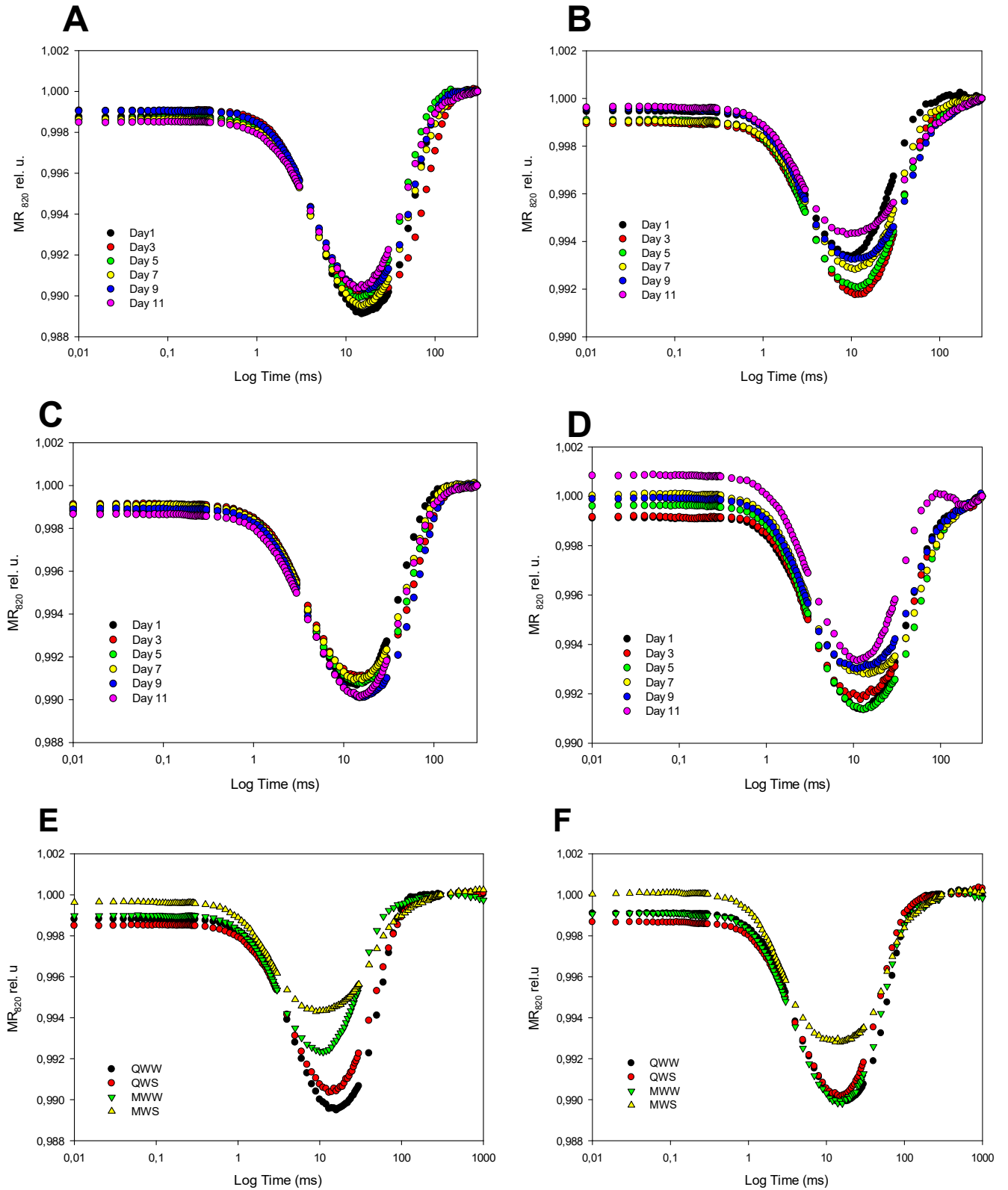


Figure 4-10: Kinetics of the modulated light reflection at 820 nm in dark adapted leaves under water stress (severe drought stress, soil moisture content $\leq 0.01 \text{ m}^3 \cdot \text{m}^{-3}$) for (A) quinoa at 20°C, (B) maize at 20°C, (C) quinoa at 30°C and (D) maize at 30°C. Comparative

MR 820 nm reflection transients for (E) both quinoa and maize at 20°C and (F) both quinoa and maize at 30°C. (MWS, maize water stress; MWW, maize well watered; QWS, quinoa water stress; QWW, quinoa well watered).

The parameters of the relative MR signal were determined for both the quinoa and maize. The V_{ox} parameter refers to the rate of initial photo oxidation of the photosystem I primary donor ($P700^+$), whereas V_{red} refers to the rate of the re-reduction of $P700^+$ via the electrons from PSII and the reduced plastoquinone pool (PQ pool) (Dąbrowski *et al.*, 2017). The V_{ox} results showed that no significant ($p>0.05$) differences occurred between the water- stressed treatments and the control treatments of both quinoa and maize at the 30°C temperature regime (Table 4-3). The water stress, therefore, had little effect on the V_{ox} of both quinoa and maize at the 30°C temperature regime. However, at the 20°C temperature regime the V_{ox} rate of the water- stressed maize was inhibited, and differed significantly ($p<0.05$) from the well-water maize and quinoa treatments. No significant ($p>0.05$) differences were found between the V_{ox} of the water- stressed quinoa and the well-water quinoa, indicating that the water stress had no effect on the photo oxidation of $P700^+$ at the 20°C temperature regime.

Significant differences were found in the V_{red} parameter between the water- stressed maize and the well- watered maize (Table 4-3). The rate of $P700^+$ re-oxidation was significantly ($p<0.05$) inhibited in the water- stressed maize. This trend was found at both temperature regimes. Once again, no significant ($p>0.05$) differences were found in the V_{red} parameter between the water- stressed quinoa and the well- watered quinoa.

Table 4-4: Parameters derived from 820 nm modulated reflection (MR_t/MR_0) in leaves of both quinoa and maize under water stress conditions (severe drought stress, soil moisture content $\leq 0.01 \text{ m}^{-3} \cdot \text{m}^{-3}$) at 20°C and 30°C (11 days of water stress). (MWS, maize water stress; MWW, maize well watered; QWS, quinoa water stress; QWW, quinoa well watered).

Treatment	30°C		20°C	
	V_{ox}	V_{red}	V_{ox}	V_{red}
MWW	-0.2400 ^a	0.3133 ^a	-0,2175 ^a	0,3225 ^a
MWS	-0.2311 ^a	0.1956 ^b	-0,1583 ^b	0,2041 ^b
QWW	-0.3017 ^a	0.3217 ^a	-0,3025 ^a	0,4051 ^a
QWS	-0.2690 ^a	0.3730 ^a	-0,2583 ^a	0,3566 ^a

V_{ox} – P700 and PC oxidation velocity (maximum slope decrease of MR_t/MR_0); V_{red} – P700 and PC re-reduction velocity (maximum slope increase of MR_t/MR_0). Treatment values not connected by the same letters are significantly different ($P < 0.05$).

In Figure 4-10 changes in the ability of both plants to oxidize P700 and to reduce P700⁺ was observed over time in both temperature regimes. The water- stressed quinoa was able to maintain its ability to oxidize P700 at both the 20°C and 30°C temperature regimes (Figure 4-10 A and B). However, a significant difference ($p < 0.05$) was found in the ability to oxidize P700 between the water- stressed quinoa and the water- stressed maize at both temperature regimes. The water- stressed quinoa had a greater ability to oxidize P700 compared to the water- stressed maize.

A significant decrease ($p < 0.05$) was found in the ability of the water- stressed maize to reduce P700⁺ (Figure 4-10 C and D). This decrease was observed at both temperature regimes. Whereas, the water- stressed quinoa was able to maintain its ability to reduce P700⁺ throughout the water stress trial.

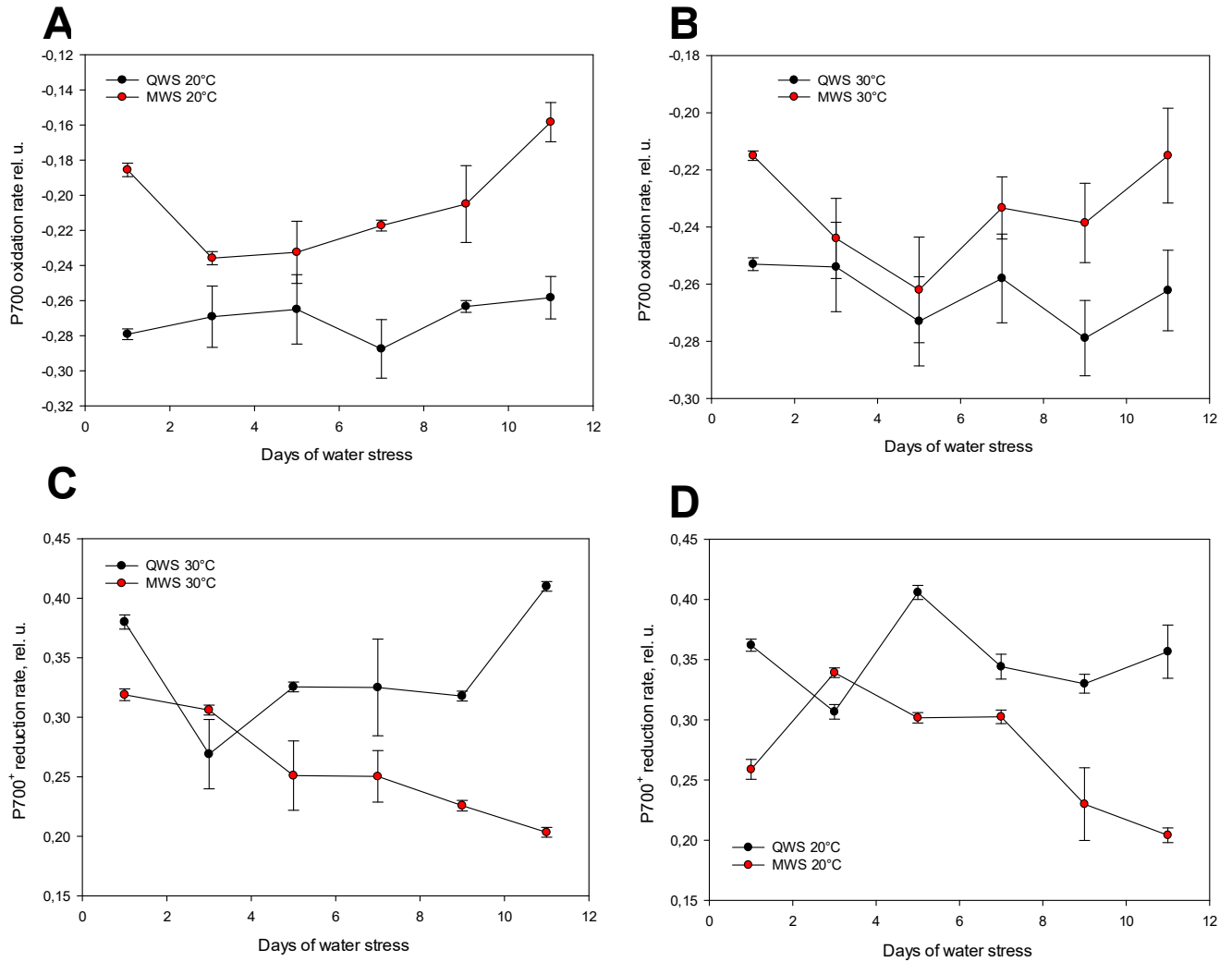


Figure 4-11: Parameters derived from 820 nm modulated reflection (MR_t/MR_0) in leaves of both quinoa and maize under water stress conditions over time (severe drought stress, soil moisture content $\leq 0.01 \text{ m}^{-3} \cdot \text{m}^{-3}$). (A) P700 oxidation rate of quinoa and maize at 20°C. (B) P700 oxidation rate of quinoa and maize at 30°C. (C) P700⁺ reduction rate of quinoa and maize at 20°C. (D) P700⁺ reduction rate of quinoa and maize at 30°C. (MWS, maize water stress; QWS, quinoa water stress).

Additionally, the difference between the MR_0 and MR_{\min} parameters were determined in order to represent the difference in the amplitudes of the $MR_{820 \text{ nm}}$ signal over time (Figure 4-11). Based on the data collected, the water-stressed quinoa had a greater difference in the MR_0/MR_{\min} value, indicating that it had a greater ability to oxidize P700⁺ and to re-reduce P700⁺. The water-stressed quinoa therefore had a greater ability to reduce NADP⁺. In contrast, the water-stressed maize had a smaller difference in the

MR_0/MR_{min} value, indicating that the water stress conditions had a more negative effect on the photochemical activities of maize. This trend was noted in both temperature regimes.

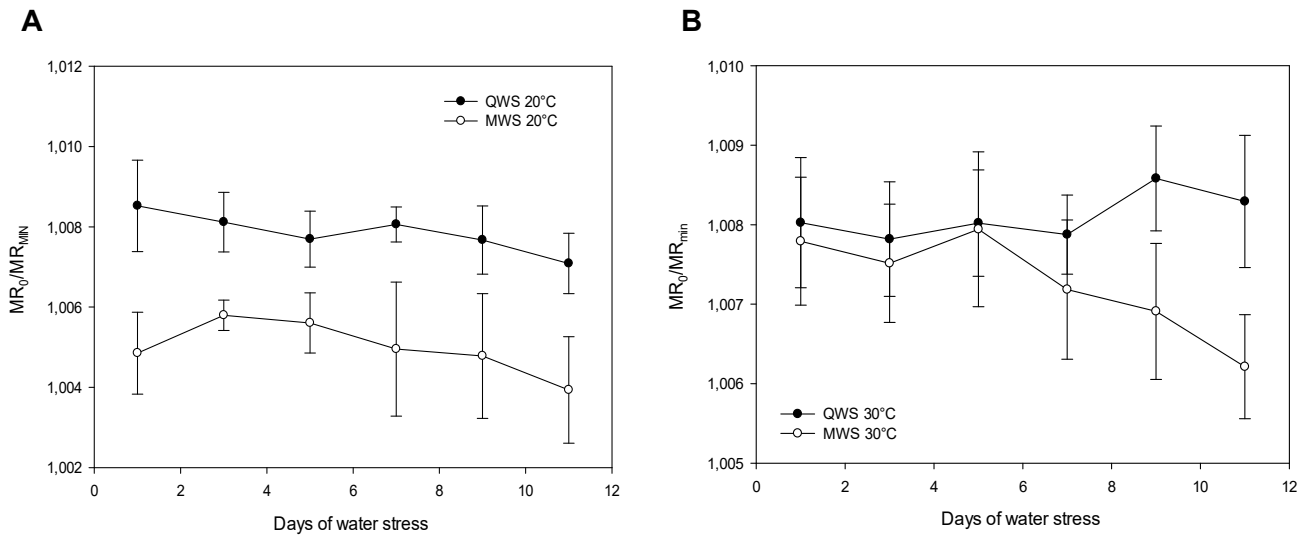


Figure 4-12: The difference between MR_0 and MR_{min} representing the difference in the amplitudes and rise of increase of the MR820 nm signal of both quinoa and maize under water stress (severe drought stress, soil moisture content $\leq 0.01 \text{ m}^{-3} \cdot \text{m}^{-3}$) at (A) 20°C and (B) 30°C. (MWS, maize water stress; QWS, quinoa water stress).

4.2 Membrane leakage

Abiotic stress tends to cause membrane damage and deterioration, thereby initiating membrane leakage (Peng *et al.*, 2004; Melkonian *et al.*, 2004). Water and temperature stress modifies the structure and composition of the cell membranes (Rahman *et al.*, 2004). For the membrane fluidity to cope with the water and temperature stress effectively, the plants alter the composition of their membranes to optimize fluidity for a given temperature (Buchanan *et al.*, 2009). In this trial there was a significant difference ($p < 0.001$) between the water- stressed quinoa and the water- stressed maize (Figure 4-12). The water- stressed quinoa had a greater ability to maintain its membrane fluidity compared to the water-stressed maize. The water- stressed maize had a 20% greater membrane leakage compared to the water- stressed quinoa at the 30°C temperature regime and a 33% greater membrane leakage at the 20°C. However, no significant ($p > 0.05$) differences were found between the two temperature regimes.

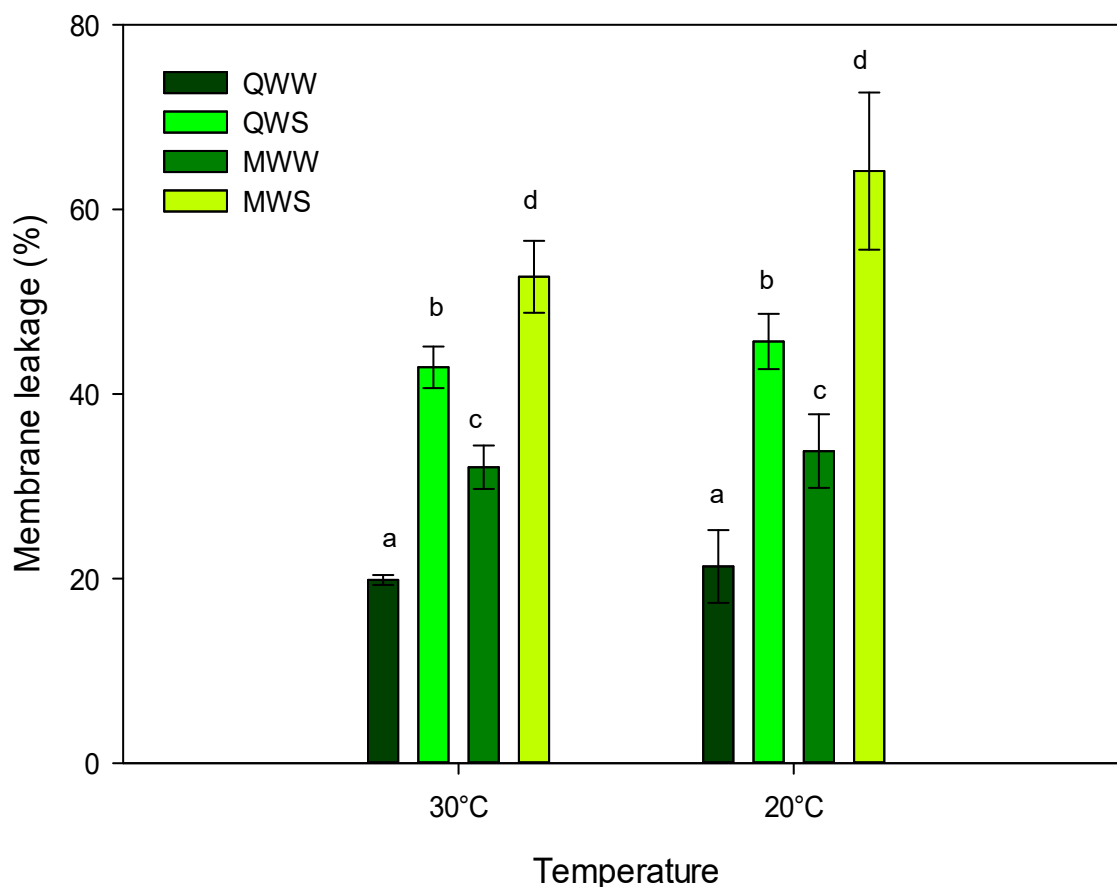


Figure 4-13: The membrane leakage (%) of both quinoa and maize under water- stressed conditions (severe drought stress, soil moisture content $\leq 0.01 \text{ m}^{-3} \cdot \text{m}^{-3}$) at 20°C and 30°C. Treatment values not connected by the same letters are significantly different ($P < 0.05$). (MWS, maize water stress; MWW, maize well watered; QWS, quinoa water stress; QWW, quinoa well watered).

4.3 Relative leaf water content

The leaf water content is one of the most suitable measures of the plant water status in terms of the physiological significance of cellular water stress. The leaf water content is useful in dealing with water transport in the soil-plant-atmosphere continuum as an estimate of the energy status of plant water (Barr and Weatherley, 1962) (Figure 4-13). During this trial, the water- stressed quinoa had a significantly higher ($p < 0.05$) leaf water content compared to the water- stressed maize at both temperature regimes. At 30°C

the water- stressed quinoa had a 16.4% higher leaf water content compared to water- stressed maize, and a 15% higher leaf water potential at the 20°C temperature regime. No significant differences were observed between the two temperature regimes.

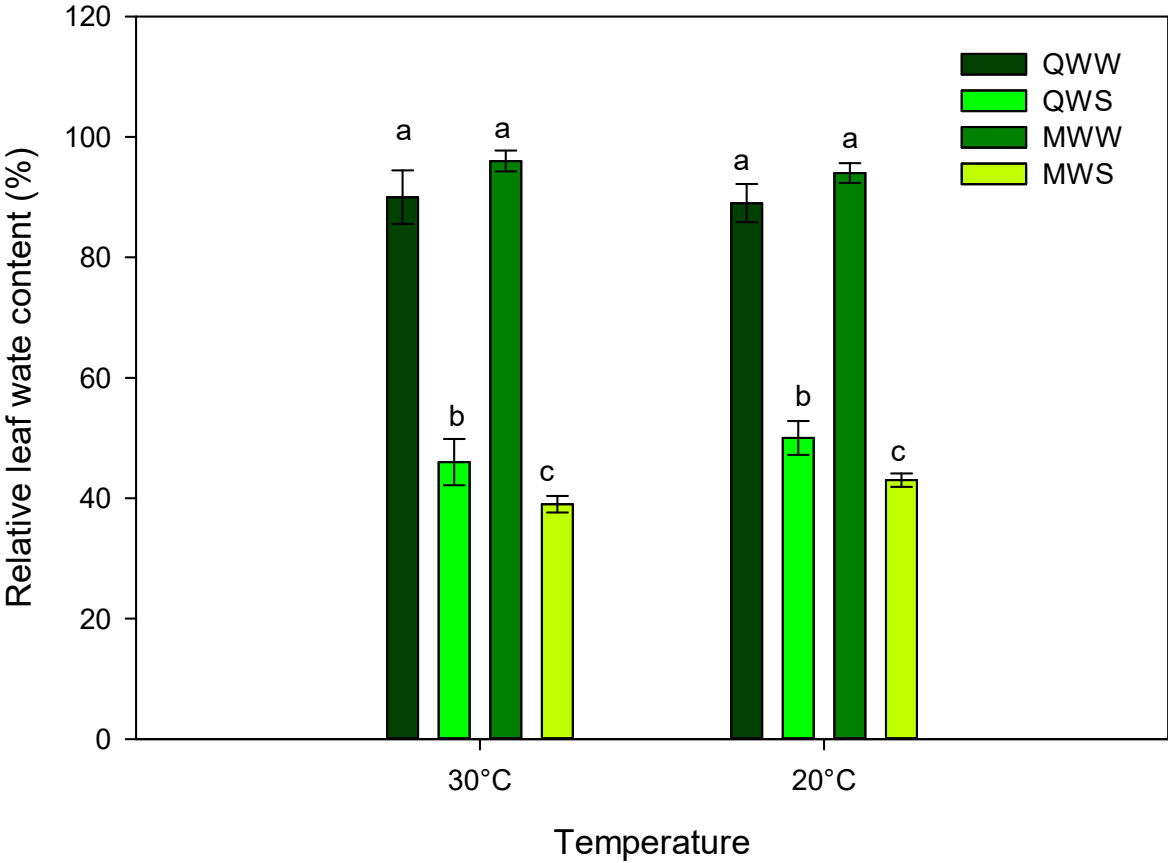


Figure 4-14: The relative leaf water content (%) of both quinoa and maize under water- stressed conditions (severe drought stress, soil moisture content $\leq 0.01 \text{ m}^{-3}.\text{m}^{-3}$) at 20°C and 30°C. Treatment values not connected by the same letters are significantly different ($P < 0.05$). (MWS, maize water stress; MWW, maize well watered; QWS, quinoa water stress; QWW, quinoa well watered).

4.4 Stomatal conductance

After 8 days of water stress, the stomatal conductance of both the quinoa and maize decreased significantly. At both temperature regimes the water- stressed quinoa had a significantly higher ($p < 0.001$) stomatal conductance compared to the water- stressed

maize (Figure 4-14). After 5 days of water stress the stomatal conductance of the water-stressed quinoa ranged between 122 and 126 $\text{mmol m}^{-2} \text{s}^{-1}$ and for the maize between 15 and 19 $\text{mmol m}^{-2} \text{s}^{-1}$ (20°C). At 30°C , the stomatal conductance of the water-stressed quinoa ranged between 169 and 173 $\text{mmol m}^{-2} \text{s}^{-1}$ and for the maize between 10 and 14 $\text{mmol m}^{-2} \text{s}^{-1}$. Once the soil moisture reached $0.01 \text{ m}^{-3} \cdot \text{m}^{-3}$, the stomatal conductance of the water-stressed quinoa ranged between 33 and 37 $\text{mmol m}^{-2} \text{s}^{-1}$ and for the maize between 8 and 11 $\text{mmol m}^{-2} \text{s}^{-1}$ (20°C). At 30°C , the stomatal conductance of the water-stressed quinoa ranged between 39 and 43 $\text{mmol m}^{-2} \text{s}^{-1}$ and for the maize between 5 and 7 $\text{mmol m}^{-2} \text{s}^{-1}$. During this trial, the water-stressed quinoa had a 108 % greater stomatal conductance at the 20°C temperature range and a 92 % greater stomatal conductance in the 30°C temperature range compared to the maize

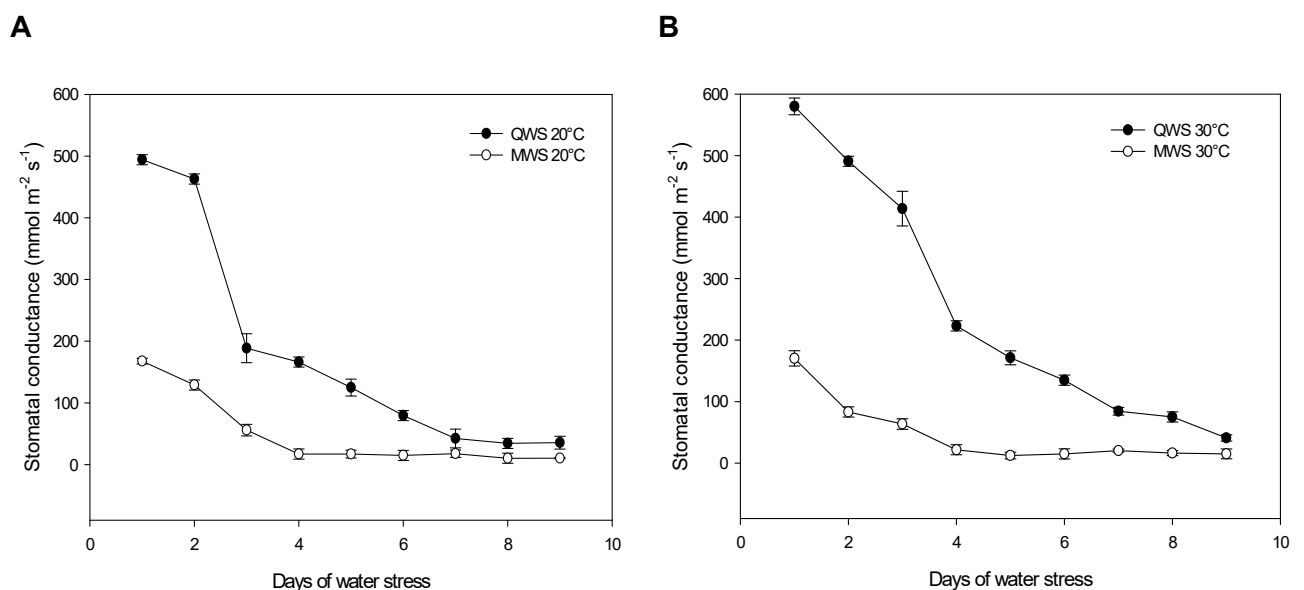


Figure 4-15: The stomatal conductance ($\text{mmol m}^{-2} \text{s}^{-1}$) of both quinoa and maize under water-stressed conditions (severe drought stress, soil moisture content $\leq 0.01 \text{ m}^{-3} \cdot \text{m}^{-3}$) at (A) 20°C and (B) 30°C . (MWS, maize water stress; QWS, quinoa water stress).

4.5 Chlorophyll content

The chlorophyll content of the water-stressed maize decreased significantly ($p < 0.05$) compared to the water-stressed quinoa (Figure 4-15). After 5 days of water stress the

chlorophyll content of the water- stressed quinoa ranged between 36 and 40 $\mu\text{mol m}^{-2}$, similarly the chlorophyll content of the water- stressed maize ranged between 34 and 38 $\mu\text{mol m}^{-2}$ (20°C). At the 30°C temperature regime the chlorophyll content ranged between 33 and 37 $\mu\text{mol m}^{-2}$ for the water- stressed quinoa and between 27 and 29 $\mu\text{mol m}^{-2}$ for the maize. After 5 days of water stress, the chlorophyll content of the water- stressed quinoa increased significantly ($P<0.05$) compared to the water- stressed maize. After 8 days of water stress the chlorophyll content of the water- stressed quinoa ranged between 47 and 51 $\mu\text{mol m}^{-2}$, similarly the chlorophyll content of the water- stressed maize ranged between 28 and 32 $\mu\text{mol m}^{-2}$ (20°C) (Figure 4-15 A). At the 30°C temperature regime the chlorophyll content ranged between 49 and 53 $\mu\text{mol m}^{-2}$ for the water- stressed quinoa and between 23 and 27 $\mu\text{mol m}^{-2}$ for the maize. After 9 days of water stress, the water- stressed quinoa had a 48% higher chlorophyll content compared to the water- stressed maize in the 30°C temperature regime and a 68% higher chlorophyll content compared to the water- stressed maize in the 30°C temperature regime (Figure 4-15 B).

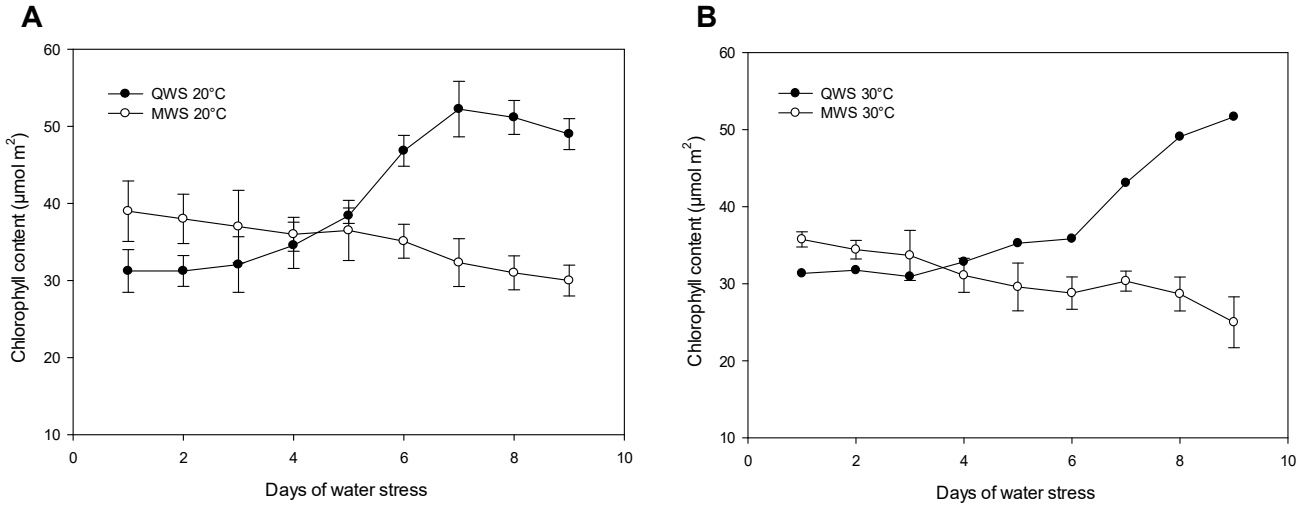


Figure 4-16: The chlorophyll content ($\mu\text{mol m}^{-2}$) of both quinoa and maize under water-stressed conditions (severe drought stress, soil moisture content $\leq 0.01 \text{ m}^{-3}.\text{m}^{-3}$) at (A) 20°C and (B) 30°C . (MWS, maize water stress; MWW, maize well watered; QWS, quinoa water stress; QWW, quinoa well watered).

4.6 Proline content

Increased levels of proline play an important role in regulating the cellular homeostasis and redox potential of plants exposed to stress conditions (Mansour and Ali, 2017). When exposed to water deficit stress, both the water- stressed quinoa and maize produced significantly ($p < 0.001$) higher levels of proline compared to the respective control treatments (Figure 4-16). However, the water- stressed quinoa produced 34.72% more proline compared to the water- stressed maize at the 20°C temperature regime. Similarly, the water- stressed quinoa produced 49% more proline at the 30°C temperature regime compared to the water- stressed maize. In addition, significant differences were found between the two temperature regimes. The water- stressed quinoa produced significantly ($p < 0.001$) more proline (48.69%) at the 30°C temperature regime compared to the 20°C temperature regime. The same trend was found when comparing the proline content of the maize between the 20°C and 30°C temperature regimes (Figure 4-16).

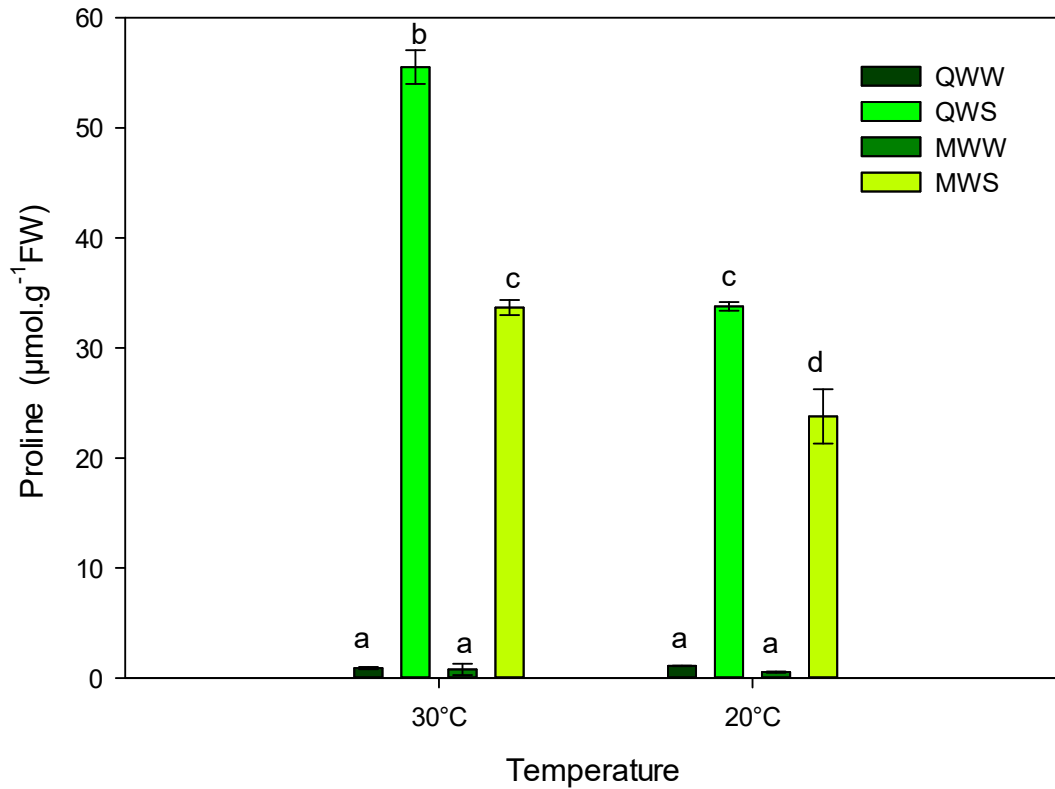


Figure 4-17: The proline content ($\mu\text{mol.g}^{-1}$ FW) of both quinoa and maize under water-stressed conditions (severe drought stress, soil moisture content $\leq 0.01 \text{ m}^{-3}.\text{m}^{-3}$) at 20°C and 30°C . Treatment values not connected by the same letters are significantly different ($P < 0.05$). (MWS, maize water stress; MWW, maize well watered; QWS, quinoa water stress; QWW, quinoa well watered).

4.7 Superoxide dismutase content

Superoxide dismutase (SOD) rapidly converts ROS into H_2O_2 and O_2 , thereby acting as the first line of antioxidant defence (Saibi and Brini, 2018). Once more the activity of the superoxide dismutase was significantly ($p < 0.05$) greater for the water-stressed quinoa when compared to the water-stressed maize (Figure 4-17). This trend was observed in both temperature regimes, however, significant differences ($p < 0.05$) were also observed between the two temperature regimes. The water-stressed quinoa had a significantly ($p < 0.05$) higher superoxide dismutase activity (27.77%) at the 20°C temperature regime compared to the water-stressed maize at the 30°C temperature regime. The water-

stressed quinoa had a 52.98% higher superoxide dismutase activity at the 20°C temperature regime compared to the water- stressed maize. In addition, the water- stressed quinoa had a 15.17% higher superoxide dismutase activity at the 30°C temperature regime compared to the water- stressed maize (Figure 4-17).

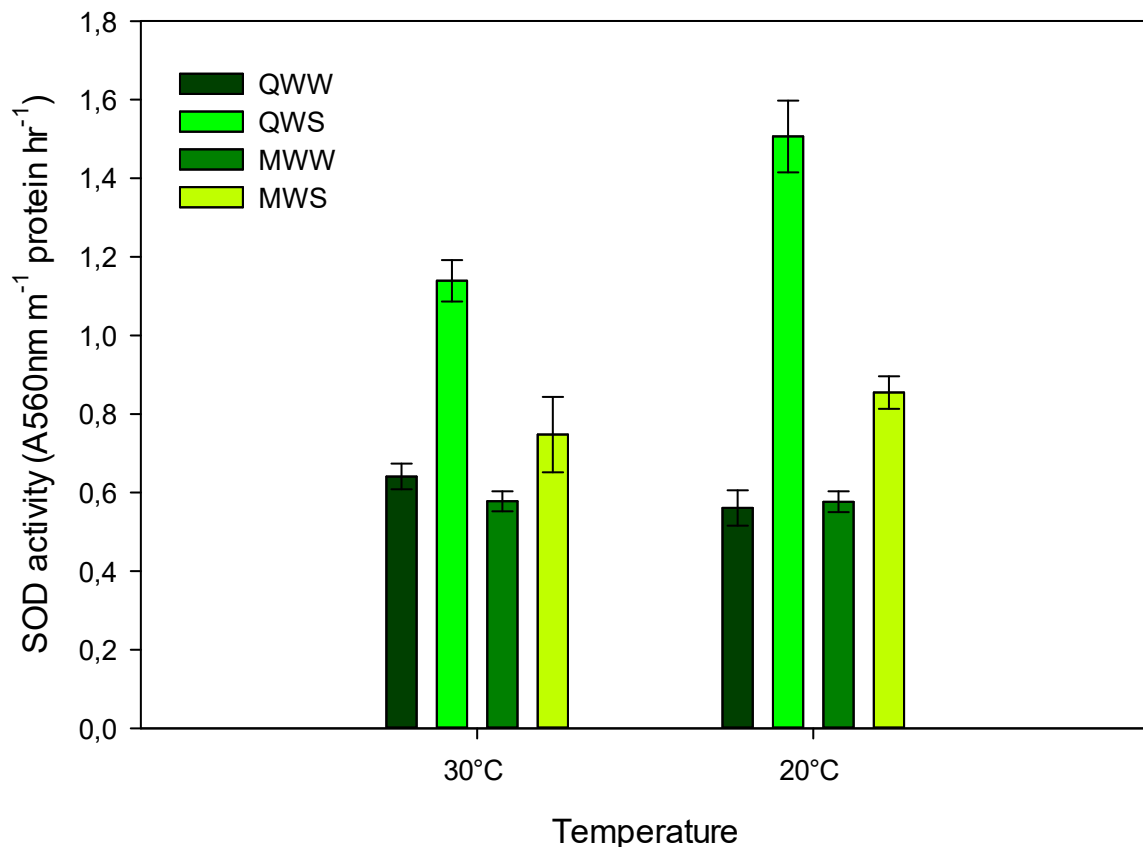


Figure 4-18: The superoxide dismutase activity ($A_{560} \text{ nm mg}^{-1} \text{ protein hr}^{-1}$) of both quinoa and maize under water- stressed conditions (severe drought stress, soil moisture content $\leq 0.01 \text{ m}^{-3} \cdot \text{m}^{-3}$) at 20°C and 30°C. Treatment values not connected by the same letters are significantly different ($P < 0.05$). (MWS, maize water stress; MWW, maize well watered; QWS, quinoa water stress; QWW, quinoa well watered).

4.8 Glutathione reductase activity

In the same way as proline and SOD, glutathione reductase (GR) is capable of protecting vital cellular components from damage caused by ROS (Trivedi *et al.*, 2013). Based on the data collected, the water- stressed quinoa had a significantly ($p < 0.005$)

higher GR activity compared to the water- stressed maize in both temperature regimes (Figure 4-18). The water- stressed quinoa had a 70.85% higher GR activity at the 20°C temperature regime compared to the water- stressed maize. Additionally, the water- stressed quinoa had a 71% higher GR activity at the 30°C temperature regime compared to the water- stressed maize. Significant differences ($p < 0.001$) were also found between the two temperature regimes. The water stressed quinoa had a 81.27% higher GR activity at the 20°C temperature regime compared to the 30°C temperature regime. The GR activity was also significantly higher in the water- stressed quinoa than in the water- stressed maize at 20°C compared to the 30°C temperature regime (Figure 4-18).

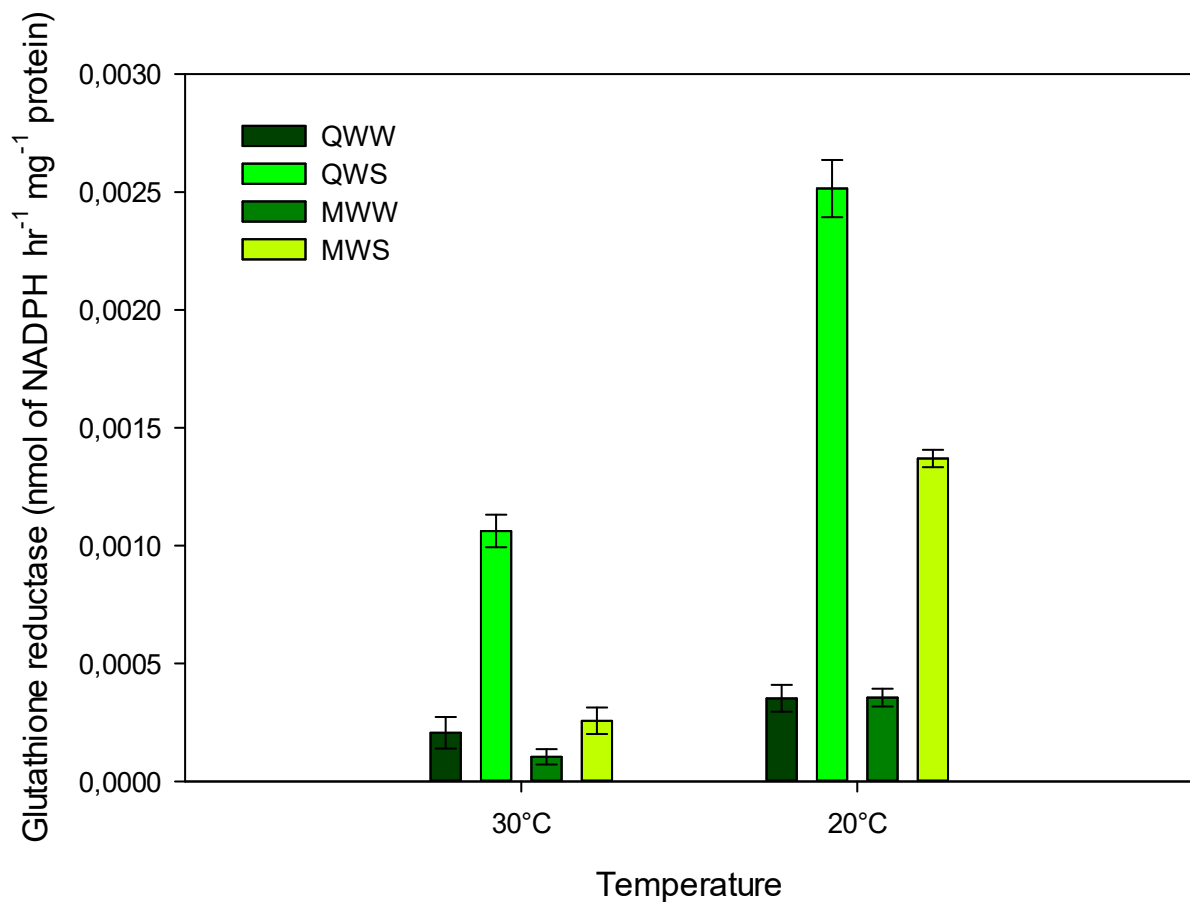


Figure 4-19: The glutathione reductase activity (nmol of NADPH hr⁻¹ mg⁻¹ protein) of both quinoa and maize under water- stressed conditions (severe drought stress, soil moisture content $\leq 0.01 \text{ m}^{-3}.\text{m}^{-3}$) at 20°C and 30°C. Treatment values not connected by the same letters are significantly different ($P < 0.05$). (MWS, maize water stress; MWW, maize well watered; QWS, quinoa water stress; QWW, quinoa well watered).

4.9 Hydrogen peroxide content

Increased levels of ROS in plants are responsible for a range of damaging effects on the DNA, RNA, oxidation of lipids and amino acids (Saxena *et al.*, 2016). During this trial the water- stressed maize produced significantly ($p < 0.001$) higher levels of hydrogen peroxide (H_2O_2) at both the 20°C and 30°C temperature regimes (Figure 4-19). The water- stressed maize produced 48.18% more H_2O_2 compared to the water- stressed quinoa at the 30°C temperature regime and 57.27% more H_2O_2 at the 20°C

temperature regime. The water- stressed quinoa produced significantly lower levels of H₂O₂ when compared to the well-watered quinoa (Figure 4-19).

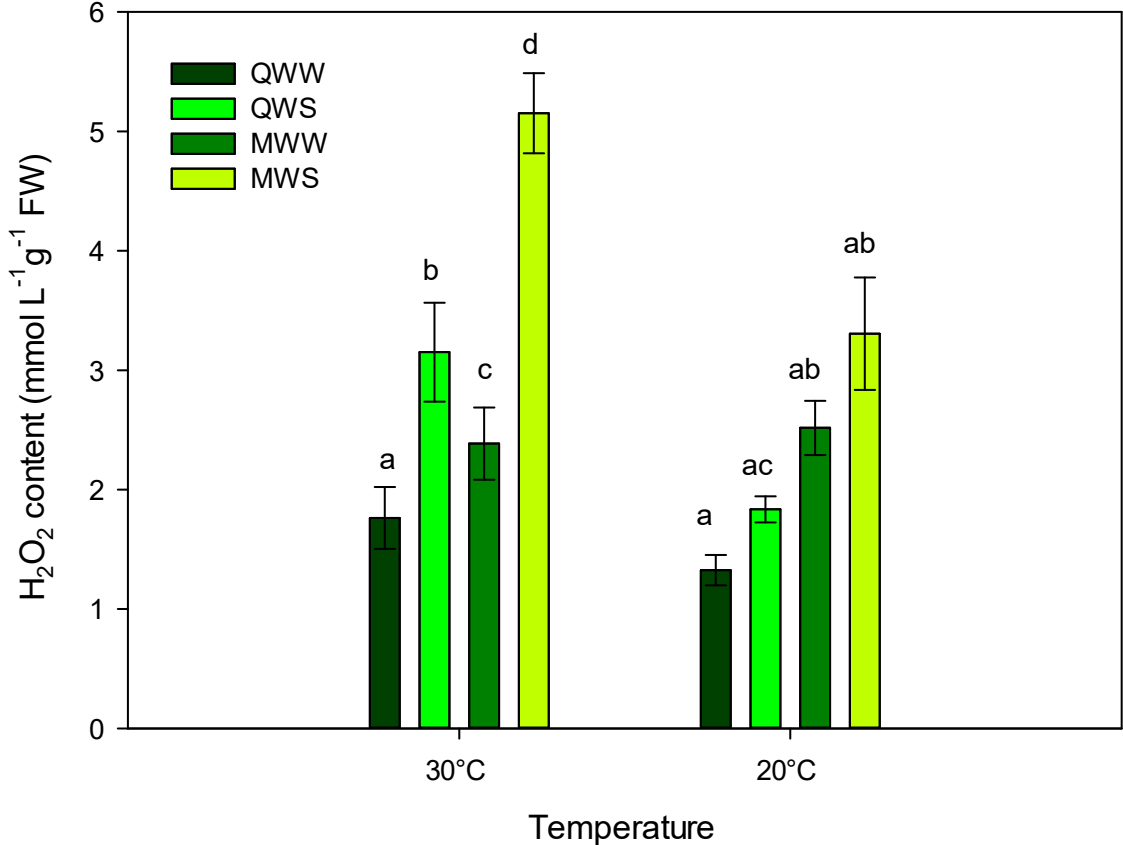


Figure 4-20: The hydrogen peroxide content (mmol L⁻¹ g⁻¹ FW) of both quinoa and maize under water- stressed conditions (severe drought stress, soil moisture content ≤ 0.01 m³.m⁻³) at 20°C and 30°C. Treatment values not connected by the same letters are significantly different (P<0.05). (MWS, maize water stress; MWW, maize well watered; QWS, quinoa water stress; QWW, quinoa well watered).

4.10 Dry Biomass

No significant ($p>0.05$) differences were found in the dry biomass between the water-stressed quinoa and the well-watered quinoa at both temperature regimes (Figure 4-20 A). A 12.30% difference in the dry biomass was observed at the 20°C temperature regime and a 17.39% difference in the dry biomass was found between the water-stressed quinoa and the well-watered quinoa at the 30°C temperature regime. Significant differences ($p<0.05$), however, were found in the dry biomass between the water-stressed maize and the well-watered maize. A 37.53% difference was observed at the 20°C temperature regime in the dry biomass was found between the water-stressed maize and the well-watered maize. At the 30°C temperature regime a 40.13% difference in the dry biomass was found between the water-stressed maize and the well-watered maize. When comparing the two temperature regimes, both crops produced significantly ($p<0.05$) more biomass at the 20°C temperature regime compared to the 30°C temperature regime. A significant decrease ($p<0.05$) in the total leaf area was also observed at both temperature regimes (Figure 4-20 B). The total leaf area of the water-stressed quinoa decreased with 78.77% compared to the well-watered quinoa at 20°C and with 70.80% at the 30°C. Whereas, a 48.74% reduction in the leaf area was observed when comparing the water-stressed maize with the well-watered maize at 20°C and 31.18% reduction at 30°C.

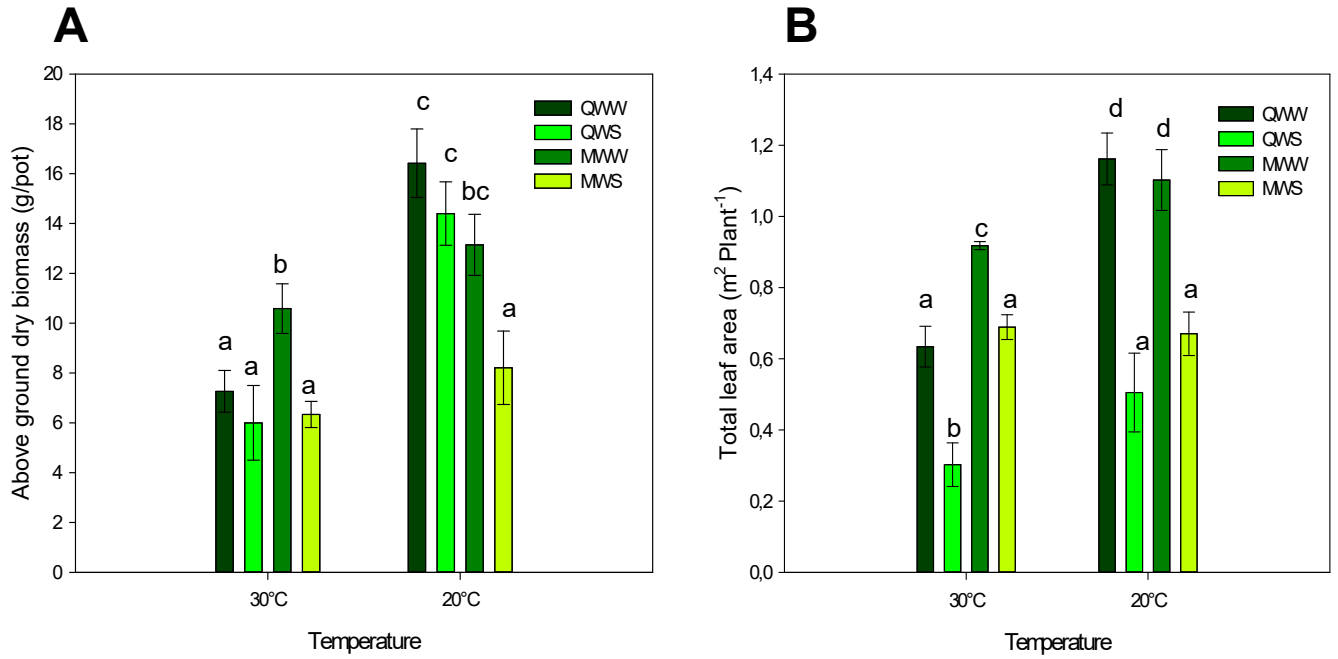


Figure 4-21: (A) The above ground dry biomass (g/pot) and (B) Total leaf area (m² Plant⁻¹) of both quinoa and maize under water- stressed conditions (severe drought stress, soil moisture content $\leq 0.01 \text{ m}^{-3} \cdot \text{m}^{-3}$) at 20°C and 30°C. Treatment values not connected by the same letters are significantly different ($P < 0.05$). (MWS, maize water stress; MWW, maize well watered; QWS, quinoa water stress; QWW, quinoa well watered).

CHAPTER 5 DISCUSSION

South Africa is a water scarce country with severe drought and high temperature events occurring frequently. The last few years a persistent decrease in the production of maize has been observed (Mangani *et al.*, 2019). This decrease in the production of maize coincided with a noticeable increase in recent drought events. Drought is considered as one of the main factors inhibiting plant growth causing increased osmotic stress (Kocheva *et al.*, 2005; Dabrowski *et al.*, 2019). Regardless of the numerous studies already conducted to understand the intrinsic mechanism by which plants respond to water stress, this subject still remains of interest (Lawson *et al.*, 2003; Liao and Wang, 2014). Various authors, however, referred to quinoa as a climate resilient crop, being able to grow in areas subjected to harsh climatic conditions, for example, drought and/or high temperatures (Jacobsen *et al.*, 2012, Miranda-Apodaca *et al.*, 2018). For this reason, the possible introduction of quinoa in the South African production system could help improve the current threat against food security. In this study we compared and evaluated the physiological acclimation strategies used by both quinoa and maize subjected to water stress under two different temperature regimes. This was done by investigating the photochemical potential and the antioxidant responses of both quinoa and maize.

One of the most common responses of plants to water stress is stomatal closure which often ensures a higher water use efficiency (Parry *et al.*, 2005; Singh and Reddy, 2011; Mathobo *et al.*, 2017). Once a decline in stomatal conductance occurs, a reduction in the supply of intercellular CO₂ could lower the photosynthetic and biochemical activities of plants (Lawlor, 2002). A decrease in the photosynthetic activity under water deficit stress could cause an imbalance in the reaction centres of photosystem II (PSII) resulting in photoinhibition (Pastenes *et al.*, 2005). Plants, however, have developed various mechanisms to avoid photoinhibition through processes such as non-photochemical quenching, transporting electrons to oxygen (O₂) and not to carbon dioxide (CO₂) (Flexas *et al.*, 2002) and changing the concentration of chlorophyll pigments (Govindjee, 1999). In this study the stomatal conductance of both the quinoa and maize decreased (Figure 4-14). The stomatal conductance of the water-stressed quinoa decreased rapidly from 500 to 190 mmol m⁻² s⁻¹ in three days at 20°C and from 620 to 230 mmol m⁻² s⁻¹ in four days at 30°C. A similar response was found in the

water- stressed maize with a stomatal conductance dropping from 170 to 55 mmol m⁻² s⁻¹ in three days at 20°C and from 170 to 63 mmol m⁻² s⁻¹ in four days at 30°C (Figure 4-14).

In general, the CO₂ concentrating mechanism of C4 plants allows for a larger diffusion gradient for CO₂. In this case, C4 species should be able to operate at a lower conductance when compared to C3 species. Following this approach, C4 species reduce water loss via transpiration, thereby maintaining a higher water use efficiency (Long, 1999). In this study the water- stressed quinoa, which is a C3 plant, was able to maintain a higher stomatal conductance compared to the water- stressed maize at both temperature regimes (Figure 4-14). According to Guidi *et al.* (2019), when certain stressors, for example, drought occurs, stomatal limitations will cause a decrease in the CO₂ uptake during photosynthesis. As a result, these limitations are more prone in C4 species compared to C3 species since C4 photosynthesis generally functions near the inflection point of the CO₂ photosynthetic response compared to C3 species (Wand *et al.*, 2001). In other studies, a decrease in the photochemical efficiency of *Alloteropsis semialata* was observed, which in turn resulted in a decreased CO₂ assimilation rate in C4 species compared to C3 species (Ripley *et al.*, 2007). In addition, it was also found that maize had a higher degree of photoinhibition and a lower photosynthetic efficiency compared to sunflower, signifying that C3 species have the ability to perform better than C4 species when exposed to stress (Killi *et al.*, 2017). Ghannoum, (2009) suggested that the limited capacity for photorespiration was more harmful under water stress due to the fact that the absorbed light largely surpassed the carboxylation energy requirement. This reasoning could further explain why C4 species are equally or sometimes even more sensitive to water stress compared to C3 species. This also explains why there is a parallel decrease between the abundance of C4 species and the annual rainfall (Guidi *et al.*, 2019).

In previous studies, Jensen *et al.* (2000) found that quinoa only started to reduce its stomatal conductance once the leaf water potential dropped below -1.2 MPa. The reduced sensitivity of the stomatal closure response in quinoa was considered as one of quinoa's unique features as a drought tolerant specie. Contrasting results, however, were found in follow-up studies, which demonstrated that quinoa closed its stomata early during a water stress trial, thereby maintaining its leaf water potential,

photosynthetic rate and water use efficiency (Jacobsen *et al.*, 2009). Sun *et al.* (2014) suggested that these contrasting results could be due to genetic variability of quinoa accessions, differences in experimental conditions and a difference in the dynamics of drought stress development. The same authors concluded that depending on the quinoa variety, a slower response in stomatal closure can occur due to a slower growth rate and smaller leaf area, whereas, increased concentrations in abscisic acid (ABA) can cause an immediate closure of the stomata.

The total leaf area is also considered as an important parameter and is related to the amount of light energy that is captured by leaves, hence affecting transpiration, photosynthesis and yield production (Xu *et al.*, 2010). During water and temperature stress, plants can reduce water loss via the production of smaller and less leaves. A reduced leaf area could, therefore ensure that a higher water use efficiency is maintained (Dong *et al.*, 2019). However, as the soil dries, the water uptake by the roots cannot meet the high transpiration rates, ultimately causing a reduction in the stomatal conductance and the total leaf area. During this study, the water- stressed quinoa had a lower total leaf area compared to the water- stressed maize (Figure 4-20 B). A lower leaf area allowed the water- stressed quinoa to maintain its osmotic potential. Similar results were found in vegetable amaranth (Liu and Stützel, 2004) and soybean (Dong *et al.*, 2019). Based on the results of this study, both quinoa and maize controlled water loss by reducing the leaf area and stomatal conductance.

Water deficit conditions and high temperatures also tend to cause a reduction in the photosynthetic pigments, for example, the chlorophyll content (Gonzales *et al.*, 2011; Ruiz *et al.*, 2016; Miranda-Apodaca *et al.*, 2018). This will usually occur as a result of a high chlorophyllase activity or because the synthesis of new pigments is inhibited (Loggini *et al.*, 1999). However, contrasting results were found in this study. The chlorophyll content of the water- stressed maize decreased significantly ($p < 0.05$), however, the water- stressed quinoa had a significantly ($p < 0.05$) higher chlorophyll content at both temperature regimes (Figure 4-15). Similar results on quinoa were found by Miranda-Apodaca *et al.* (2018) under drought and saline stress. These authors suggested that the increased chlorophyll content could be due to a concentrating effect of the chlorophylls since the mass production was equivalently greater than the increase in the degradation of the chlorophylls. Furthermore, Iqbal *et al.* (2019) suggested that

proline over producing mutants could also inhibit the synthesis of ethylene. During leaf senescence and fruit ripening, ethylene is known to promote the degradation of chlorophyll pigments (Ceusters and Van de Poel, 2018). Therefore, suggesting that ethylene is involved in establishing a normal level of chlorophyll content in young leaves and initiates chlorosis in mature leaves. Additionally, a higher proline content can also maintain the integrity of the chlorophyll molecules (Wani *et al.*, 2019) and the water potential necessary for photosynthesis (Iqbal *et al.*, 2019). Wani *et al.* (2019) reported that an increase in the proline content resulted in an increase in the chlorophyll content in saline stressed mustard. In this study we found that the water- stressed quinoa produced significantly higher ($p < 0.05$) levels of proline (Figure 4-16) compared to the water- stressed maize, therefore, suggesting that the water- stressed quinoa was able to protect the chlorophyll molecules from degradation.

Drought and high temperatures influences numerous cellular components and metabolic processes (Sung *et al.*, 2003; Chen *et al.*, 2016). The photosynthetic apparatus has been described as one of the most sensitive physiological process to heat and drought stress on many occasions (Goltsev *et al.*, 2012; Oukarroum *et al.*, 2016; Chen *et al.*, 2016). Fluorescence, mainly emitted by PSII can essentially be used to monitor the successive steps of excitation energy transformation (Willmont, 1982; Paschenko *et al.*, 1975; Goltsev *et al.*, 2012). One of the most variable parts of chlorophyll *a* fluorescence is directly linked to the reduction of Quinone A (Q_A^-), which increases during the photo-induced reduction of Q_A^- (Goltsev *et al.*, 2012). Additionally, the photo-induced kinetics of the modulated reflection at 820 nm is in accordance with the accumulation and reduction of the photosystem I primary donor ($P700^+$) (Schansker *et al.*, 2003).

In this trial, the shape of the OJIP curve was sensitive to the development of water stress in the leaf tissue and demonstrates changes induced by the water stress regarding the function of PSII. Further analysis of the fast polyphasic fluorescence transient revealed that the water stress significantly ($p \leq 0.05$) decreased the photochemical potential of both quinoa and maize (Figure 4-1 and 4-9). These differences were especially noticeable in the multiple turnover phase of the OJIP-transient (Figure 4-1). The change in the fluorescence intensity was determined by the differences in the reduction of Q_A to Q_A^- (Haldiman and Strasser, 1995; Redillas *et al.*,

2011). The water stress decreased both the ratio of the reduced electron acceptors, Q_A^- to the reaction centre (RC) and from Quinone B (Q_B^-) to Q_A^- (Kalaji *et al.*, 2016).

High temperatures will generally influence the shape of the OJIP curve resulting in a reduction in the maximum quantum (F_M) yield of PSII. This was observed for both the quinoa and maize. The effect of the water stress at both temperature regimes was more noticeable in the maize compared to the quinoa (Figure 4-6 B). The water-stressed maize had a significantly ($p < 0.05$) lower F_M value compared to the water-stressed quinoa. According to Yamane *et al.* (1997) the decrease in the F_M value is associated with the denaturation of the chlorophyll molecules. Various authors also reported an increase in the minimal fluorescence value (F_0) when plants are exposed to heat stress (Chen *et al.*, 2009; Mathur *et al.*, 2011; Redillas *et al.*, 2011; Brestic *et al.*, 2013; Chen *et al.*, 2016; Kalaji *et al.*, 2016). According to Kalaji *et al.* (2016) the increase in the F_0 value could occur due an inhibition in the flow of electrons caused by a reduced transfer of Q_A to Q_B . Additionally, it could also occur due to the release of the light harvesting complex II (LHC II) from the PSII complex and/or the inactivation of the photochemical reactions centres associated with PSII (Mathur *et al.*, 2011). In spinach and rice, Yamane *et al.* (1997) found that an increase in the F_0 was associated with the permanent dissociation of LHC II from the PSII complex and partial reversible inactivation of PSII RCs. However, in this study, no significant differences were found in the F_0 value between the control treatments and the water-stressed treatments of both quinoa and maize (Figure 4-6 A). Various authors also found that PSII is quite insensitive to drought stress (Cornic and Fresneau 2002, Tezara *et al.*, 2003).

The quantum yield of the primary photosystem (F_v/F_m) is commonly used to provide information regarding the amount of light absorbed by the chlorophyll pigments present in the photochemical processes (Genty *et al.*, 1989; Liu *et al.*, 2019). An F_v/F_m value of 0.750 has been identified as a boundary value indicating a fully functional PSII (Strasser *et al.*, 2004). In this study we found that the water-stressed quinoa had the ability to maintain a high F_v/F_m value (0.818 at 30°C and 0.816 at 20°C), suggesting that there was no damage to the structure of PSII (Figure 4-6 C). Electrons were therefore, able to move into the electron transport chain without much difficulty. The water-stressed maize, however, had F_v/F_m values of 0.580 (30°C) and 0.703 (20°C), indicating that the flow of electrons into the electron transport chain was effected more negatively (Figure

4-6 C). Yang *et al.* (2016), however, found a decrease in the F_v/F_m value when exposing quinoa to water deficit conditions. In this study, no significant differences were observed between the water-stressed and well-watered quinoa treatments. The decrease in the F_v/F_m in the water-stressed maize was similar to results found by Efeoglu *et al.* (2009).

To fully visualize and understand the changes in the redox potential of the O-J-I-P transient, other normalizations and corresponding subtractions of the fluorescence rise kinetics were done. The difference in variable fluorescence was, normalized and plotted on a logarithmic time scale. By doing so, different ΔV -bands were revealed, describing the movement of electrons through the electron transport chain. The main changes observed in the fluorescence rise kinetics of both maize and quinoa was the appearance of the ΔV_K , ΔV_J and ΔV_I bands (Figure 4-2 and 4-3).

The ΔV_K - band (0.3 ms) revealed information regarding the reactions present on the donor side of the PSII reaction centre (Zushi *et al.*, 2012, Oukarroum *et al.*, 2016, Chen *et al.*, 2016). Various studies demonstrated that water stress in plants tend to lead to the inactivation of the oxygen evolving complex (OEC), therefore resulting in an imbalance in the flow of electrons between the RC and the acceptor side, as well as the flow of electrons between the RC and donor side of PSII (Yusuf *et al.*, 2010; Bussotti *et al.*, 2011; Chen *et al.*, 2016; Kalaji *et al.*, 2017; Banks, 2018; Kalaji *et al.*, 2018). According to the results observed, the amplitude of the ΔV_K - band for the water stressed maize was higher at both temperature regimes compared to the water stressed quinoa (Figure 4-4). The water- stressed maize had a higher ΔV_K - band at the 30°C temperature regime compared to the 20°C temperature regime. On the other hand, the quinoa had a higher ΔV_K - band at the 20°C temperature regime compared to the 30°C temperature regime (Figure 4-4). In previous studies it has been proposed that proline has the ability to protect the OEC under water deficit stress (De Ronde *et al.*, 2004; Oukarroum *et al.* 2012a; Gilberti *et al.*, 2014; Rejeb *et al.*, 2014; Chen *et al.*, 2016) and simultaneously stabilize the manganese (Mn) cluster (Allakhverdiev *et al.*, 1996). According to the model of De Ronde *et al.* (2004), an alternative electron donor such as proline can also donate electrons to PSII instead of water. This will result in a short-lived increase in the reduced Pheo⁻/Q_A⁻ concentration, leading to the appearance of a ΔV_K - band. Hence, the

degree of OEC injury is directly proportional to the amplitude of the ΔV_K - band (Strasser, 1997; Chen *et al.*, 2016).

Under water deficit stress, higher levels of proline could therefore, maintain the redox potential at a suitable level for metabolism (Giberti *et al.*, 2014; Rejeb *et al.* 2014). Further, it has been suggested that proline may be synthesised from glutamate in chloroplasts (Székely *et al.*, 2008). In this case, the oxidation of two Nicotinamide adenine dinucleotide phosphate (NADPH) molecules to $NADP^+$ is required and possibly recycling $NADP^+$ under stress. By restoring the terminal electron acceptor pool, proline synthesis could lower ROS production and protect the plant from photo-inhibition under water deficit conditions (Rejeb *et al.*, 2014). And so, there would be a link between the synthesis of proline and the reduction of $NADP^+$ via the pentose phosphate pathway (Shetty, 2004). In this pathway the production of ribulose-5-phosphate generates two molecules of NADPH and one of CO_2 . The regeneration of CO_2 would allow the carbon reduction to continue. The NADPH could be utilized for the synthesis of proline, thereby preventing the production of harmful ROS (Verslues and Sharma, 2010, Rejeb *et al.*, 2014).

Based on the results from this study, we found that the detoxification metabolism of quinoa was more efficient compared to maize. In both temperature regimes the water-stressed quinoa had significantly ($p < 0.001$) higher levels of proline compared to the water-stressed maize, suggesting that the water-stressed quinoa had a greater capability to function under the water deficit condition compared to the water-stressed maize (Figure 4-17). Additionally, the quinoa produced more proline at 30°C compared to the 20°C temperature regime. This is reasonable as quinoa prefers a lower optimal growth temperature, and as a result the increased production of proline coincides with an increase in the temperature. The significantly lower ($p < 0.001$) production of proline observed in the water-stressed maize indicated that its osmotic adjustment to water stress was ineffective compared to that of the quinoa. However, it should be noted that the water-stressed maize produced more proline at the 30°C temperature regime compared to the 20°C temperature regime (Figure 4-17).

Recent studies, however, revealed that various important crops, including, maize, wheat and rice are not able to synthesize the necessary levels of proline that are needed to

counteract the damaging effects of drought stress (Slama *et al.* 2015). This was further supported by the lower leaf water content (Figure 4-14) and lower membrane leakage (Figure 4-13) that was observed in the water- stressed maize compared to the water- stressed quinoa. The membrane leakage of the water- stressed quinoa was significantly lower ($p < 0.05$) compared to the water- stressed maize, suggesting that the maize had higher levels of electron leakage and higher levels of cell injury (Figure 4-13).

The increased levels of proline present in the water- stressed quinoa prevented the dissociation of the OEC by providing more electrons for PSII. In addition, the water- stressed quinoa produced significantly ($p < 0.001$) more proline in the 30°C temperature regime when compared to the 20°C temperature regime. As a result, it had a greater ability to exert a more protective effect on the OEC at the 30°C temperature regime (Figure 4-17). By doing so, an acceptable level of NADPH was maintained, thereby avoiding more damage (Oukarroum *et al.*, 2012a). During this trial the water- stressed quinoa was able to maintain its ability to reduce NADP⁺ to NADPH ($\delta_{R0}/(1-\delta_{R0})$) compared to the decrease in NADPH reduction found in the water- stressed maize (Figure 4-7 and Figure 4-8 E).

Chen *et al.* (2016) found that temperatures below 40°C only partially inhibited the OEC, without creating a visible ΔV_K - band. These authors further suggest that RCs of PSII will also be affected to some extent, without significantly affecting the antenna complexes, primary light reactions, energy dissipation and the electron transfer between the photosystems.

However, in this study the dissipation of heat energy from the active reaction centres (Dlo/RC) increased significantly ($p < 0.05$) for the water- stressed maize when compared to the well-watered maize, which coincides with the increase in the effective antenna size of active RCs (ABS/RC) (Figure 4-7; 4-8 and Table 4-1). The same trend was observed for the quinoa, but the degree with which the quinoa was affected by the water stress was significantly lower ($p < 0.05$), compared to the water- stressed maize. The same effect for both the quinoa and maize was found at both temperature regimes, although the effect of water stress was more pronounced at the 30°C temperature regime (Figure 4-7; 4-8 and Table 4-1). If the antenna complexes deliver too much energy under water stress conditions, the production of singlet oxygen is promoted. This

can cause photo-oxidation in the chlorophyll and irreversible peroxidation of membrane lipids (Lauriano *et al.*, 2006; Kalaji *et al.*, 2017). These results, suggests that maize is less tolerant to water deficit stress when compared to the quinoa.

Furthermore, a reduced TRo/RC and ETo/RC indicates that the active RCs were converted into inactive RCs, thereby decreasing the efficiency of trapping and consequently causing a decline in PSII activity (Figure 4-7 and Table 4-1). Several studies have been identified with similar results regarding the effect of water stress on *Calluna vulgaris* (Albert *et al.*, 2011), tomato plants (Zushi *et al.*, 2012) and maize (Liu *et al.*, 2018). In addition, the PI_{TOTAL} of the water- stressed maize decreased significantly ($p < 0.05$) in both temperature regimes, whereas the PI_{TOTAL} of the water-stressed quinoa was significantly higher ($p < 0.05$) (Figure 4-7 and Figure 4-9 B). Therefore, the higher PI_{TOTAL} values of the quinoa indicated that more energy was conserved between the photons absorbed by PSII and the reduction of the intersystem electron acceptors.

A positive ΔV_J -band suggested that the temperature and water stress depressed the flow of electrons further than Q_A (Chen *et al.*, 2016; Kalaji *et al.*, 2018; Liu *et al.*, 2018) (Figure 4-2 D and Figure 4-3 D). This effect was more noticeable in the water- stressed maize at both temperature regimes. However, the water stress and temperature stress had different effects on the water- stressed quinoa. A significant increase ($p < 0.05$) in the ΔV_J was found at the 30°C temperature regime compared to the 20°C. Similar results were found by Chen *et al.* (2016). This data agrees with the decrease that was observed for the water- stressed maize in the amount of light energy trapped per RC ($\phi_{PO}/(1-\phi_{PO})$) and the reduced efficiency with which an electron moved further than Q_A - ($\Psi_{E0}/(1-\Psi_{E0})$) (Figure 4-7). In both these instances, no significant differences were observed when comparing the water- stressed quinoa with the well-watered quinoa, suggesting that the water stress had a minor effect on the amount of light energy trapped per RC and on the movement of electrons further than Q_A^- (Figure 4-7).

Water stress can also affect the relative amplitude of the I - P phase, which has been described as the slowest phase of the fluorescence transient and runs parallel with the re- reduction of plastocyanin (PC^+) and $P700^+$ of photosystem I (PSI) (Schansker *et al.*, 2003; Kalaji *et al.*, 2016). Ceppi *et al.* (2012) noted that the I – P phase was related to

the content of the PSI RCs, whereas Zivcak *et al.* (2014) found that the I – P phase was related to the availability of linear electron transport. In this study, the water- stressed maize had a significantly lower V_{IP} phase in both the 20°C and 30°C temperatures regimes (Figure 4-5). Similar results were found in barley (Oukarroum *et al.*, 2009) and two desert shrubs (Van Heerden *et al.*, 2007). According to these authors, extensive drought stress can cause a restriction on the acceptor side of PSI, thus leading to an increase in the reduction of the plastoquinone (PQ) pool. However, the water- stressed quinoa had a higher V_{IP} phase compared to the water- stressed maize at the 30°C temperature regime and a V_{IP} phase equivalent to the well-watered maize at the 20°C temperature regime (Figure 4-5). This suggests that the efficiency of PSI was not compromised by the water stress in the water- stressed quinoa.

The response of both the water- stressed maize and quinoa was also established based on the analysis of the MR parameters. At the 20°C temperature regime a significant decrease ($p < 0.05$) in both the V_{ox} and V_{red} was found for the water- stressed maize and at the 30°C temperature regime a decrease was found for the V_{red} (Table 4-3). For quinoa, no significant differences were found for the V_{ox} and V_{red} parameters between the water- stressed treatment and the well-watered treatment. A decrease in the V_{ox} was also observed by Oukarroum *et al.* (2012b) and Gao *et al.* (2014), which signifies a simultaneous decrease in the rate of photo-induced electron transfer through PSI. This will generally occur as a result of the reduction of the PSI photochemical activity. These authors also found a decrease in the V_{red} parameter under drought stress which, indicated a slower re-reduction of $P700^+$, caused by the slower electron donation from P680. In this study, similar results were found at the 20°C temperature regime for the water- stressed maize. However, at the 30°C temperature regime no decrease in the V_{ox} parameter was found for the water- stressed maize (Table 4-3) and this corresponds to the same trend found by Dabrowski *et al.* (2019).

According to Schansker *et al.* (2003) the MR signal is mostly affected by the rate of electron flow from PSII to PSI. A limitation on the acceptor side of PSI, for example drought stress, could cause changes in the MR signal. Additionally, these authors also concluded that the fast phase relates to the photo-induced changes of $P700^+$ and that the slow phase reflects the re-reduction of $P700^+$, which tends to change under stress. In the present study, the MR fast and MR slow parameters changed significantly

between the water- stressed maize and the well-watered maize, signifying that the water stress had a more negative effect on PSI. However, no significant changes in the MR fast and MR slow occurred between the two quinoa treatments, indicating that the PSI activity of the water- stressed quinoa was more stable under the water- stressed conditions (Table 4-3).

When higher plants are exposed to drought stress, photosynthesis is inhibited by stomatal closure, thereby limiting the flow of CO₂ to the chloroplasts (Cornic, 2000; Chaves *et al.*, 2003; Oukarroum *et al.*, 2009). As stated previously, a significant decrease ($p < 0.05$) was found in the stomatal conductance of both the water- stressed quinoa and maize (Figure 4-15). This type of event will cause a decrease in the internal CO₂ concentration leading to a reduction in the activity of Rubisco (Maroco *et al.*, 2002). When a limit in the available CO₂ occurs, PSI can become a possible source of oxygen radicals (Oukarroum *et al.*, 2009). According to Ke (2001), the reaction of oxygen with the FeS cluster can be catalysed by methylviologen. However, this reaction can also occur in the absence of methylviologen via the water-water cycle found in the chloroplast (an elaborate detoxification system) (Asada, 1999; Heber, 2002; Makino *et al.*, 2002; Rizhsky *et al.*, 2003)

Mittler (2002) and Dat *et al.* (2000) both stated that a reduction in the PSI content in response to various stresses could occur due to an increase in the production of PSI oxygen radicals. Similar to PSII, PSI can also undergo photoinhibition instigated by ROS (Sejima *et al.*, 2014; Takagi *et al.*, 2016). When the electron transport chain is in a highly reduced state, the over production of ROS can occur at the PSI site (Oelze *et al.*, 2012; Grieco *et al.*, 2012). Once the PSI electron carriers become reduced, photoinhibition will occur, thereby damaging the net carbon assimilation and plant growth (Suorsa *et al.*, 2012; Grieco *et al.*, 2012; Kono *et al.*, 2014). Several authors concluded that PSII could relatively be drought tolerant and only decreases under water stress (Souza *et al.*, 2004). Additionally, Oukarroum *et al.* (2009) further suggested that the decrease in the I – P phase occurred due to an increased change in the ratio between PSII and PSI.

Furthermore, PSI tends to recover slower than PSII after photo-inhibition (Sonoike, 2011) therefore; PSI photoinhibition has a more negative effect on the reduction of end

electron acceptors (Takagi *et al.*, 2016). When the activity of the Calvin-Benson cycle is reduced due to water stress, an increase in the production of superoxide can occur on the acceptor side of PSI. Superoxide can form by means of several processes, but the main sources are the photosynthetic electron transport and the respiratory chains (Pilon *et al.*, 2011). Generally, superoxide will form when electrons from the electron transport chain react with molecular oxygen. However, the enzyme superoxide dismutase (SOD) is responsible for the conversion of superoxide to the more stable form, H₂O₂ (Sekmen *et al.*, 2014).

Various authors found increased levels of SOD in citrus genotypes exposed to drought and heat stress (Zandalinas *et al.* 2017), *Scutellaria baicalensis* Georgi (Cheng *et al.*, 2018), *Cerasus humilis* (Ren *et al.*, 2016) and rice (Lum *et al.*, 2014). In the present study, the water- stressed quinoa had a significantly higher ($p<0.05$) SOD activity compared to the water- stressed maize (Figure 4-18). Quinoa therefore, has a greater ability to convert superoxide into H₂O₂, compared to maize. The water- stressed quinoa also had significantly lower ($p<0.05$) hydrogen peroxide (H₂O₂) levels when compared to the water- stressed maize (Figure 4-20). This suggests that quinoa possibly had a greater concentration of catalase (CAT) and ascorbate peroxidase (APX) enzymes available to convert H₂O₂ into water and oxygen, whereas the water- stressed maize would have had lower concentrations of CAT and APX available. Similar results were also found in pigeon pea (Kumar *et al.*, 2011), wheat (Omar *et al.*, 2012) and black gram (Pratap and Sharma, 2010). The higher H₂O₂ levels present in the water- stressed maize increased the oxidative damage in the cells, thereby decreasing the activity of both PSII and PSI. As previously mentioned, halophytes generally have higher activities of SOD (Bose *et al.*, 2014), supporting the fact that the water- stressed quinoa had a greater ability to reduce superoxide to H₂O₂.

An increased glutathione reductase (GR) activity is associated with stress tolerance in plants. One of the main contributions of GR in conferring stress tolerance lies in the recycling of reduced glutathione (GSH) and maintaining the GSH/GSSG ratio in a cell (Pang *et al.*, 2010). When under stress, increased GR activities can also alter the redox state of important components of the electron transport chain (Gill *et al.*, 2013). In the present study, a significantly higher ($p<0.05$) GR activity was found in the water- stressed quinoa at both temperature regimes (Figure 4-19). The water- stressed maize

had a significantly lower GR activity ($p < 0.05$). The increased GR activity in the water-stressed quinoa decreased the accumulated H_2O_2 in the cell, thereby decreasing oxidative stress. Additionally, Ding *et al.* (2012) found that a decrease in the GR activity resulted in a higher accumulation of H_2O_2 in the chloroplast, which resulted in a decrease in the PSII activity. This resulted in a slow transfer of electrons between Q_A and Q_B , a decrease in the redox potential of Q_B and PSII protein accumulation. These authors further suggested that an increased GR activity stabilizes the PSII complexes and it also protects the function of PSII by maintaining the flow of electrons to the acceptor side of PSII. Similar results were found by Melchiorre *et al.* (2009) where the overexpression of GR enhanced photo-oxidative stress tolerance in plants, which was accompanied by positive changes in the cellular redox state.

The water-stressed quinoa had a higher SOD and GR activity at the 20°C temperature regime compared to the 30°C temperature regime (Figures 4-18 and 4-19). Various authors, for example, Verbruggen and Hermans (2008) and Sekmen *et al.* (2014) demonstrated that proline can also act as an OH^\cdot scavenger. This gives proline the additional trait to protect cells from oxidative stress (Ashraf and Foolad, 2007). In the present study, a significantly higher ($p < 0.05$) proline activity was found for the water-stressed quinoa at the 30°C temperature regime, therefore not only did the proline stabilize the osmotic potential and membranes, but it also protected the cells from damaged caused by ROS. Due to the high proline activity at 30°C, a reduced amount of ROS, for example, superoxide was present in the cells. As a result, lower SOD and GR activities occurred in the cells at 30°C compared to the water-stressed quinoa at 20°C. As the water-stressed quinoa had a lower proline content, it stabilized the ROS activity with higher SOD and GR activities at the 20°C temperature regime (Figure 4-17, 4-18 and 4-19).

Quinoa was able to acclimatize to the water-stressed conditions more successfully compared to the water-stressed maize. The water-stressed quinoa was able to produce more proline, thereby protecting the OEC and increasing the flow of electrons between PSII and PSI. This effect was more pronounced at 30°C (Figure 4-4). With increasing temperature, quinoa therefore, had the ability to acclimatize more efficiently compared to the maize. The water-stressed maize's inability to acclimatize to the water stress at both temperature regimes, drastically down regulated the photochemical

efficiency of maize and its capacity to withstand osmotic stress. Additionally, no significant changes in the MR fast and MR slow occurred between the two quinoa treatments, indicating that the PSI activity of the water-stressed quinoa was more stable under water-stressed conditions. In contrast, a significant change in the MR fast and MR slow parameters were found between the water-stressed maize and the well-watered maize, signifying that the water stress had a more negative effect on PSI (Table 4-3). Furthermore, the water-stressed quinoa also had a higher SOD and GR activity, thereby playing an active role in abiotic stress induced oxidative damage.

CHAPTER 6 CONCLUSIONS

As a C₃ specie, quinoa was able to adapt more successfully to the abiotic stress compared to maize, a C₄ species. The water deficit stress had detrimental effects on the quinoa and maize at both temperature regimes. However, the water- stressed quinoa was able to acclimate more efficiently to the water- stressed conditions compared to the water- stressed maize. The water- stressed quinoa produced higher levels of proline compared to the water- stressed maize; thereby, increasing the tolerance of PSII to the water deficit stress. As a result, the flow of electrons between PSII and PSI continued unhindered. The water- stressed quinoa also produced more proline at 30°C compared to the 20°C temperature regime. The water- stressed quinoa was able to acclimatize more efficiently compared to the maize at the 30°C temperature regime.

Furthermore, the water- stressed quinoa had a higher SOD and GR activity, thus playing an active role against abiotic stress induced damage. The water- stressed quinoa was able to maintain a higher photochemical potential and it had a higher antioxidant capability, thereby eliminating the harmful effects of ROS. On the other hand, the water- stressed maize produced less proline and had lower SOD and GR activities compared to the water- stressed quinoa. A decrease in the photochemical potential of the water- stressed maize was also observed along with a decrease in its capacity to withstand osmotic stress. The water- stressed maize was unable to acclimatize successfully to the water stress at both temperature regimes.

The PSI activity of the water- stressed quinoa was also more stable, as no significant changes occurred when comparing the MR fast and MR slow parameters to the well-watered quinoa. Whereas, a significant change was found between the water- stressed maize and well- watered maize when comparing the MR fast and MR slow parameters. This indicated that the PSI activity of the water- stressed maize was affected more negatively by the water deficit stress.

As quinoa has the ability to be cultivated in areas with a wide temperature range making it possible to produce this crop where the majority of food crops, for example, maize cannot be produced. The production of quinoa in marginal production areas affected by water stress, salinity and alkalinity would be profitable. Additionally, quinoa could also

be used as an alternative winter crop in crop rotation systems where water deficit stress is likely to occur.

Quinoa could also be used to facilitate small- scale farmers. As quinoa can grow in very poor soils with a low soil moisture its production by small- scale farmers could improve their livelihoods in the face of climate change. To produce quinoa successfully in South Africa it should fit in the current crop production systems and prove its value in properly designed farm trials. As quinoa is a new crop, more effort would also be needed to increase the market demands and to improve the crop yields by way of creating more awareness of its social, cultural and dietary benefits. Compared to maize, quinoa would definitely be a more suitable crop to face the current climatic conditions in South Africa.

CHAPTER 7 RECOMMENDATIONS AND FUTURE STUDIES

Quinoa is one of the few crops with the ability to grow and produce yield in adverse environmental conditions. It has a great ability to acclimatize to various climatic conditions thereby making quinoa an excellent crop in the face of climate change. Quinoa is also known to have various mechanisms to withstand unfavourable conditions, such as the production of an osmoprotectant.

The current study was conducted in glasshouses and even though it gave a good idea of the effect of water stress on both quinoa and maize, it would be beneficial to compare the current results to field conditions, taking the complexity and interaction of environmental stresses into account. Different varieties also display a wide range of sensitivity to water and temperature stress, therefore understanding variety sensitivity would be beneficial in the development of tolerant species.

It would also be beneficial to research the combined effect of water and temperature stress on quinoa. Usually this approach comes with a set of difficulties as maintaining different heat stress temperatures, such as 40°C and 45°C, could become problematic without the correct infrastructure. Nevertheless, this research would be beneficial to further understand the different defence mechanisms used by quinoa during abiotic stress.

In addition, not much is known of the osmoprotectants present in quinoa and how they are synthesized. Further research is needed to understand the regulation and syntheses of the antioxidant capabilities, such as, proline, glycine betaine and mannitol in quinoa, and how these metabolites accumulate during the onset and through a time period of water stress. Additionally, the recovery potential of quinoa should also be observed and what roles the different osmoprotectants play during recovery. By understanding how the defence mechanisms in quinoa works, this information can be used to possibly incorporate these tolerant genes into other susceptible crops in the future.

References

Adolf, V.I., Jacobsen, S. E. and Shabala, S. 2013. Salt tolerance mechanisms in quinoa (*Chenopodium quinoa* Willd.). *Environmental and experimental botany*, 92:43-54.

Ahanger, M. A., Tyagi, S. R., Wani, M. R. and Ahmad, P. 2014. Drought Tolerance: Role of Organic Osmolytes, Growth Regulators, and Mineral Nutrients. (In Ahmad, P., Wani, M. R., eds. *Physiological Mechanisms and Adaptation Strategies in Plants Under Changing Environment*. New York. Springer. p. 3249-296).

Ahmed, I. M., Cao, F., Zhang, M., Chen, X., Zhang, G. and Wu, F. 2013. Difference in yield and physiological features in response to drought and salinity combined stress during anthesis in Tibetan wild and cultivated barleys. *Ploset one*, 8(10):77869.

Alam, R., Das, D.K., Islam, M.R., Murata, Y. and Hoque, M.A. 2017. Exogenous proline enhances nutrient uptake and confers tolerance to salt stress in maize (*Zea mays* L.). *Progressive agriculture*, 27(4):409-417.

Albert, K. R., Mikkelsen, T. N., Michelsen, A., Ro-Poulsen, H. and van der Linden, L. 2011. Interactive effects of drought, elevated CO₂ and warming on photosynthetic capacity and photosystem performance in temperate heath plants. *Journal of plant physiology*, 168:1550-1561.

Allakhverdiev, S. I., Feyziev, Y. M., Ahmed, A., Hayashi, H., Aliev, J. A. and Klimov, V. V. 1996. Stabilization of oxygen evolution and primary electron transport reactions in photosystem II against heat stress with glycine betaine and sucrose. *Journal of photochemistry and photobiology*, 34:149–157.

Alscher, R. G. 1989. Biosynthesis and antioxidant function of glutathione in plants. *Physiologia plantarum*, 77:457–464.

Alscher, R. G., Erturk, N. and Heath, L. S. 2002. Role of superoxide dismutases (SODs) in controlling oxidative stress in plants. *Journal of experimental botany*, 53:1331–1341.

Alvarez-Flores, R., Winkel, T., Degueudre, D., Del Castillo, C. and Joffre, R. 2013. Plant growth dynamics and root morphology of little-known species of *Chenopodium* from contrasted Andean habitats. *Botany*, 92:101–108.

- Asada, K. 1999. The water-water cycle in chloroplasts: scavenging of active oxygen and dissipation of excess photons. *Annual review of plant physiology and plant molecular biology*, 50:601–639.
- Ashraf, M. and Foolad, M. 2007. Roles of glycine betaine and proline in improving plant abiotic stress resistance. *Environmental and experimental botany*, 59(2):206-216.
- Awasthi, R., Bhandari, K. and Nayyar, H. 2015. Temperature stress and redox homeostasis in agricultural crops. *Frontiers in environmental science*, 3:11.
- Banks, J. M. 2018. Chlorophyll fluorescence as a tool to identify drought stress in *Acer* genotypes. *Environmental and experimental botany*, 155:118-127.
- Barnabas, B., Jager, K., Feher, A. 2008. The effect of drought and heat stress on reproductive processes in cereal. *Plant cell environment*, 31:11-38.
- Barr, H. D. and Weatherley, P. E. 1962. A re-examination of the relative turgidity technique for estimating water deficit in leaves. *Australian journal of biological sciences*, 15:413-428.
- Bascuñán-Godoy, L., Reguera, M., Abdel-Tawab, Y.M. and Blumwald, E. 2016. Water deficit stress-induced changes in carbon and nitrogen partitioning in *Chenopodium quinoa* Willd. *Planta*, 243:591–603.
- Baudoin, M. A., Vogel, C., Nortje, K. and Naik, M. 2017. Living with drought in South Africa: lessons learnt from the recent El Niño drought period. *International journal of disaster risk reduction*, 23:128–137.
- Bazile, D., Jacobsen, S. E. and Verniau, A. 2016. The global expansion of quinoa: Trends and limits. *Frontiers in environmental science*, 7:622.
- Beauchamp, C. and Fridovich, I. 1971. Superoxide dismutase: improved assay and an assay applicable to acrylamide gels. *Analytical biochemistry*, 44:276-287.
- Behnamnia, M., Kalantari, K.M. and Rezanejad, F. 2009. Exogenous application of brassinosteroids alleviates drought-induced oxidative stress in *Lycopersicon esculentum* L. *General and applied plant physiology*, 35:22–34.

- Benhin, J. K. A. 2006. Climate change and South African agriculture: Impact and adaptation options. CEEPA Discussion Paper #21. University of Pretoria, South Africa.
- Bertero, H. D., King, R. W. V Hall, A. J. 1999. Photoperiod-sensitive development phases in quinoa (*Chenopodium quinoa* Willd). *Field crops research*, 60:231-243.
- Bertero, H.D., De la Vega, A.J., Correa, G., Jacobsen, S.E. and Mujica, A. 2004. Genotype and genotype-by-environment interaction effects for grain yield and grain size of quinoa (*Chenopodium quinoa* Willd.) as revealed by pattern analysis of international multi-environment trials. *Field crops research*, 89:299–318.
- BFAP (Bureau for Food and Agricultural Policy). 2007. Modelling the economic impact of climate change on the South African maize industry. BFAP Report #2007-02.
- Bhargava, A., Shukla, S., Katiyar, R. S. and Ohri, D. 2003. Selection parameters for genetic improvement in *Chenopodium* grain on sodic soil. *Journal of applied horticulture*, 5:45-48.
- Bhargava, A., Shukla, S. and Ohri, D. 2006. *Chenopodium quinoa*—An Indian perspective. *Industrial crops and products*, 23:73–87.
- Bhargava, A., Shukla, S., Rajana, S. and Ohri, D. 2007. Genetic diversity for morphological and quality traits in quinoa (*Chenopodium quinoa* Willd) germplasm. *Genetic resources and crop evolution*, 54:167-173.
- Bitá, C.E. and Gerats, T. 2013. Plant tolerance to high temperature in a changing environment: Scientific fundamentals and production of heat stress-tolerant crops. *Frontiers in environmental science*, 4:273.
- Bois, J. F., Winkel, T., Lhomme, J. P., Raffailac, J. P. and Rocheteau, A. 2006. Response of some Andean cultivars of quinoa (*Chenopodium quinoa* Willd) to temperature: effects on germination, phenology, growth and freezing. *European journal of agronomy* 25:299-308.
- Bose, J., Rodrigo-Moreno, A. and Shabala, S. 2014. ROS homeostasis in halophytes in the context of salinity stress tolerance. *Journal of experimental botany*, 65:1241– 1257.

Bosque Sanchez, H., Lemeur, R., Damme, P.V. and Jacobsen, S. E. 2003. Ecophysiological analysis of drought and salinity stress of quinoa (*Chenopodium quinoa* Willd.). *Food reviews international*, 19:111–119.

Bradford, M. M. 1976. A rapid and sensitive method for the quantification of microgram quantities of protein utilizing the principle of protein-dye binding. *Analytical biochemistry*, 72:248-254.

Breenan, T. and Frenkel, C. 1977. Involvement of Hydrogen Peroxide in the Regulation of Senescence in Pear. *Plant physiology*, 59:411-416.

Brestic, M. and Zivcak, M. 2013. PSII Fluorescence techniques for measurement of drought and high temperature stress signal in crop plants: protocols and applications. *Molecular stress physiology of plants*. Springer, Berlin, pp 87–131.

Buchanan, B. B., Gruissem, W. and Jones, R. L. 2000. *Biochemistry and molecular biology of plants*. Rockville, Maryland.

Bukhov, N. G., Boucher, N. and Carpentier, R. 1997. Aftereffect of short-term heat shock on photosynthetic reactions in barley leaves. *Russian journal of plant physiology*, 44:526–32.

Bussotti, F., Desotgiu, R., Cascio, C., Pollastrini, M., Gravano, E., Gerosa, G., Marzuoli, R., Nali, C., Lorenzini, G., Salvatori, E., Manes, F., Schaub, M. and Strasser, R.J. 2011. Ozone stress in woody plant assessed with chlorophyll a fluorescence. A critical reassessment of existing data. *Environmental and experimental botany*, 73:19–30.

Carillo, P. and Gibon, Y. 2011. Extraction and Determination of Proline. https://www.researchgate.net/publication/211353600_PROTOCOL_Extraction_and_determination_of_proline Date of access: 25 Jan. 2019.

Ceppi, M. G., Oukarroum, A., Cicek, N., Strasser, R. J. and Schansker, G. 2012. The IP amplitude of the fluorescence rise OJIP is sensitive to changes in the photosystem I content of leaves: a study on plants exposed to magnesium and sulfate deficiencies, drought stress and salt stress. *Physiologia plantarum*, 144(3):277–288.

- Ceusters, J., and Van de Poel B. 2018. The control of photosynthesis by the hormone ethylene. *Plant physiology*, 76:2601-2612.
- Chaves, M. M., Maroco, J. P. and Pereira, J. S. 2003. Understanding plant response to drought: from genes to the whole plant. *Functional plant biology*, 30:239–264.
- Chen, L. S., Li, P. and Cheng, L. 2009. Comparison of thermotolerance of sun-exposed peel and shaded peel of 'Fuji'apple. *Environmental and experimental botany*, 66(1):110–116.
- Chen, S., Yang, J., Zhang, M., Strasser, R. J. and Qiang, S. 2016. Classification and characteristics of heat tolerance in *Ageratina adenophora* populations using fast chlorophyll a fluorescence rise O-J-I-P. *Environmental and experimental botany*, 122:126-140.
- Cheng, L., Han, M., Yang, L., Yang, L., Sun, Z., and Zhang, T. 2018. Changes in the physiological characteristics and baicalin biosynthesis metabolism of *Scutellaria baicalensis* Georgi under drought stress. *Industrial crops & products*, 122:473–482.
- Cornic, G. 2000. Drought stress inhibits photosynthesis by decreasing stomatal aperture, not by affecting ATP synthesis. *Trends in plant science*, 5:187–188.
- Cornic, G. and Fresneau, C. 2002. Photosynthetic Carbon Reduction and Carbon Oxidation Cycles Are the Main Electron Sinks for Photosystem II Activity during a Mild Drought. *Annals of botany*, 89:887-894.
- Cocoza, C., Pulvento, C., Lavini, A., Riccardi, M., d'Andria, R. and Tognetti, R. 2013. Effects of increasing salinity stress and decreasing water availability on ecophysiological traits of quinoa (*Chenopodium quinoa* Willd.) Grown in a mediterranean-type agroecosystem. *Journal of agronomy and crop science*, 199:229–240.
- Corpas, F.J., Fernández-Ocaña, A., Carreras, A., Valderrama, R. and Luque, F. 2006. The expression of different superoxide dismutase forms is cell-type dependent in olive (*Olea europaea* L.) leaves. *Plant and cell physiology*, 47:984–994.

Cui, X., Tang, Y., Gu, S., Nishimura, S., Shi, S. and Zhao, S. 2003. Photosynthetic depression in relation to plant architecture in two alpine herbaceous species. *Environmental and experimental botany*, 50:125-135.

Cusack, D. 1984. Quinoa: grain of Incas. *Ecologist*, 14:21-31.

Dabrowski, P., Kalaji, H. M., Baczewska, A. H., Pawluśkiewicz, B., Mastalerczuk, G., Borawska-Jarmułowicz, B., Paunov, M. and Goltsev, V. 2017. Delayed chlorophyll a fluorescence, MR820, and gas exchange changes in perennial rye grass under salt stress. *Journal of luminescence*, 183:322–333.

Dabrowski, P., Baczewska-Dabrowska, A. H., Kalaji, H. M., Goltsev, V., Paunov, M., Rapacz, M., Wójcik-Jagła, M., Pawlusiewicz, B., Baba, W. and Brestic, M. 2019. Exploration of chlorophyll a fluorescence and plant gas exchange parameters as indicators of drought tolerance in perennial ryegrass. *Sensors*, 19:2736. doi:10.3390/s19122736.

DAFF (Department of Agriculture, Forestry and Fisheries). 2016. A profile of the South African maize market value chain. Department of Agriculture, Forestry and Fisheries, Pretoria, South Africa. <https://www.nda.agric.za/doaDev/sideMenu/Marketing/Annual%20Publications/Commodity%20Profiles/field%20crops/Maize%20Market%20value%20Chain%20Profile%202016.pdf>. Date of access: 16 May 2018.

Dar, M. I., Naikoo, M. I., Khan, F. A., Rehman, F., Green, I. D., Naushin, F. and Ansari, A. A. 2017. An Introduction to reactive oxygen species metabolism under changing climate in plants (In Khan, M. I. R., Khan, N, A. eds. *Reactive Oxygen Species and Antioxidant System in Plants: role and regulation under abiotic stress*. New York: Springer Nature, p. 25-52).

Dat, J., Vandenabeele, S., Vranova, E., Montagu, M., Inze, D. and Van Breusegem, F. 2000 Dual action of the active oxygen species during plant stress responses. *Cellular and molecular life sciences*, 57:779–795.

Department of Agriculture, Forestry and Fisheries (DAFF). 2016. A profile of the South African maize market value chain. Department of Agriculture, Forestry and Fisheries,

Pretoria, South Africa. <https://www.nda.agric.za/doaDev/sideMenu/Marketing/Annual%20>

[Publications/Commodity%20Profiles/field%20crops/Maize%20Market%20value%20Chain%20Profile%202016.pdf](https://www.nda.agric.za/Marketing/Annual%20Publications/Commodity%20Profiles/field%20crops/Maize%20Market%20value%20Chain%20Profile%202016.pdf). Date of access: 16 May 2018.

De Ronde, J. A., Cress, W. A., Krüger, G. H J., Strasser, R. J. and Van Staden, J. 2004. Photosynthetic response of transgenic soybean plants, containing an *Arabidopsis* P5CR gene, during heat and drought stress. *Journal of plant physiology*, 161(11):1211-1224.

Digrado, A., Bachy, A., Mozaffar, A., Schoon, N., Bussotti, F., Amelynck, C., Dalcq, A. C., Fauconnier, M. L., Aubinet, M., Heinesch, B., du Jardin, P. 2017. Long-term measurements of chlorophyll a fluorescence using the JIP-test show that combined abiotic stresses influence the photosynthetic performance of the perennial ryegrass (*Lolium perenne*) in a managed temperate grassland. *Physiologia plantarum*, 161(3), 355–371.

Ding, S., Lei, M., Lu, Q., Zhang, A., Yin, Y., Wen, X., Zhang, L. and Lu, C. 2012. Enhanced sensitivity and characterization of photosystem II in transgenic tobacco plants with decreased chloroplast glutathione reductase under chilling stress, *Biochimica et Biophysica Acta (BBA) - Bioenergetics*, 1817(11):1979-1991.

Dong, S., Jiang, Y., Dong, Y., Wang, L., Wang, W., Ma, Z. and Yan, C. 2019. A study on soybean responses to drought stress and rehydration, *Saudi journal of biological sciences*, <https://doi.org/10.1016/j.sjbs>. Date of access: 05 Aug 2019.

Dupont, C.L., Neupane, K., Shearer, J. and Palenik, B. 2008. Diversity, function and evolution of genes coding for putative Ni-containing superoxide dismutases. *Environmental microbiology*, 10:1831–1843.

Durand, W. 2006. Assessing the impact of climate change on crop water use in South Africa. CEEPA Discussion Paper #28. University of Pretoria, South Africa.

Dutta, T., Neelapu, N. R. R., Wani, S. H. and Surekha, C. 2019. Role and regulation of osmolytes as signalling molecules to abiotic stress tolerance (*In* Khan, I. R., Reddy, P. S., Ferrante, A., Khan, N. eds. *Plant Signalling Molecules*. 1st ed. United Kingdom, Elsevier Science. p. 459-477).

DWAF (Department of Water Affairs and Forestry), 2004. National Water Resource Strategy, Pretoria.

Edwards, E. A., Rawsthorne, S. and Mullineaux, P. M. 1990. Subcellular distribution of multiple forms of glutathione reductase in leaves of pea (*Pisum sativum* L.). *Planta*, 180:278–284.

Edwards, J. K., Solsona, B., Ntainjua, E., Carley, A. F., Herzing, A. A., Kiely, C. J. and Hutchings, G. J. 2009. Switching off hydrogen peroxide hydrogenation in the direct synthesis process. *Science*, 323(5917):1037-1041.

Edwards, E. J., Osborne, C. P., Strömberg, C. A., Smith, S. A., C4 Grasses Consortium, Bond, W. J., Christin, P. A., Cousins, A. B., Duvall, M. R., Fox, D. L., Frecjleton, R. P., Ghannoum, O., Hertwell, J., Huang, Y., Janis, C. M., Keely, J. E., Kellogg, E. A., Leakey, A. D., Nelson, D. M., Saarela, J. M., Sage, O. E., Salamin, N., Still, C. J., Tipple, B. 2010. The origins of C4 grasslands: integrating evolutionary and ecosystem science. *Science*, 328:587–591.

Efeoglu, B., Ekmekci, Y. and Cicek. N. 2009. Physiological responses of three maize cultivars to drought stress and recovery. *South African journal of botany*, 75:34-42.

Ehleringer, J. R., Sage, R. F., Flanagan, L. B. and Pearcy, R. W. 1991. Climate change and the evolution of C4 photosynthesis. *Trends in ecology & evolution*, 6:95–99.

Eisa, S. S., Eid, M. A., Abd, E. S., Hussin, S. A., Abdel-Ati, A. A., El-Bordeny, N. E., Ali, S. H., Al-Sayed, H. M. A., Lotfy, M. E., Masoud, A. M. El-Naggar, A. M. and Ebrahim, M. 2017. *Chenopodium quinoa* Willd. A new cash crop halophyte for saline regions of Egypt. *Australian journal of crop science*, 11:343–351.

Estes, L. D., Beukes, H., Bradley, B. A., Debats. S., R., Oppenheimer, M., Ruane, A. C., Schulze, R. and Tadross, M. 2013. Projected climate impacts to South African maize and wheat production in 2055: a comparison of empirical and mechanistic modelling approaches. *Global change biology*, 19(12):3762–3774.

- Farooq, M., Aziz, T., Basra, S. M. A., Cheema, M. A. and Rehman, H. 2008. Chilling Tolerance in Hybrid Maize Induced by Seed Priming with Salicylic Acid. *Journal of agronomy and crop science*, 194:161–168.
- Farooq, M., Wahid, A., Kobayashi, N., Fujita, D. and Basra, S. M. A. 2009. Plant drought stress: effects, mechanisms and management. *Agronomy for sustainable development*, 29:185–212.
- FAO (Food and Agriculture Organisation). 2012. FAOStat: production. <http://www.fao.org/faostat/en/#data/QC>. Date of Access: 18 March 2019.
- FAO (Food and Agriculture Organisation). 2013. Agroclimatological Data. The United Nations Regional Office for Latin America and the Caribbean. Vitacura. Santiago, Chile.
- Filippou, P., Tanou, G., Molassiotis, A. and Fotopoulos, V. 2013. Plant acclimation to environmental stress using priming agents. (*In* Tuteja, N. and Gill, S. S. eds. *Plant acclimation to environmental stress*. New York, Springer. p. 1- 27).
- Fink, R. C. and Scandalios, J. G. 2002. Molecular evolution and structure function relationships of the superoxide dismutase gene families in angiosperms and their relationship to other eukaryotic and prokaryotic superoxide dismutase. *Archives of biochemistry and biophysics*, 399: 19–36.
- Flexas, J., Bota, J., Escalona, J. M., Sampol, B. and Medrano, H. 2002. Effects of drought on photosynthesis in grapevines under field conditions: an evaluation of stomatal and mesophyll limitations, *Functional plant biology*. 29:461–471.
- Fukao, T. and Bailey-Serres, J. 2004. Plant responses to hypoxia - is survival a balancing act? *Trends in plant science*, 9:449–456.
- Funck, D., Winter, G., Baumgarten, L. and Forlani, G., 2012. Requirement of proline synthesis during Arabidopsis reproductive development. *BMC plant biology*, 12(1):191.
- Garcia, M., Raes, D. and Jacobsen, S. E. 2003. Evapotranspiration analysis and irrigation requirements of quinoa (*Chenopodium quinoa*) in the Bolivian highlands. *Agricultural water management*, 60:119–134.

Gao, J., Li, P., Ma, F. and Goltsev, V. 2014. Photosynthetic performance during leaf expansion in *Malus micromalus* probed by chlorophyll a fluorescence and modulated 820 nm reflection. *Journal of photochemistry and photobiology : biology*, 137:144–150.

Garg, N. and Manchanda, G. 2009.) ROS generation in plants: boon or bane? *Plant biosystems*, 143:8–96.

Geerts, S., Reas, D., Garcia, M., Vacher, J., Mendoza, J., Huanca, R., Morales, B., Miranda, R., Cusicanqui, J. and Taboada, C. 2008. Introducing deficit irrigation to stabilize yields of quinoa (*Chenopodium quinoa* Willd). *European journal of agronomy*, 28:427-436.

Genty, B., Briantais, J. M. and Baker, N. R. 1989. The relationship between the quantum yield of photosynthetic electron transport and quenching of chlorophyll fluorescence. *Biochimica et biophysica acta*, 990:87-92.

Ghannoum, O. 2009. C4 photosynthesis and water stress. *Annals of botany*, 103:635–644.

Ghannoum, O., Evans, J. R. and von Caemmerer, S. 2011. Nitrogen and water use efficiency of C₄ plants. (In Raghavendra, A.S. and Sage, R.S. eds. C₄ photosynthesis and related CO₂ concentrating mechanisms. Netherlands, Springer Dordrecht Science and Business Media B.V. p. 129-146).

Gilberti, S., Funk, D. and Forlani, G. 2014. Δ^1 -pyrroline-5-carboxylate reductase from *Arabidopsis thaliana*: stimulation or inhibition by chloride ions and feedback regulation by proline depend on whether NADPH or NADH acts as co-substrate. *New phytologist*, 202:911-919.

Gill, S. S and Tuteja, N. 2010. Reactive oxygen species and antioxidant machinery in abiotic stress tolerance in crop plants. *Plant physiology and biochemistry*, 2010(48):909–930.

Gill, S. S., Anjum, N. A., Hasanuzzaman, M., Gill, R., Trivedi, D. K. Ahmad, I., Pereira, E. and Tuteja, N. 2013. Glutathione and glutathione reductase: a boon in disguise for plant abiotic stress defence operations. *Plant physiology and biochemistry*, 70:204– 212.

Gill, S. S., Anjum, N. A., Gill, R., Yadav, S., Hasanuzzaman, M., Fujita, M., Mishra, P., Sabat, S. C. and Tuteja, N. 2015. Superoxide dismutase-mentor of abiotic stress tolerance in crop plants. *Environmental science and pollution research*. 14:10375-10394.

Goltsev, V., Zaharieva, I., Chernev, P., Kouzmanova, M., Kalaji, H. M., Yordanov, I., Krasteva, V., Alexandrov, V., Stefanov, D., Allakhverdiev, S. I. and Strasser, R. J. 2012. Drought-induced modifications of photosynthetic electron transport in intact leaves: Analysis and use of neural networks as a tool for a rapid non-invasive estimation. *Biochimica et biophysica acta*, 1817:1490–1498.

González, J. A., Bruno, M., Valoy, M. and Prado, F. E., 2011. Genotypic variation of gas exchange parameters and leaf stable carbon and nitrogen isotopes in ten quinoa cultivars grown under drought. *Journal of agronomy and crop science*. 197:81–93.

González, J. A., Eisa, S. S. S., Sayed A. E. S. Hussin, S. A. E. S. and Prado, F. E. 2015. Quinoa: An Incan Crop to Face Global Changes in Agriculture. (In Murphy, K. and Matanguihan, J. eds. Quinoa: Improvement and Sustainable Production. 1st ed. John Wiley & Sons, Inc. p. 1-18).

Gorbe, E. and Calatayud, A. 2012. Applications of chlorophyll fluorescence imaging technique in horticultural research: a review. *Scientia horticultrae*, 138:24–35.

Govindjee. 1999. On the requirement of minimum number of four versus eight quanta of light for the evolution of one molecule of oxygen in photosynthesis: a historical note, *Photosynthesis research*, 59:249–254.

Grieco, M., Tikkanen, M., Paakkarinen, V., Kangasjärvi, S. and Aro, E. M. 2012. Steady state phosphorylation of light-harvesting complex II proteins preserves photosystem under fluctuating white light. *Plant physiology*, 160:1896–1910.

Guidi, L., Piccolo, E. L. and Landi, M. 2019. Chlorophyll Fluorescence, Photoinhibition and Abiotic Stress: Does it Make Any Difference the Fact to Be a C₃ or C₄ Species? *Frontiers in plant science*, 10:174.

- Gunes, A., Inal, A., Alpaslan, M., Eraslan, F., Bagci, E.G. and Cicek, N. 2007. Salicylic acid induced changes on some physiological parameters symptomatic for oxidative stress and mineral nutrition in maize (*Zea mays* L.) grown under salinity. *Journal of plant physiology*, 164:728–736.
- Guo, P., Baum, M., Varshney, R., Graner, A., Grando, S. and Ceccarelli, S. 2008. QTLs for chlorophyll and chlorophyll fluorescence parameters in barley under post-flowering drought. *Euphytica*, 163(2):203-214.
- Hamdani, S., Qu, M., Xin, C. P., Li, M., Chu, C., Govindjee and Zhu, X. G. 2015. Variations between the photosynthetic properties of elite and landrace Chinese rice cultivars revealed by simultaneous measurements of 820 nm transmission signal and chlorophyll a fluorescence induction. *Journal of plant physiology*, 177:128–138.
- Haldiman, P. and Strasser, R. J. 1999. Effects of anaerobiosis as probed by the polyphasic chlorophyll a fluorescence rise kinetic in pea (*Pisum sativum* L.). *Photosynthesis research*, 62:67-83.
- Hare, P.D., Cress, W.A. and Van Staden, J., 1998. Dissecting the roles of osmolyte accumulation during stress. *Plant, cell & environment*. 21:535-553.
- Hatch, M. D. 1987. C4 photosynthesis: a unique blend of modified biochemistry, anatomy and ultrastructure. *Biochimica et biophysica acta*, 895:81–106.
- Hatch, M. D. 1992. C4 photosynthesis: an unlikely process full of surprises. *Plant and cell physiology*, 33:333-342.
- Heber, U. 2002. Irrungen, Wirungen? The Mehler reaction in relation to cyclic electron transport in C3 plants. *Photosynthesis research*, 73:223–231.
- Heuer, B. 2003. Influence of exogenous application of proline and glycine betaine on growth of salt-stressed tomato plants. *Plant science*, 165(4):693-699.
- Hinojosa, L., González, J. A., Barrios-Masias, F. H., Fuentes, F. and Murphy, K. M. 2018. Quinoa Abiotic Stress Responses: A Review. *Plants*, 7(4):106.

- Horton, P. and Hague, A. 1988. Studies on the induction of chlorophyll fluorescence in isolated barley protoplasts. IV. Resolution of non-photochemical quenching. *Biochimica et biophysica acta (BBA) – bioenergetics*, 932:107-115.
- Hossain, M. A., Bhattacharjee, S., Armin, S. M., Qian, P., Wang, X., Li, H. Y., Burritt, D. J., Fujita, M. and Tran, L. S. 2015. Hydrogen peroxide priming modulates abiotic oxidative stress tolerance: insights from ROS detoxification and scavenging. *Frontiers in plant science*, 6:420. doi:10.3389/fpls.2015.00420
- Hung, S., Yu, C. and Lin, C. H. 2005. Hydrogen peroxide functions as a stress signal in plants. *Botanical bulletin of academia sinica*, 46:1–10.
- Hunziker, A. T. 1943. Los especies alimenticias de *Amaranthus* y *Chenopodium* cultivadas por los indios de America. *Revista argentina de agronomia*, 30:297-353.
- Iqbal, H., Yaning, C., Waqas, M., Shareef, M., Raza, S. T. 2018. Differential response of quinoa genotypes to drought and foliage-applied H₂O₂ in relation to oxidative damage, osmotic adjustment and antioxidant capacity. *Ecotoxicology and environmental safety*, 164:344–354.
- Jacobsen, S. E. and Stolen, O. 1993. Quinoa morphology, phenology and prospects for its production as a new crop in Europe. *European journal of agronomy*, 2:19-29.
- Jacobsen, S. E., Mujica, A. and Jensen, C. R. 2003. The resistance of quinoa (*Chenopodium quinoa* Willd) to adverse abiotic factors. *Food reviews international*, 19:99-109.
- Jacobsen, S. E., Monteros, C., Christiansen, J.L., Bravo, L.A., Corcuera, L.J. and Mujica, A. 2005. Plant responses of quinoa (*Chenopodium quinoa* Willd.) to frost at various phenological stages. *European journal of agronomy*, 22:131–139.
- Jacobsen, S. E., Liu, F. and Jensen, C. R. 2009. Does root sourced ABA play a role for regulation of stomata under drought in quinoa (*Chenopodium quinoa* Willd.). *Scientia Horticulturae*, 122:281-287.

Jacobsen, S. E. 2011. The situation for quinoa and its production in southern Bolivia: from economic success to environmental disaster. *Journal of agronomy and crop science*, 197:390-399.

Jacobsen, S. E., Jensen, C. R. and Lui, F. 2012. Improving crop production in the arid Mediterranean climate. *Field crops research*, 128:34-47.

Jaleel, C. A., Manivannan, P., Kishorekumar, A., Sankar, B. Gopi, R., Somasundaram, R. and Panneerselvam, R. 2007. Alterations in osmoregulation, antioxidant enzymes and indole alkaloid levels in *Catharanthus roseus* exposed to water deficit. *Colloids and surfaces B: biointerfaces*, 59:150–157.

Jawahar, G., Rajasheker, G., Maheshwari, P., Punita, D. L., Jalaja, N., Kumari, P. H., Kumar, S. A., Afreen, R., Karumanchi, A. P., Rathnagiri, P Sreenivasulu, N. and Kishor, P. B. K. 2019. Osmolyte diversity, distribution, and their biosynthetic pathways. (In Khan, I. R., Reddy, P. S., Ferrante, A., Khan, N. eds. *Plant signalling molecules*. 1st ed. United Kingdom, Elsevier Science. p. 499-458).

Jensen, C. R., Jacobsen, S. E., Andersen, M. N., Nunez, N., Andersen, S. D., Rasmussen, L. and Mogensen V. O. 2000. Leaf gas exchange and water relation characteristics of field quinoa (*Chenopodium quinoa* Willd.) during soil drying. *European journal of agronomy*, 13:11–25.

Ji, H., Pardo, J.M., Batelli, G., Van Oosten, M.J., Bressan, R.A. and Li, X. 2013. The salt overly sensitive (SOS) pathway: established and emerging roles. *Molecular plant*, 6(2):275-286.

Jiménez, A., Hernández, J. A., del Río, L. A. and Sevilla, F. 1997. Evidence for the presence of the ascorbate-glutathione cycle in mitochondria and peroxisomes of pea (*Pisum sativum* L.) leaves. *Plant physiology*, 114:275–284.

Joshi, R., Singla-Pareek, S.L. and Pareek, A. 2018. Engineering abiotic stress response in plants for biomass production. *The journal of biological chemistry*, 293(14):5035-5043.

Kajala, K., Covshoff, S., Karki, S., Woodfield, H., Tolley, B. J., Dionora, M. J., Mogul, R. T., Mabilangan A. E., Danila, F. R., Hibberd, J. M. and Quick, W. P. 2011. Strategies for engineering a two-celled C₄ photosynthetic pathway into rice. *Journal of experimental botany*, 62:3001–3010.

Kahane, R., Hodgkin, T., Jaenicke, H., Hoogendoorn, C., Keatinge, H. M. J. D. H., d'Arros Hughes, J., Padulosi, S. and Looney, N. 2013. Agrobiodiversity for food security, health and income. *Agronomy sustainable development*, 33:671-693.

Kalaji, H.M. and Loboda, T., 2007. Photosystem II of barley seedlings under cadmium and lead stress. *Plant, soil and environment*, 53(12):511-516.

Kalaji, H. M., Jajoo, A., Oukarroum, A., Brestic, M., Zivcak, M., Samborska, I. A., Cetner, M. D., Łukasik, I., Goltsev, V. and Ladle, R. J. 2016. Chlorophyll a fluorescence as a tool to monitor physiological status of plants under abiotic stress conditions. *Acta physiologiae plantarum*, 38:102.

Kalaji, H. M., Schansker, G., Brestic, M., Bussotti, F., Calatayud, A., Ferroni, L., Goltsev, V., Guidi, L., Jajoo, A., Li, P., Losciale, P., Mishra, V. K., Misra, A. N., Nebauer, S. G., Pancaldi, S., Penella, C., Pollastrini, M., Suresh, K., Tambussi, E., Yanniccari, M., Zivcak, M., Cetner, M. D., Samborska, I. A., Stirbet, A., Olsovska, K., Kunderlikova, K., Shelonzek, H., Rusinowski, S. and Baba, W. 2017. Frequently asked questions about chlorophyll fluorescence, the sequel. *Photosynthesis research*, 132(1):13–66.

Kalaji, H. M., Rackova, L., Paganova, V., Swoczyna, T., Rusinowski, S. and Sitko, K. 2018. Can chlorophyll a fluorescence parameters be used as bio- indicators to distinguish between drought and salinity stress in *Tilia cordata* Mill? *Environmental and experimental botany*, 152:149-157.

Kaminaka, H., Morita, S, Nakajima, M., Masumura, T. and Tanaka, K. 1998. Gene cloning and expression of cytosolic glutathione reductase in rice (*Oriza sativa* L.). *Plant and cell physiology*, 39:1269–1280.

Kavi Kishor, P. B., Sangam, S., Amrutha, R. N., Laxmi, P. S., Naidu, K. R., Rao, K. R. S. S., Rao, S., Reddy, K. J., Theriappan, P. and Sreenivasulu, N. 2005. Regulation of

proline biosynthesis, degradation, uptake and transport in higher plants: its implications in plant growth and abiotic stress tolerance. *Current science*, 88:424–438.

Ke, B. 2001. P430: the spectral species representing the terminal electron acceptor of photosystem I. (In Ke, B. ed. *Photosynthesis: Photobiochemistry and Photobiophysics*. Volume 10. Dordrecht, The Netherlands: Kluwer Academic Publishers. p. 305–322).

Keppler, L. D. and Novacky, A. 1987. The initiation of membrane lipid peroxidation during bacteria-induced hypersensitivity reaction. *Physiological and molecular plant pathology*, 30:233-245.

Killi, D., Bussotti, F., Raschi, A. and Haworth, M. 2017. Adaptation to high temperature mitigates the impact of water deficit during combined heat and drought stress in C3 sunflower and C4 maize varieties with contrasting drought tolerance. *Physiologia plantarum*, 159:130–147.

Killi, D. and Haworth, M. 2017. Diffusive and metabolic constraints to photosynthesis in quinoa during drought and salt stress. *Plants*, 6:49.

Kocheva, K. V., Busheva, M. C., Georgiev, G. I., Lambrev, P. H. and Goltsev, V. N. 2005. Influence of short-term osmotic stress on the photosynthetic activity of barley seedlings. *Biologia plantarum*, 49:145–148.

Kono, M., Noguchi, K. and Terashima, I. 2014. Roles of the cyclic electron flow around PSI (CEF-PSI) and O₂-dependent alternative pathways in regulation of the photosynthetic electron flow in short-term fluctuating light in *Arabidopsis thaliana*. *Plant and cell physiology*, 55:990–1004.

Kornyeyev, D., Logan, B. A., Payton, P., Allen, R. D. and Holaday, A. S. 2003. Elevated chloroplastic glutathione reductase activities decrease chilling-induced photoinhibition by increasing rates of photochemistry, but not thermal energy dissipation, in transgenic cotton. *Functional plant biology*, 30:101–110.

Krall, J. P. and Edwards, G. E. 1990. Quantum Yields of Photosystem II Electron Transport and Carbon Dioxide Fixation in C₄ Plants. *Australian journal of plant physiology*, 17(5):579 – 588.

- Kubien, D. S., von Caemmerer, S., Furbank, R. T. and Sage, R. F. 2003. C₄ photosynthesis at low temperature: a study using transgenic plants with reduced amounts of Rubisco. *Plant physiology*, 132:1577–1585.
- Kumar, M., Sirhindi, G., Bhardwaj, R., Kumar, S. and Jain, G. 2010. Effect of exogenous H₂O₂ on antioxidant enzymes of *Brassica juncea* L. seedlings in relation to 24-epibrassinolide under chilling stress. *Indian journal of biochemistry and biophysics*, 47:378–382.
- Kumar, R. R., Karajol, K. and Naik, G. R. 2011. Effect of polyethylene glycol induced water stress on physiological and biochemical responses in pigeonpea (*Cajanus cajan* L. Millsp.). *Recent research in science and technology*, 3:148–152.
- Laino, M. 2006. Características Climáticas de Ancovinto Durante. Boletín Técnico FIA-CODE-CITE. Iquique, Chile. pp. 1-3.
- Lara, M.V. and Andreo, C.S. 2005. Photosynthesis in non- typical C₄ species. (In Pessaraki, M. ed. Handbook of Photosynthesis. 2nd ed. Boca Raton, FL, USA: CRC press, Taylor & Francis Group. p. 391-421).
- Lara, M.V. and Andreo, C.S. 2011. C₄ plants adaptation to high levels of CO₂ and to drought environments (In Shanker, A. ed. Abiotic stress in plants - mechanisms and adaptations. In Tech. <http://www.intechopen.com/books/abiotic-stress-in-plantsmechanisms-and-adaptations/c4-plants-adaptation-to-high-levels-of-co2-and-to-drought-environments>. Date of access: 17 Feb. 2018.
- Larkindale, J., and Huang, B. 2004. Thermo-tolerance and antioxidant systems in *Agrostis stolonifera*: Involvement of salicylic acid, abscisic acid, calcium, hydrogen peroxide, and ethylene. *Journal of plant physiology*, 161:405–413.
- Lauriano, J. A., Ramalho, J. C., Lindon, F. C., Céu Matos, M. 2006. Mechanisms of energy dissipation in peanut under water stress. *Photosynthetica*, 44:404-410.
- Lawlor, D.W. 2002. Limitation to photosynthesis in water-stressed leaves: stomata vs. metabolism and the role of ATP. *Annals of botany*, 89:871–885.

- Lawson, T., Oxborough, K., Morison, J.L. and Baker, N.R. 2003. The responses of guard and mesophyll cell photosynthesis to CO₂, O₂, light, and water stress in a range of species are similar. *Journal of experimental botany*, 54:1743–1752.
- Liao, J. X. and Wang, G. X. 2014. Effects of drought stress on leaf gas exchange and chlorophyll fluorescence of *Glycyrrhiza uralensis*. *Russian journal of ecology*, 46:532–538.
- Lin, W. C. and Block, G. S. 2010. Can H₂O₂ application reduce chilling injury of horticultural crops? *Acta horticulturae*, 875:33–36.
- Liu, F. and Stützel, H. 2004. Biomass partitioning, specific leaf area, and water use efficiency of vegetable amaranth (*Amaranthus* spp.) in response to drought stress. *Scientia horticulturae*, 102:15–27.
- Liu, J., Guo, Y. Y., Bai, Y. W., Camberato, J. J., Xue, J. Q. and Zhang, R. H. 2018. Effect of drought stress on the photosynthesis in maize. *Russian journal of plant physiology*, 65:849–856.
- Liu, B., Liang, J., Tang, G., Wang, X., Liu, F., Zhao, D. 2019. Drought stress effects on growth, water use efficiency, gas exchange and chlorophyll fluorescence of *Juglans* rootstocks. *Scientia horticulturae*, 250:230-235.
- Loggini, B., Scartazza, A., Brugnoli, E. and Navari-Izzo, F., 1999. Antioxidative defense system, pigment composition, and photosynthetic efficiency in two wheat cultivars subjected to drought. *Plant physiology*, 119:1091–1100.
- Long, S.P. 1999. Environmental responses. (In Sage, R.F. & Monson, R.K. ed. C₄ plant biology. San Diego, USA: Academic Press. p. 215–249).
- Long, S.P., Zhu, X.G., Naidu, S.L. and Ort, D.R. 2006. Can improvement in photosynthesis increase crop yields? *Plant cell and environment*. 29:315-330.
- Longenberger, P.S., Smith, C.W., Duke, S.E. and Mcmichael, B.L., 2009. Evaluation of chlorophyll fluorescence as a tool for the identification of drought tolerance in upland cotton, *Euphytica*. 166(1):25-33.

- Lum, M. S., Hanafi, M.M., Rafii, Y. M., Akmar, A. S. N. 2014. Effect of drought stress on growth, proline and antioxidant enzyme activities of upland rice. *The Journal of animal & plant sciences*, 24(5):1487-1493.
- Majeran, W., Friso, G., Ponnala, L., Connolly, B., Huang, M., Reidel, E., Zhang, C., Asakura, Y., Bhuiyan, N. H., Sun, Q., Turgeon, R. and van Wijk, K. J. 2010. Structural and metabolic transitions of C4 leaf development and differentiation defined by microscopy and quantitative proteomics in maize. *Plant cell*, 22(11):3509–3542.
- Makino, A., Miyake, C. and Yokota, A. 2002. Physiological functions of the water–water cycle (Mehler reaction) and the cyclic electron flow around PSI in rice leaves. *Plant and cell physiology*, 43:1017–1026.
- Mangani, R., Tesfamariam, E. H., Engelbrecht, C. J., Bellocchi, G., Abubeker Hassen, A. and Mangani, T. 2019. Potential impacts of extreme weather events in main maize (*Zea mays* L.) producing areas of South Africa under rainfed conditions. *Regional environmental change*, 19:1441–1452.
- Manivannan, P., Jaleel, C. A., Kishorekumar, A., Sankar, B. Somasundaram, R., Sridharan, R. and Panneerselvam, R. 2007. Changes in antioxidant metabolism of *Vigna unguiculata* (L.) Walp. by propiconazole under water deficit stress. *Colloids and surfaces B: biointerfaces*, 57:69–74.
- Mansour, M. M. F., and Ali, E. F. 2017. Evaluation of proline functions in saline conditions. *Phytochemistry*, 140:52-56.
- Maroco, J. P., Rodrigues, M. L., Lopes, C. and Chaves, M. M. 2002. Limitations to leaf photosynthesis in grapevine under drought-metabolic and modelling approaches. *Functional plant biology*, 29:1–9.
- Martinez, C. A., Loureiro, M. E., Oliva, M. A., Maestri, M. 200. Differential responses of superoxide dismutase in freezing resistant *Solanum curtilobum* and freezing sensitive *Solanum tuberosum* subjected to oxidative and water stress. *Plant science*, 160: 505–515.

- Mathobo, R., Marais, D. and Steyn, J. M. 2017. The effect of drought stress on yield, leaf gaseous exchange and chlorophyll fluorescence of dry beans (*Phaseolus vulgaris* L.). *Agricultural water management*, 108:118-125.
- Mathur, S., Mehta, P., Jajoo, A and Bharti, S. 2011. Analysis of elevated temperature induced inhibition of Photosystem II using Chl a fluorescence induction kinetics. *Plant biology*, 13:1–6.
- Mattioli, R., Costantino, P. and Trovato, M. 2009. Proline accumulation in plants. Not only stress. *Plant signaling & behaviour* 4:1016–1018.
- Maxwell, K. and Johnson, G. N. 2000. Chlorophyll fluorescence- a practical guide. *Journal of experimental biology*, 55:659-668.
- McCree, K. J. 1972. The action spectrum, absorptance and quantum yield of photosynthesis in crop plants. *Agricultural meteorology*, 9:191–216.
- Melchiorre, M. Robert, G. Trippi, V. Racca, R. and Lascano, H.R. 2009. Superoxide dismutase and glutathione reductase overexpression in wheat protoplast: photo-oxidative stress tolerance and changes in cellular redox state. *Plant growth regulation*, 57:57-68.
- Melkonian, J., Yu, L.X. and Setter, T.L. 2004. Chilling response of maize (*Zea Mays* L.) seedlings: root hydraulic conductance, abscisic acid, and stomatal conductance. *Journal of experimental botany*, 55:1751-1760.
- Miller, A. F. 2004. Superoxide dismutases: active sites that save, but a protein that kills. *Current opinion in chemical biology*, 8:162–168.
- Miranda-Apodaca, J., Yoldi-Achalandabaso, A., Aguirresarobe, A., del Canto, A. and Pérez-Lópe, U. 2018. Similarities and differences between the responses to osmotic and ionic stress in quinoa from a water use perspective. *Agricultural water management*, 203:344–352.
- Mittler, R. 2002. Oxidative stress, antioxidants and stress tolerance. *Trends in plant science*, 7:405–410.

- Mittler, R., Vanderauwera, S., Gollery, M. and Van Breusegem, F. 2004. Reactive oxygen gene network of plants. *Trends in plant science*, 9:490–498.
- Mittler, R. and Blumwald, E. 2010. Genetic Engineering for Modern Agriculture: Challenges and Perspectives. *Annual review of plant biology*, 61(1):443.
- Moore, P. H., Paterson, A. H and Tew, T. 2014. Sugarcane: The crop, the plant, and development. (In Moore, P. H. & Botha, F. C, ed. Sugarcane physiology, biochemistry & functional biology. Iowa, USA: John Wiley & Sons, Inc. p. 1- 34).
- Mujica, A. 1994. Andean grains and legumes. (In Hernando Bermujo, J. E. and Leon, J. eds. Neglected Crops. Volume 26. Rome, Italy. p. 131-148).
- Mullineaux, P. M., Enard, C., Hellens, R. and Creissen, G. 1996. Characterization of a glutathione reductase gene and its genetic locus from pea (*Pisum sativum* L.). *Planta*, 200:186–194.
- Muscolo, A., Panuccio, M.R., Giofrè, A.M. and Jacobsen, S. E. 2016. Drought and salinity differently affect growth and secondary metabolites of “*Chenopodium quinoa* Willd” seedlings. (In Khan, M.A., Ozturk, M., Gul, B., Ahmed, M.Z., eds. Halophytes for Food Security in Dry Lands. San Diego, CA, USA: Elsevier Inc. p. 259–275).
- National Research Council. 1989. Lost crops of Incas. Little known plants of the Andes with promise for worldwide cultivation. Washington, DC, National Academy Press.
- Oelke, E. A., Putnam, D. H., Teynor, T. M. and Oplinger, E. S. 1992. Alternative field crops manual. University of Wisconsin Cooperative Extension Service. University of Minnesota Extension Service. Center for alternative Plant and Animal products.
- Oelze, M. L., Vogel, M. O., Alsharafa, K., Kahmann, U., Viehhauser, A., Maurino, V. G. and Dietz, K. J. 2012. Efficient acclimation of the chloroplast antioxidant defence of *Arabidopsis thaliana* leaves in response to a 10- or 100-fold light increment and the possible involvement of retrograde signals. *Journal of experimental botany*, 63:1297–1313.
- Omar, A. A. 2012. Impact of drought stress on germination and seedling growth parameters of some wheat cultivars. *Life science journal*, 9(1):590-598.

Orsini, F., Accorsi, M., Gianquinto, G., Dinelli, G., Antognoni, F., Carrasco, K. B. R., Martinez, E. A., Alnayef, M., Marotti, I., Bosi, S. and Biondi, S. 2011. Beyond the ionic and osmotic response to salinity in *Chenopodium quinoa*: Functional elements of successful halophytism. *Functional plant biology*, 38:818–831.

Oukarroum, A., El Madidi, S., Schansker, G. and Strasser, R. J. 2007. Probing the responses of barley cultivars (*Hordeum vulgare* L.) by chlorophyll *a* fluorescence OLKJIP under drought stress and re-watering. *Environmental and experimental botany*, 60:438–446.

Oukarroum, A., Schansker, G. and Strasser, R. J. 2009. Drought stress effects on photosystem I content and photosystem II thermotolerance analyzed using Chl *a* fluorescence kinetics in barley varieties differing in their drought tolerance. *Physiologia plantarum*, 137(2):188–199.

Oukarroum, A., El Madidi, S. and Strasser, R. J. 2012a. Exogenous glycine betaine and proline play a protective role in heat-stressed barley leaves (*Hordeum vulgare* L.): A chlorophyll *a* fluorescence study. *Plant biosystems*, 146:1037–1043.

Oukarroum, A., Strasser, R.J. and Schansker, G. 2012b. Heat stress and the photosynthetic electron transport chain of the lichen *Parmelina tiliacea* (Hoffm.) Ach. in the dry and the wet state: Differences and similarities with the heat stress response of higher plants. *Photosynthesis research*, 111:303–314.

Oukarroum, A., Madidi, S. and Strasser, R. J. 2016. Differential heat sensitivity index in barley cultivars (*Hordeum vulgare* L.) monitored by chlorophyll *a* fluorescence OKJIP. *Plant physiology and biochemistry*, 105:102-108.

Pang, C.H. and Wang, B.H. 2010. Role of ascorbate peroxidase and glutathione reductase in ascorbate–glutathione cycle and stress tolerance in plants. (In Anjum, N. A., Chan, M. T., Umar, S. eds. *Ascorbate-glutathione pathway and stress tolerance in plants*. Netherlands: Springer. p. 91–113).

Parry, M. A. J., Flexas, J. and Medrano, H. 2005. Prospects for crop production under drought: research priorities and future directions, *Annals of applied biology*, 147:211–226.

- Paschenko, V. Z., Protasov, S. P., Rubin, A. B., Timofeev, K. N., Zamazova, L. M. and Rubin, L. B. 1975. Probing the kinetics of photosystem I and photosystem II fluorescence in pea chloroplasts on a picosecond pulse fluorometer. *Biochimica et biophysica acta (BBA)*, 408:143–153.
- Pastenes, C., Pimentel, P. and Lillo, J. 2005. Leaf movements and photoinhibition in relation to water stress in field-grown beans, *Journal of experimental botany*. 56:425–433.
- Peng, S. H., Sheehy, J., Laza, J. E., Visperas, R. E., Zhong, R. M., Centeno, X., Khush, G. S., and Cassman, K. G. 2004. Rice yields decline with higher night temperature from global warming. *Proceedings of the national academy of sciences of the United States of America*, 101:9971-9975.
- Per, T.S., Khan, N.A., Reddy, P.S., Masood, A., Hasanuzzaman, M., Khan, M.I.R. and Anjum, N. A. 2017. Approaches in modulating proline metabolism in plants for salt and drought stress tolerance: phytohormones, mineral nutrients and transgenics. *Plant physiology and biochemistry*, 115:126-140.
- Percival, G. C., Keary, I. P. and Al-Habsi, S. 2006. An assessment of the drought tolerance of *Fraxinus* genotypes for urban landscape plantings. *Urban forestry and urban greening*, 5:17-27.
- Peterson, A. and Murphy, K. 2015. Tolerance of lowland quinoa cultivars to sodium chloride and sodium sulphate salinity. *Crop science*, 55:331–338.
- Pilon, M., Ravet, K. and Tapken, W. 2011. The biogenesis and physiological function of chloroplast superoxide dismutases. *Biochimica et biophysica acta*, 1807:989–998.
- Porcar-Castell, A., Tyystjärvi, E., Atherton, J., van der Tol, C., Flexas, J., Pfundel, E. E., Moreno, J., Frankenberg, C. and Berry, J. A. 2014. Linking chlorophyll *a* fluorescence to photosynthesis for remote sensing applications: mechanisms and challenges. *Journal of experimental botany*, 65:4065–4095.

Portis, A.R. Jr and Parry, M. A. J. 2007. Discoveries in Rubisco (ribulose 1,5-bisphosphate carboxylase/oxygenase): a historical perspective. *Photosynthesis research*, 94:121–143.

Prasad, P. V. V., Pisipati, S. R., Momcilovic, I. and Ristic, Z. 2011. Independent and combined effects of high temperature and drought stress during grain filling on plant yield and chloroplast EF-Tu expression in spring wheat. *Journal of agronomy and crop science*, 197:430-441.

Prasad, V., Bheemanahalli, R. and Jagadish, S. V. K. 2017. Field crops and the fear of heat stress - Opportunities, challenges and future directions. *Field crops research*, 200:114–121.

Pratap, V. and Sharma Y. K. 2010. Impact of osmotic stress on seed germination and seedling growth in black gram (*Phaseolus mungo*). *Journal of environmental biology*, 31(5):721-726.

Pšidová, E., Živčák, M., Stojnić, S., Orlović, S., Gömöry, D., Kučerová, J., Ditmarová, L., Střelcová, K., Brestič, M., Kalaji, H. M. 2018. Altitude of origin influences the responses of PSII photochemistry to heat waves in European beech (*Fagus sylvatica* L.). *Environmental and experimental botany*, 152, 97–106.

Pulvento, C., Riccardi, M., Lavini, A., D'Andria, R., Iafelice, G. and Marconi, E. 2010. Field trial evaluation of two *Chenopodium quinoa* genotypes grown under rain-fed conditions in a typical Mediterranean environment in south Italy. *Journal of agronomy and crop science*, 196:407–411.

Rahman, H. U., Malik, S. A. and Saleem, M. 2004. Heat tolerance of upland cotton during the fruiting stage evaluated using cellular membrane thermostability. *Field crops research*, 85:149-158.

Ralph, P. J. and Gademann, R. 2005. Rapid light curves: a powerful tool to assess photosynthetic activity. *Aquatic botany*, 82:222–237.

Rapacz, M., Gasior, D., Zwierzykowski, Z., Lesniewska-Bocianowska, A., Humphreys, M. W. and Gay, A. P. 2004. Changes in cold tolerance and the mechanisms of

acclimation of photosystem II to cold hardening generated by anther culture of *Festuca pratensis* x *Lolium multiflorum* cultivars. *New phytology* 162:105-114.

Redillas, M. C. F. R., Strasser, R. J., Jeong, J. S., Kim, Y. S. and Kim, J. 2011. The use of JIP test to evaluate drought-tolerance of transgenic rice overexpressing OsNAC10. *Plant biotechnology reports*, 5:169-175.

Reddy, A.R., Chaitanya, K.V. and Vivekanandan, M. 2004. Drought-induced responses of photosynthesis and antioxidant metabolism in higher plants. *Journal of plant physiology*, 161:1189-1202.

Reddy, A.R., Rasineni, G.K. and Raghavendra, A.S. 2010. The impact of global elevated CO₂ concentration on photosynthesis and plant productivity. *Current science*, 99:46-57.

Rejeb, K. B., Abdelly, C. and Saviouré, A. 2014. How reactive oxygen species and proline face stress together. *Plant physiology and biochemistry*, 80:278-284.

Ren, J., Sun, L. N., Zhang, Q. Y. and Song, X. S. 2016. Drought tolerance is correlated with the activity of antioxidant enzymes in *Cerasus humilis* seedlings. *BioMed research international*, 2016:9851095.

Rhee, J., Kim, R., Choi, H., Lee, J., Lee, Y. and Lee, J. 2011. Molecular and biochemical modulation of heat shock protein 20 (Hsp20) gene by temperature stress and hydrogen peroxide (H₂O₂) in the monogonont rotifer, *Brachionus* sp. *Comparative biochemistry and physiology*, 154:19–27.

Ripley, B. S., Gilbert, M. E., Ibrahim, D. G., and Osborne, C. P. 2007. Drought constraints on C₄ photosynthesis: stomatal and metabolic limitations in C₃ and C₄ subspecies of *Alloteropsis semialata*. *Journal of experimental botany*, 58:1351–1363.

Rizhsky, L., Liang, H. and Mittler, R. 2002. The combined effect of drought stress and heat shock on gene expression in tobacco. *Plant physiology*, 130:1143-1151.

Rizhsky, L., Liang, H. and Mittler, R. 2003. The water-water cycle is essential for chloroplast protection in the absence of stress. *The journal of biological chemistry*, 278:38921–38925.

Romanowska, E., Buczyńska, A., Wasilewska, W., Krupnik, T., Drozak, A., Rogowski, P., Parys, E. and Zienkiewicz, Z. 2017. Difference in photosynthetic responses of NADP-ME type C₄ species to high light. *Planta*, 245:641-657.

Rosa, M., Hilal, M., Gonzalez, J. A. and Prado, F. E. 2004. Changes in soluble carbohydrates and related enzymes induced by low temperature during early developmental stages of quinoa (*Chenopodium quinoa*) seedlings. *Journal of plant physiology*, 161:683-689.

Ruiz, K., Biondi, S., Oses, R., Acuña-Rodríguez, I., Antognoni, F., Enrique A. Martínez-Mosqueira, E. A., Coulibaly, A., Canahua-Murillo, A., Pinto, M., Zurita-Silva, A., Bazile, D., Jacobsen, S. and Molina-Montenegro, M. A. 2014. Quinoa biodiversity and sustainability for food security under climate change. *Agronomy for sustainable development*, 34:349–359.

Ruiz, K.B., Biondi, S., Martínez, E.A., Orsini, F., Antognoni, F. and Jacobsen, S.E., 2016. Quinoa – a model crop for understanding salt-tolerance mechanisms in halophytes. *Plant biosystems*, 150:357–371.

Sabagh, A.E., Sorour, S., Ragab, A., Saneoka, H. and Islam, M.S., 2017. The effect of exogenous application of proline and glycine betaine on the nodule activity of soybean under saline condition. *Journal of agriculture biotechnology*, 2(1):1-5.

Sage, R. F. and McKown, A. D. 2006. Is C₄ photosynthesis less phenotypically plastic than C₃ photosynthesis? *Journal of experimental botany*. 57:303–317.

Sage, R. F., Peixoto, M. M. and Sage, T. L. 2014. Photosynthesis in sugarcane. (In Moore, P. H. & Botha, F. C, ed. Sugarcane physiology, biochemistry & functional biology. Iowa, USA: John Wiley & Sons, Inc. p. 121-154).

Sage, R. F., and Sultmanis, S. 2016. Why are there no C₄ forests? *Journal of plant physiology*, 203:55–68.

Saibi, W. and Brini, F. 2018. Superoxide dismutase (SOD) and abiotic stress tolerance in plants: an overview. (In Magliozzi, S. ed. Superoxide Dismutase. New York, United States: Nova Science Publishers, Inc. p. 101-142)

- Sairam, R. K., Rao, K. V. and Srivastava, G. C. 2002. Differential response of wheat genotypes to long term salinity stress in relation to oxidative stress, antioxidant activity and osmolyte concentration. *Plant science*, 163:1037–1046.
- Saxena, I., Srikanth, S. and Chen, Z. 2016. Cross talk between H₂O₂ and interacting signal molecules under plant stress response. *Frontiers in plant science*, 7: 570. doi: 10.3389/fpls.2016.00570
- Schaedle, M. and Bassham, J. A. 1977. Chloroplast glutathione reductase. *Plant physiology*, 59:1011-1012.
- Schansker, G., Srivastava, A., Govindjee and Strasse, R. J. 2003. Characterization of the 820-nm transmission signal paralleling the chlorophyll *a* fluorescence rise (OJIP) in pea leaves. *Functional plant biology*, 30(7):785–796.
- Schansker, G., To' th, S. Z. and Strasser, R. J. 2005. Methylviologen and dibromothymoquinone treatments of pea leaves reveal the role of photosystem I in the Chl *a* fluorescence rise OJIP. *Biochimica et biophysica acta*, 1706:250–261.
- Schmöckel, S. M., Lightfoot, D. J., Razali, R., Tester, M. and Jarvis, D. E. 2017. Identification of putative transmembrane proteins involved in salinity tolerance in *Chenopodium quinoa* by integrating physiological data, RNAseq, and SNP analyses. *Frontiers in plant science*, 8.
- Schreiber, U. 1986. Detection of rapid induction kinetics with a new type of high-frequency modulated chlorophyll fluorometer. *Photosynthesis research*, 9:261–272.
- Schreiber, U., Neubauer, C. and Klughammer, C. 1989. Devices and methods for room-temperature fluorescence analysis. *Philosophical transactions of the Royal Society B: biological* 323(1216):241–251.
- Schreiber, U., Klughammer, C. and Kolbowski, J. 2012. Assessment of wavelength-dependent parameters of photosynthetic electron transport with a new type of multi-color PAM chlorophyll fluorometer. *Photosynthesis research*, 113(1–3):127–144.

Schurr, U. 1997. Growth physiology and measurement of growth. (In Behnke, H. D., Lüttge, U., Esser, K., Kadereit, J. W. and Runge, M. eds. Progress in Botany 59. Berlin: Springer Verlag. p. 355-373).

Sekmen, A. H., Ozgur, R., Uzilday, B. and Turkan, I. 2014. Reactive oxygen species scavenging capacities of cotton (*Gossypium hirsutum*) cultivars under combined drought and heat induced oxidative stress. *Environmental and experimental botany*, 99:141–149.

Sejima, T., Takagi, D., Fukayama, H., Makino, A. and Miyake, C. 2014. Repetitive short-pulse light mainly inactivates photosystem I in sunflower leaves. *Plant and cell physiology*, 55:1184–1193.

Sharma, P. and Dubey, R. S. 2005. Drought induces oxidative stress and enhances the activities of antioxidant enzymes in growing rice seedlings. *Plant growth regulation*, 46(3): 209–221.

Shetty, K., 2004. Role of proline-linked pentose phosphate pathway in biosynthesis of plant phenolics for functional food and environmental applications: a review. *Process Biochemistry*, 39:789-803.

Signorelli, S., Corpas, F. J., Borsani, O., Barroso, J. B. and Monza, J. 2013. Water stress induces a differential and spatially distributed nitro-oxidative stress response in roots and leaves of *Lotus japonicus*. *Plant science*, 201–202:137–146.

Singh, S. K. and Reddy, K. R. 2011. Regulation of photosynthesis, fluorescence, stomatal conductance and water-use efficiency of cowpea (*Vigna unguiculata* [L.] Walp.) under drought. *Journal of photochemistry and photobiology B: biology*, 105:40–50.

Slama, I., Abdelly, C., Bouchereau, A., Flowers, T. and Savoure, A., 2015. Diversity, distribution and roles of osmoprotective compounds accumulated in halophytes under abiotic stress. *Annals of botany*, 115(3):433-447.

Solanki, J. K. and Sarangi, S. K. 2014. Effect of drought stress on proline accumulation in peanut genotypes. *International journal of advanced research*, 2:301-309.

- Sonoike, K. 201. Photoinhibition of photosystem I. *Physiologia plantarum*, 142:56–64.
- South African Grain Quality. 2011. South African Maize-Crop Quality Report 2010/2011 Season, 2011.
- Sosa-Zuniga, V., Brito, V., Fuentes, F. and Steinfort, U. 2017. Phenological growth stages of quinoa (*Chenopodium quinoa*) based on the BBCH scale. *Annals of applied biology*, 171:117–124.
- Souza, R. P., Machado, E. C., Silva, J. A. B., Lagoa, A. M. M. A. and Silveira, J. A. G. 2004. Photosynthetic gas exchange, chlorophyll fluorescence and some associated metabolic changes in cowpea (*Vigna unguiculata*) during water stress and recovery. *Environmental and experimental botany*, 51:45–56.
- Stevens, R. G., Creissen, G. P. and Mullineaux, P. M. 1997. Cloning and characterization of a cytosolic glutathione reductase cDNA from pea (*Pisum sativum* L.) and its expression in response to stress. *Plant molecular biology*, 35:641–654.
- Strasser, B. J. 1997. Donor side capacity of Photosystem II probed by chlorophyll a fluorescence transient. *Photosynthesis research*, 52:147–155.
- Strasser, R.J. and Tsimilli-Michael, M. 2001. Stress in plants, from daily rhythm to global changes, detected and quantified by the JIP-test. *Chimie-New*, 75:3321-3326.
- Strasser, R. J., Tsimilli-Michael, M. and Srivastava, A. 2004. Analysis of the chlorophyll a fluorescence transient. (In Papageorgiou, G., Govindjee. eds. Chlorophyll a fluorescence a signature of photosynthesis. Dordrecht: Springer International Publishing. p. 321-362).
- Strasser. R, J., Tsimilli-Michael, M., Dangre, D. and Rai, M. 2007. Biophysical phenomics reveals functional building blocks of plants systems biology: a case study for the evaluation of the Impact of Mycorrhization with *Piriformospora indica*. (In Varma, A. and Oelmüller, R. eds. Advanced techniques in soil microbiology. Berlin Heidelberg: Springer International Publishing. p. 319-341).
- Strasser, R. T., Tsimilli-Michael, M., Qiang, S. and Goltsev, V. 2010. *Simultaneous in vivo* recording of prompt and delayed fluorescence and 820-nm reflection changes

during drying and after rehydration of the resurrection plant *Haberlea rhodopensis*. *Biochimica et biophysica acta*, 1797:1313-1326.

Sun, Y., Liu, F., Bendevis, M., Shabala, S. and Jacobsen, S. E. 2014. Sensitivity of two quinoa (*Chenopodium quinoa* Willd.) varieties to progressive drought stress. *Journal of agronomy and crop science*, 200:12-23.

Sung, D. Y., Kaplan, F., Lee, K. J. and Guy, C. L. 2003. Acquired tolerance to temperature extremes. *Trends in plant science*, 8:179-187.

Suorsa, M., Järvi, S., Grieco, M., Nurmi, M., Pietrzykowska, M., Rantala, M., Kangasjärvi, S., Paakkari, V., Tikkanen, M., Jansson, S. and Aro, E. M. 2012. Proton gradient regulation is essential for proper acclimation of *Arabidopsis* photosystem I to naturally and artificially fluctuating light conditions. *Plant Cell*, 24:2934–2948.

Sullivan, C. Y. 1971. The techniques for measuring plant drought stress. (In Larson, K. L. and Epstein, J. D. eds. *Drought injury and resistance in crop*. Madison, Wisconsin: Crop Science Society of America. p. 1-18).

Suprasanna, P., Nikalje, G. C. and Rai, A. N. 2016. Osmolyte accumulation and implications in plant abiotic stress tolerance. (In Iqbal, N., Nazar, R., Khan, N. A. eds. *Osmolytes and Plants Acclimation to Changing Environment: Emerging Omics Technologies*. India: Springer. p. 1-12).

Székely, G., Abraham, E., Cselo, A., Rigo, G., Zsigmond, L., Csiszar, J., Ayaydin, F., Strizhov, N., Jasik, J., Schmelzer, E., Koncz, C. and Szabados, L., 2008. Duplicated P5CS genes of *Arabidopsis* play distinct roles in stress regulation and developmental control of proline biosynthesis. *The plant journal*, 53:11-28.

Takagi, D., Takumi, S., Hashiguchi, M., Sejima, T. and Miyake, C. 2016. Superoxide and singlet oxygen produced within the thylakoid membranes both cause photosystem I photoinhibition. *Plant physiology*, 171:1626–1634.

- Tanko, M. U. and Hassan, U. T. 2016. Leaf area determination for maize (*Zea mays* L), okra (*Abelmoschus esculentus* L) and cowpea (*Vigna unguiculata* L) crops using linear measurements. *Journal of biology, agriculture and healthcare*. 4:103-111.
- Tanou, G., Job, C., Belghazi, M., Molassiotis, A., Diamantidis, G. and Job, D. 2010. Proteomic signatures uncover hydrogen peroxide and nitric oxide cross-talk signaling network in citrus plants. *Journal of proteome research*, 9:5994–6006.
- Tapia, M. 1997. Cultivos Andinos Subexplotados y su Aporte a la Alimentacion. Santiago, Chile: Oficina Regional de la FAO para America Latina y el Caribe.
- Tapia, M. 2009. La quinua. Historia, distribución geográfica actual, producción y usos. *Revista Ambienta*, 99:104–119.
- Tapia, M. 2015. The Long Journey of Quinoa: Who wrote its history? (In Bazile, D., Bertero, H.D., Nieto, C. eds. State of the Art Report on Quinoa around the World 2013. FAO: Santiago, Chile; CIRAD: Montpellier, France, Volume 1, pp. 1–7).
- Tezara, W., Martínez, D., Rengifo, E. and Herrera, A. 2003. Photosynthetic responses of the tropical spiny shrub *Lycium nodosum* (solanaceae) to drought, soil salinity and saline spray. *Annals of botany*, 92(6):757–765.
- Trivedi D., Gill, S. S., Yadav, S. and Tuteja N. 2013. Genome-wide analysis of glutathione reductase (GR) genes from rice and *Arabidopsis*. *Plant signaling & behavior*, 8(2):23021.
- Tsimilli-Michael, M. and Strasser, R.J. 2008. *In vivo* assessment of stress impact on plant's vitality: applications in detecting and evaluating the beneficial role of mycorrhization on host plants. In mycorrhiza (In: Varma, A., eds. Mycorrhiza: state of the art, genetics and molecular biology, eco-function, biotechnology, eco-physiology, structure and systematics. Springer, Berlin, Heidelberg. p. 679-670).
- Tsimilli-Michael, M. and Strasser, R.J. 2013. Biophysical Phenomics: Evaluation of the Impact of Mycorrhization with *Piriformospora indica* (In: Varma, A., Kost, G. and Oelmüller, R., eds. *Piriformospora indica*. Soil Biology 33, Springer-Verlag Berlin Heidelberg, pp. 173-189).

Uchida, A., Jagendorf, A. T., Hibino, T., Takabe, T. and Takabe, T. 2002. Effects of hydrogen peroxide and nitric oxide on both salt and heat stress tolerance in rice. *Plant Science*, 163:515–523.

Uzilday, B., Turkan, I., Ozgur, R., Sekman, A. H. 2014. Strategies of ROS regulation and antioxidant defense during transition from C₃ to C₄ photosynthesis in the genus *Flaveria* under PEG-induced osmotic stress. *Journal of plant physiology*. 171: 65-75.

van Heerden, P.D.R., Swanepoel, J.W. and Krüger, G.H.J., 2007. Modulation of photosynthesis by drought in two desert scrub species exhibiting C₃-mode CO₂ assimilation. *Environmental and experimental botany*. 61:124-136.

Verbruggen, N. and Hermans, C. 2008. Proline accumulation in plants: a review. *Amino acids*, 35(4):753–759.

Verslues, P.E. and Sharma, S., 2010. Proline metabolism and its implications for plant-environment interaction. *Arabidopsis Book*, 8:0140.

Vives-Peris, V., Go´mez-Cadenas, A. and Pe´rez-Clemente, R. M., 2017. Citrus plants exude proline and phytohormones under abiotic stress conditions. *Plant cell reports*, 36(12):1971-1984.

Vogel, C. and van Zyl, K. 2016. Drought: In Search of Sustainable Solutions to a Persistent, ‘Wicked’ Problem in South Africa. (In Salzmann, N., Huggel, C., Nussbaumer, S., Ziervogel, G. eds. *Climate Change Adaptation Strategies – An Upstream-downstream Perspective*. Switzerland: Springer International Publishing. p. 195–211).

Volkov, R. A., Panchuk II, Mullineaux, P. M. and Schöffl, F. 2006. Heat stress-induced H₂O₂ is required for effective expression of heat shock genes in *Arabidopsis*. *Plant molecular biology*, 61:733–746.

Vredenberg, W., Kasalicky, V., Durchan, M. and Prasil, O. 2006. The chlorophyll a fluorescence induction pattern in chloroplasts upon repetitive single turnover excitations: Accumulation and function of QB--nonreducing centers. *Biochimica et biophysica acta*. 1757:173-181.

- Wahid, A., Gelani, S., Ashraf, M. and Foolad, M.R. 2007. Heat tolerance in plants: An overview. *Environmental and experimental botany*, 61:199–223.
- Wand, S. J. E., Midgley, G. F. and Stock, W. D. 2001. Growth responses to elevated CO₂ in NADP-ME, NAD-ME and PCK C₄ grasses and a C₃ grass from South Africa. *Australian journal of plant physiology*, 28:13–25.
- Wani, A. S., Ahmad, A., Hayat, S. and Tahir, I. 2019. Epibrassinolide and proline alleviate the photosynthetic and yield inhibition under salt stress by acting on antioxidant system in mustard. *Plant physiology and biochemistry*, 135:385–394.
- Willmott, C. J. 1982. Some comments on the evaluation of model performance. *Bulletin of the American meteorological society*, 63:1309–1313.
- Wilson, H. D. 1990. Quinoa and relatives (*Chenopodium* sect. *Chenopodium* subsect. *Cellulata*). *Economic botany*, 44:92-110.
- Winkel, T., Lhomme, J. P., Nina Laura, J. P., Mamani Alcón, C., del Castillo, C. and Rocheteau, A. 2009. Assessing the protective effect of vertically heterogeneous canopies against radiative frost: The case of quinoa on the Andean Altiplano. *Agriculture and forest meteorology*, 149:1759-1768.
- Xu, Z., Zhou, G. and Shimizu, H. 2010. Plant responses to drought and rewatering, *Plant signaling & behaviour*, 5(6):649-654.
- Yamane, Y., Kashino, Y., Koike, H. and Satoh, K. 1997. Increases in the fluorescence Fo level and reversible inhibition of Photosystem II reaction center by high-temperature treatments in higher plants. *Photosynthesis research*, 52:57–64.
- Yang, A., Akhtar, A. S. S. M., Iqbal, S. and Jacobsen, S. E. 2016. Growth and Physiological Responses of Quinoa to Drought and Temperature Stress. *Journal of agronomy and crop science*, 202:445–453.
- Yordanov, I., Velikova, V. and Tsonev, T. 2000. Plant responses to drought, acclimation and stress tolerance. *Photosynthetica*, 38(1):171-186.

Yusuf, M. A., Kumar, D., Rajwanshi, R., Strasser, R. J., Tsimilli-Michael, M, Govindjee and Sarin, N. B. 2010. Overexpression of γ -tocopherol methyl transferase gene in transgenic Brassica juncea plants alleviates abiotic stress: physiological and chlorophyll a fluorescence measurement. *Biochimica et biophysica acta*, 1797:1428-1438.

Yousuf, P. Y., Hakeem, K. U. R., Chandna, R. and Ahmad, P. 2012. Role of Glutathione Reductase in Plant Abiotic Stress. (In Ahmad, P. and Prasad, M. N. V. eds. Abiotic Stress Responses in Plants: Metabolism, Productivity and Sustainability, Springer Science + Business Media, LLC 2012. p. 149-158).

Zandalinas, S. I., Balfagón, D., Arbona, V. and Gómez-Cadenas, A. 2017. Modulation of antioxidant defense system is associated with combined drought and heat stress tolerance in citrus. *Frontiers in plant science*, 8:953.

Zandalinas, S.I., Mittler, R., Balfago´ n, D., Arbona, V. and Gomez Cadenas, A., 2018. Plant adaptations to the combination of drought and high temperatures. *Physiologia Plantarum*, 162(1):2-12.

Zarattini, M. and Forlani, G., 2017. Toward unveiling the mechanisms for transcriptional regulation of proline biosynthesis in the plant cell response to biotic and abiotic stress conditions. *Frontiers in plant science*, 8:927.

Zhang, L. and Becker D. F. 2015. Connecting proline metabolism and signaling pathways in plant senescence. *Frontiers in plant science*, 6:552. doi: 10.3389/fpls.2015.00552

Zhang, J. and Kirkham, M. 1995. Water relations of water-stressed, split-root C₄ (*Sorghum bicolor*; Poaceae) and C₃ (*Helianthus annuus*; Asteraceae) plants. *American journal of botany*, 82:1220–1229.

Ziervogel, G., New, M., van Garderen, Midgley, Taylor, A., Hamann, R., Stuart-Hill, S., Myers, J. and Warburton, M. 2014. Climate change impacts and adaptation in South Africa. *WIREs climate change*, 5:605–620.

Zlatev, Z. and Stotanov, Z. 2005. Effect of water stress on leaf water relations of young bean plants. *Journal of central European agriculture*, 6(1):5–14.

Zurita, S. A., Fuentes, F., Zamora, P., Jacobsen, S. and Schwember, A. R. 2014. Breeding quinoa (*Chenopodium quinoa Willd.*): potential and perspectives. *Molecular breeding*, 34:13–30.

Zurita, S. A., Jacobsen, S. E., Razzaghi, F., Álvarez Flores, R., Ruiz, K. B., Morales, A. and Silva Ascencio, H. 2015. Quinoa drought responses and adaptation (*In* Bazile, D., Bertero, D. & Nieto, C. eds. State of the art report on quinoa around the world in 2013. Chapter 2.4. Chile: Santiago, FAO/CIRAD. p. 157-171).

Zushi, K., Kajiwara, S. and Matsuzoe, N. 2012. Chlorophyll *a* fluorescence OJIP transient as a tool to characterize and evaluate response to heat and chilling stress in tomato leaf fruit. *Scientia horticultrae*, 148:39-46.

Zivcak, M., Kalaji, M. H., Shao, H. B., Olsovska, K. and Brestic, M. 2014. Photosynthetic proton and electron transport in wheat leaves under prolonged moderate drought stress. *Journal of photochemistry and photobiology B: biology*, 137:107-115.

LAST UPDATED: 19 February 2020